NUREG/CR--4343
SAND85--1639
R4
Printed December 1985

Integrated Severe Accident Containment Analysis with the CONTAIN Computer Code

K. D. Bergeron, D. C. Williams, P. E. Rexroth, J. L. Tills

Prepared by
Sandia National Laboratories
Albuquerque, New Mexico 87185 and Livermore, California 94550
for the United States Department of Energy
under Contract DE-AC04-76DP00789

Prepared for
U. S. NUCLEAR REGULATORY COMMISSION

Available from

Superintendent of Documents
U.S. Government Printing Office
Post Office Box 37082
Washington, D.C. 20013-7982

and

National Technical Information Service
Springfield, VA 22161

NUREG/CR-4343
SAND85-1639
R4

INTEGRATED SEVERE ACCIDENT CONTAINMENT ANALYSIS WITH THE CONTAIN COMPUTER CODE

K. D. Bergeron
D. C. Williams
P. E. Rexroth
J. L. Tills*

December 1985

Sandia National Laboratories
Albuquerque, New Mexico 87185
Operated by
Sandia Corporation
for the
U.S. Department of Energy

Prepared for
Division of Accident Evaluation
Office of Nuclear Regulatory Research
U.S. Nuclear Regulatory Commission
Washington, DC 20555
Under Memorandum of Understanding DOE 40-550-75
NRC FIN NO. A1198

* J. L. Tills and Associates, Inc., Albuquerque, NM

ABSTRACT

Analysis of physical and radiological conditions inside the containment building during a severe (core-melt) nuclear reactor accident requires quantitative evaluation of numerous highly disparate yet coupled phenomenologies. These include two-phase thermodynamics and thermal-hydraulics, aerosol physics, fission product phenomena, core-concrete interactions, the formation and combustion of flammable gases, and performance of engineered safety features. In the past, this complexity has meant that a complete containment analysis would require application of suites of separate computer codes each of which would treat only a narrower subset of these phenomena, e.g., a thermal-hydraulics code, an aerosol code, a core-concrete interaction code, etc. In this paper, we describe the development and some recent applications of the CONTAIN code, which offers an integrated treatment of the dominant containment phenomena and the interactions among them. We describe the results of a series of containment phenomenology studies, based upon realistic accident sequence analyses in actual plants. These calculations highlight various phenomenological effects that have potentially important implications for source term and/or containment loading issues, and which are difficult or impossible to treat using a less integrated code suite. The results described show that analyses with nonintegrated, separate-effects codes can neglect interactions that are important to the source term and, furthermore, that it is impossible to generalize whether the errors in such treatments would be "conservative" or "nonconservative." It is concluded that integrated phenomenological analysis will play an increasingly important role as the technology for severe accident analysis matures.

TABLE OF CONTENTS

LIST OF FIGURES

LIST OF FIGURES (Con't.)

LIST OF TABLES

ACKNOWLEDGMENT

There have been many individuals who have contributed, knowingly or not, to this work, but we will single out only two. Ken Murata's work in model development and calculational studies were very important for this project. And S. Bradley Burson of the NRC has been a continuous source of insight on integrated severe accident analysis for all the years he has been program monitor for the CONTAIN project.

EXECUTIVE SUMMARY

Computational Tools for Severe Accident Containment Analysis

Commercial nuclear power reactors have been designed and constructed with extraordinary precaution against the possibility that radioactive materials should be released from the plant under any conceivable circumstances. The remarkable safety record of these plants attests to the success of the "defense in depth" strategy of these designs. Numerous studies of hypothetical event sequences reinforce the conclusion that accidents leading to core melt and vessel failure are extremely unlikely. Nonetheless, these studies, as well as the historical record of the arrested sequence at TMI-2, suggest that core-melt accidents cannot be considered impossible. As with other advanced technologies, a significant fraction of the total risk to society associated with the operation of nuclear power plants resides in these low-probability, high-consequence events. It is therefore prudent to invest some fraction of the total regulatory and research effort in studying the consequences of severe accidents.

In the absence of any history of reactor accidents involving release of molten material into the containment building and in view of the complexity of the systems under consideration, a natural approach for such studies is to develop system-level computer codes embodying the best current understanding of the relevant phenomena. However, such a task is remarkably difficult, since it requires the code developer with limited resources to translate an incomplete knowledge base into a practical calculational tool. A logical first step in this task is to divide the problem into manageable subelements. A natural division is to consider the primary system, containment building, and ex-plant environment as separate subsystems. This analysis requires only one-way transfers of information in most situations. The second step is to narrow the range of questions intended for the particular calculational tool under consideration. For severe accident containment analysis, there are a broad variety of issues that need to be addressed, such as containment loading and failure prediction, source term prediction, probabilistic risk assessment, and equipment survival and accident management questions.

In this report, we focus on the containment loading and source term issues, particularly those questions for which the well-mixed atmosphere assumption is acceptable. We use the USNRC's CONTAIN code[1] as an example of a calculational tool designed for such problems. This code is unique among containment analysis codes in that it does not rely on the further subdivision of the problem into separate treatments of thermal-hydraulic, aerosol, and fission product phenomena. In CONTAIN, these are treated simultaneously, so it is possible to include some of the two-way feedback effects that might occur.

These feedback effects are not always important, but without an integrated analysis tool, it is often difficult to predict whether they need to be considered or not.

The range of phenomena which must be considered in CONTAIN is quite large. As in the analysis of Design Basis Accidents (DBAs), prediction of the pressure and temperature of the atmosphere requires analysis of the thermodynamics of mixtures of steam and noncondensible gases, as well as sources and sinks of heat and mass. Condensation heat transfer to walls and other structures is is an important mass and energy sink, while internal heat sources include hydrogen combustion, radiant heat transfer from molten pools, and decay heat from suspended or deposited radioisotopes. An important source of gases that must be modeled is the decomposition of concrete due to ablation by molten core debris. The flow of gases and liquids between compartments is modeled in CONTAIN, as is the effect of engineered safety features (e.g., containment sprays or ice condenser) on atmospheric thermodynamic conditions.

Besides these thermal-hydraulic phenomena, detailed modeling of the evolution of the aerosol particle size distribution is included in the code. This requires not only analysis of natural agglomeration and deposition processes, but also the decontaminating effects of engineered safety features. A critical aspect of the coupling between aerosols and thermal-hydraulics is the modeling of condensation onto and evaporation from aerosol particles.

In addition to aerosols and thermal-hydraulics, CONTAIN also includes models for the inventory and location of radioisotopes in the containment. These models include the effects of radioactive decay and the resulting generation of heat. The migration of each radioactive species from one material to another is also considered, albeit by means of parametric models.

The models implemented in the CONTAIN code are intended to reflect the current state of understanding of severe accident phenomenology, to the extent possible in a system-level code. Nonetheless there are identifiable limitations in the code, and a proper understanding of the significance of calculational results requires an awareness of these limitations. Perhaps the most important of these is the reliance on the well-mixed atmosphere assumption in each control volume (or cell) and the use of an orifice flow model to govern the transfer of gas between cells. The well-mixed assumption is invoked primarily for calculational tractability (e.g., to keep the number of calculational cells to a minimum), but many other limitations in the models are simply a reflection of an incomplete knowledge base, which can be remedied only by additional phenomenological research. Where possible, provisions have been incorporated in the code to allow the user to investigate the consequences of alternative hypotheses concerning such uncertain phenomena.

Despite such unavoidable limitations, CONTAIN provides a significantly more complete description of severe accident containment phenomenology in pressurized water reactors than calculational tools that have been available up until now. Of particular importance is the fact that the calculation is not fragmented into separate analyses of thermal-hydraulics, aerosol behavior, and fission product inventories. One of the principal goals of this report is to investigate the importance of performing integrated analyses of these phenomena for realistic severe accident sequences--in other words, to determine the importance of closed-loop feedback effects on containment loads and the source term.

The focus of this work is a series of calculational studies performed with the CONTAIN code, involving a variety of hypothetical accident sequences at different plants. These are primarily sensitivity studies, with the goal of illustrating the role played by a particular phenomenon or coupling. This approach is somewhat different from the studies presented in Reference 2 (referred to as the QUEST study), which was a more complete uncertainty study of source term modeling in severe accident analysis. In the latter, the focus of attention is the error band that should be assigned to the source term calculations as a result of uncertainties in containment phenomenology; the precise role of each phenomenon or each synergism was not always revealed in that analysis.

Highlights of Sensitivity Studies

Five topics are addressed in this report, each involving a specific accident sequence at actual power plants. Thus, the issues are investigated in a realistic context, although the calculations are not intended as best estimates for those plants and sequences. Many of the results are discussed with an emphasis on couplings between thermal-hydraulics, aerosols, and fission product behavior, but there are numerous other aspects of the calculations that are also of interest.

Aerosol Deposition and Decay Heating

The first sensitivity study involves an investigation of the effects of the location of decay heat sources on containment pressure and temperature histories. The sequence studied was the Station Blackout (TMLB') at a plant similar to the Bellefonte station. It was shown that the pressure and temperature at late times (e.g., twenty hours into the accident) are sensitive to the inclusion of the decay heat associated with volatile and aerosolized fission products. The predicted pressure changes from about three atmospheres to almost five when these fission products are treated as a gas in the atmosphere. More to the point, however, is what happens when, instead of treating the fission products as a gas, we invoke the aerosol model in CONTAIN to allow for the deposition of the decay heat sources onto surfaces of heat sinks. The

resulting pressure is about four atmospheres, midway between the two extremes. This exercise illustrates that realistic treatment of radionuclide transport may be important for accurate prediction of such thermal-hydraulic quantities as pressure, temperature, relative humidity, and steam concentration.

Depressurization Condensation on Aerosols

If the containment building fails at high pressure under conditions of high relative humidity, the resulting depressurization may lead to supercooled conditions, which will cause rapid condensation of water vapor on suspended aerosols. Since the subsequent growth in particle size (through agglomeration as well as condensation) can lead to rapid aerosol removal by gravitational settling, it is of interest to investigate the effects of these processes on the source term. A series of calculations was performed for this purpose based on a TMLB' sequence in a containment building whose geometry and heat sinks were those of the Zion plant. It was found that the effects of depressurization condensation could be significant, but only if the failure hole size is small enough that the depressurization process is slow compared to characteristic times for aerosol removal via condensation, agglomeration. and gravitational settling. In particular, a large hole (0.8 m^2) depressurizes the containment in minutes, and there is virtually no effect on the amount of radionuclides released to the environment, whereas with a smaller hole (0.02 m^2) the pressure takes over an hour to be substantially reduced, and the deposition processes have time to work; consequently, the source term is reduced by about forty percent. In the context of other uncertainties in the source term, this is not a large effect, but it is not insignificant, and might be larger in other scenarios.

Effects of Steam and Heat Sources on the TMLB' Sequence

There is a good deal of uncertainty in the steam and heat sources to the containment building, both from the primary system and from phenomena occurring in the reactor cavity. Variations in these sources may have significant effects on subsequent events, especially when hydrogen burns are part of the scenario, since gas combustion is a "threshold effect." A series of calculations was performed with CONTAIN involving, again, the TMLB' (or Station Blackout) sequence, but this time the containment was that of the subatmospheric Surry plant.

In the base case of this calculational series a hydrogen burn due to steam de-inerting was predicted at about eight hours from scram. The first effect noted in the variations from the base case is that a moderate increase in the assumed rate of steam injection resulted in a delay of the burn because de-inerting took longer. Since there was a continuous hydrogen source in these calculations, the burn was also more severe. It

was also found that similar results are predicted when an equivalent amount of heat is added to the atmosphere without additional mass (e.g., due to radiant heat transfer from the molten pool). Larger sources of steam or heat had a sufficiently large effect that de-inerting was not observed during the entire calculational period, and burns did not occur. As in virtually all CONTAIN accident sequence calculations, it was observed that saturated steam conditions are rare in containment, and significant superheat the norm. The resulting low-humidity conditions may have significant effects on aerosol behavior.

TMLB' Sequences with Spray Recovery

An important potential mechanism for de-inerting steam-laden laden atmospheres in the TMLB' sequence is activation of the containment sprays in the event that power is restored. In this case, the steam removal process is quite fast, but so is the decontaminating effect of the sprays. It is therefore of interest to study the possibility of hydrogen burns following spray recovery, and also to evaluate the effect of the sprays on the suspended radioactive inventory under such conditions. CONTAIN predictions for such sequences indicate that the sprays substantially reduce the pressures and temperatures due to burns initiated by the de-inerting effect of the sprays, unless the default correlation for burn duration was overridden to give near-adiabatic burns. Also, the decontaminating effect of the sprays was very large both prior to burn initiation and for a period of time after the burn. Careful examination of the aerosol removal rate histories indicates that the interplay between aerosol agglomeration, condensation on aerosols, condensation on spray droplets, and the effects of the hydrogen burns, is quite complex, and leads to higher removal rates than might be predicted on the basis of simple models.

Integrated Analysis of Isolation Failure Sequences

A series of calculations was performed to study the sensitivity of the source term to hole size for sequences in which a pre-existing leak in the containment was assumed. The accident studied was the AB sequence at the Surry plant, and an important goal was to compare results with calculations performed for the American Nuclear Society (ANS) on the same sequence with different calculational tools.[3] It was found that there were a number of qualitative similarities between the results obtained in the two studies, but there were significant quantitative differences as well. The most notable qualitative similarity is the existence of a hole size which gives a larger source term than either smaller or larger holes, i.e., a local maximum in the source term vs. hole size curve.

The reasons for quantitative differences were difficult to trace, since there were so many differences in the code suites

used. However, it appeared that some of the more important differences could be traced to issues involving integrated aerosol/thermal-hydraulics analysis. In particular, the modeling of the suspended atmospheric water poses problems for a thermal-hydraulic code which (like that used in the ANS study) does not perform aerosol calculations. The suspended liquid inventory predicted by CONTAIN was depleted by aerosol deposition processes to the extent that hot gases released prior to the release of fission product aerosols evaporated all of the remaining aerosolized water. This depletion of the atmospheric liquid inventory also permitted significant superheat to develop, as well as steam concentrations low enough to permit hydrogen burns (which were not predicted in the ANS study). On the aerosol side of the problem there were related effects: CONTAIN predicted no water aerosol remaining at the time solid aerosols were released, so the removal process was slow compared to the ANS aerosol model prediction, which assumed that the high suspended liquid water inventory predicted by the thermal-hydraulics code would be depleted only by agglomeration and settling, without evaporation.

The examples studied here illustrate the variety of synergistic effects which are possible in severe accident containment analysis when the couplings among apparently disparate phenomena are taken into account. The quantitative effects observed in these cases ranged from modest to orders of magnitude. The explanations for the feedback effects were sometimes simple and sometimes surprisingly complex. As additional severe accident analysis is performed with CONTAIN (for example, studies involving Boiling Water Reactors or Ice Condensers), it is expected that additional evidence of the importance of integrated analysis will be discovered.

1. INTRODUCTION

Over the last twenty years, calculational tools for the analysis of the physical conditions inside nuclear reactor containment buildings during Design Basis Accidents (DBAs) have developed to a relatively mature stage. Best-estimate codes have been able to perform blind predictions of almost-full-scale large break Loss-of-Coolant Accident (LOCA) experiments[4] with a degree of accuracy which establishes very high levels of confidence that reactor containments will not fail during DBAs. Part of the reason for this success is simply that there are only a small number of basic phenomena involved, and in the narrow parameter ranges of interest, they are well understood and amenable to simple modeling approaches (e.g., control volumes, heat slabs, condensation correlations). Indeed, most analytic effort for DBAs has been devoted to primary system phenomena, which are not so simple.

In contrast, containment analysis for core-melt accidents is incomparably more difficult a task than the design basis accident problem. The number and diversity of phenomena involved is much greater, and the current state of scientific knowledge about these phenomena is often inadequate. Because of the difficulty of the modeling challenge, and also the perception that accidents beyond the design basis could be justifiably neglected, little work was done in the area of system-level severe accident containment code development until recently. There are two reasons for a sharp increase in interest in developing such a calculational capability. The first is the accident at the TMI-2 power plant, which has changed perceptions about the likelihood of such events. The second is the growing understanding that, because of natural removal and deposition processes, the containment building can play a major role in reducing the release of radioisotopes to the environment, even if the pressure vessel and the containment should fail. Furthermore, there appears to be considerably less uncertainty about the extent of such decontamination in containment than there is about hold-up of the radioisotope inventory in the primary system.

Thus, there is a great deal of incentive to face the challenge of developing system-level codes for severe accident containment analysis. Such a code must include models for all the phenomena which are treated by the LOCA codes (steam-gas thermodynamics, intercell gas flow, condensation heat transfer, conduction in heat sinks, operation of engineered safety features) and in addition, phenomena which are unique to core-melt accidents. These include hydrogen or carbon monoxide burns, molten core-concrete interactions, steam generation due to contact of water with hot debris, aerosol behavior, fission product decay, decay heating, and various other processes which affect the transport of radioisotopes throughout the containment and/or into the environment.

The relevant phenomena can be conveniently grouped into three categories; these categories also needed in DBA codes are indicated by (DBA):

a. Thermal-hydraulic phenomena

gas flow (DBA)

liquid flow (DBA)

condensation (DBA)

gas combustion

heat transfer to sinks (DBA)

conduction in heat sinks (DBA)

thermodynamics of steam/
non-condensible gas mixtures (DBA)

ablation of concrete by core debris

b. Aerosol behavior

aerosol generation processes

particle size distribution

particle agglomeration

deposition on structures

c. Radioisotope decay, heating and transport

radioisotope inventories and decay chains

release from materials

absorption

heating of gases and structures

Clearly, only a small subset of these phenomena is needed for the DBA codes. Efforts to analyze the severe accident containment problem have considered a larger number of items from this list, but because of the complexity of the problem, computational analysis has typically been fragmentary. That is to say, accident sequences have been analyzed with various combinations of computer codes each of which deals with a different subset of the phenomena in question. Interfaces between the codes are typically output-input data transfers, with no accounting for possible feedback effects. For example, a debris-concrete interaction model might be run first, providing gas and energy sources for a thermal-hydraulic

containment code, and other input to an aerosol generation code. Then, an aerosol behavior code is run based on the outputs of the thermal-hydraulic code and aerosol generation code. The result is an estimate of the source term. Such a one-way linkage of codes has been used for most of the recent re-evaluations of the source term. Figure 1-1 shows the sequence of codes used for the studies[5] (for both primary system and containment) performed by Battelle Columbus Laboratories for the U.S. Nuclear Regulatory Commission (USNRC).

Such a calculational approach has distinct practical advantages; engineers and scientists have learned that the best initial approach to complex problems is to "divide and conquer." However, the success of this strategy depends on the absence of important feedback effects which have been neglected because of the fragmentation of the calculation. There are also practical disadvantages to using a sequence of several codes to analyze the complete accident sequence: the logistics of interfacing all of the codes becomes quite cumbersome, errors in the code interfaces are common, and maintaining the various links between the codes as they each evolve becomes an additional burden.

For these reasons, it is desirable to develop "second generation" computer codes that deal with all of the relevant phenomena in an integrated manner. The CONTAIN[1] code is such a tool, intended for analysis of the physical and radiological conditions inside the containment building (or other attached buildings) during and following severe accidents. It also can calculate the release to the environment in the event of containment leakage or failure. It should be made clear, however, that CONTAIN is not a complete accident sequence code; only phenomena occurring inside containment are modeled. Phenomena occurring within the primary system or outside the plant must be treated with other tools.

In this report, we will be discussing a number of aspects of integrated phenomenological analysis in the containment, in some cases using CONTAIN to exemplify some of the first steps in this new direction. However, a few cautionary words about terminology may be in order. The term "integrated analysis" is sometimes used to refer to a calculation that simultaneously models both the primary system and the containment. The MARCH computer code,[6] for example, handles thermal-hydraulic phenomena in both systems. For clarity, one might call this a "vertically integrated" code, in contrast to the "horizontally integrated" CONTAIN code, which models a wider range of phenomena, but only inside the containment system. A parallel second-generation "horizontally integrated" code for in-vessel analysis is MELPROG,[7] which is currently under development for the USNRC. Like CONTAIN, it models aerosols and fission products as well as thermal-hydraulic behavior. Ultimately, it would be desirable to have a "fully integrated" code that incorporates both the vertical and horizontal integration

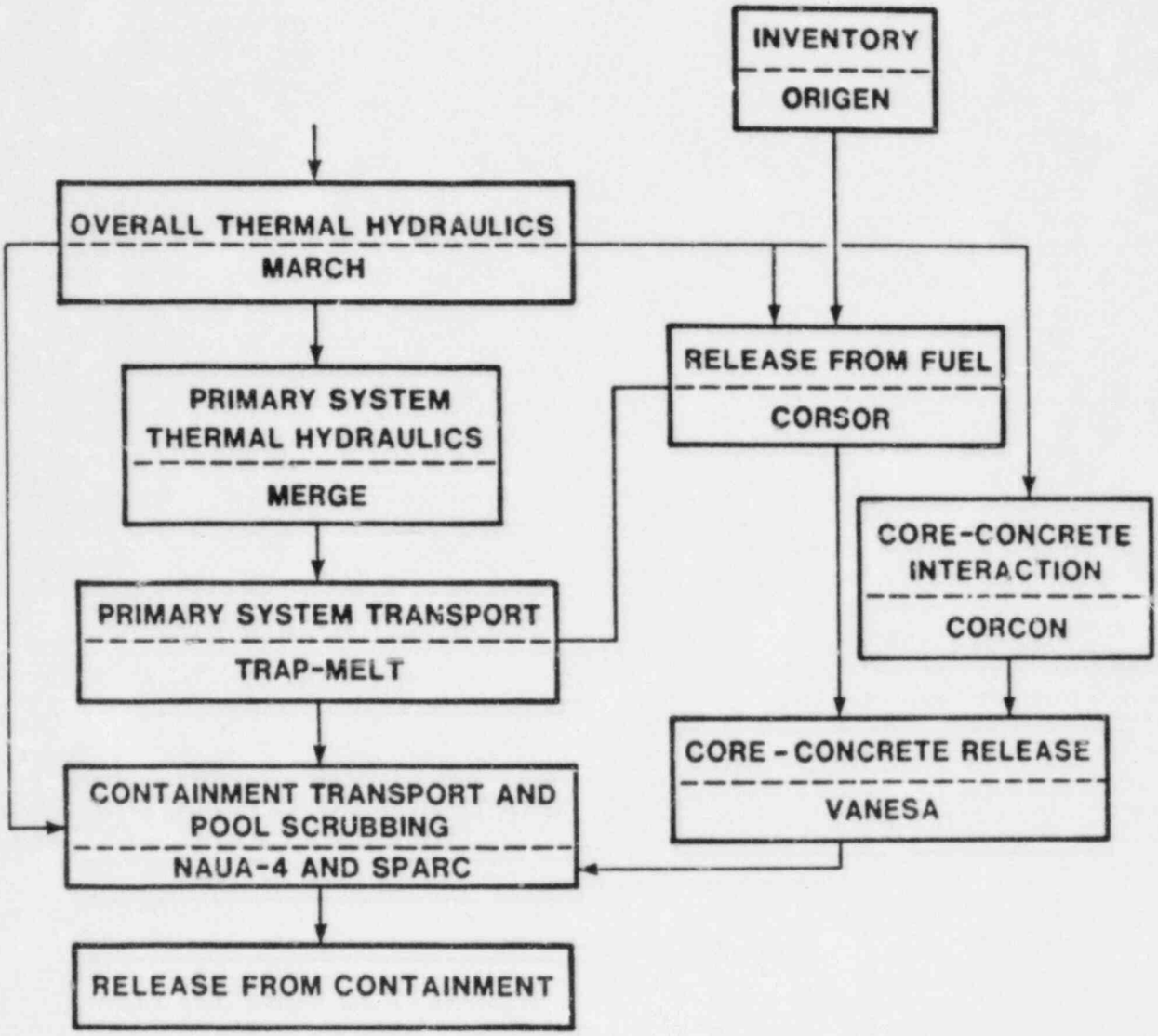

Figure 1-1. Sequence of computer codes used with one-way coupling for the BMI-2104 source term study.[5]

capabilities. For best-estimate analysis, such a code would presumably be very large and complex. The closest approximation to such a code being developed for the USNRC is the MELCOR[8] code, which is being developed primarily for risk analysis rather than for best-estimate calculations.

Thus, using a code like CONTAIN represents a different approach to "divide and conquer" than has been used in the past--a different way of breaking up a complex problem into tractable pieces. It is based on the assumption that closed-loop feedback effects between containment and the primary system, or between the ex-plant environment and containment, are negligible. This is probably a much more justifiable assumption than the neglect of two-way coupling between aerosols, fission products, and thermal-hydraulics. A few situations in which in-vessel/ex-vessel or in-plant/ex-plant coupling may be important can be identified, and they will be briefly discussed in Section 3.7. However, one of the principal purposes of this report is to explore some of the ways that the various phenomena inside containment can interact, and the effects of these feedback loops on quantities of importance to reactor safety. Many aspects to be discussed will make use of the CONTAIN code, but it must be kept in mind that not all of the couplings are included in CONTAIN, and those that are included are sometimes based on rather simplistic models. Thus, a complete or definitive study of integrated containment analysis cannot be made at this time. The intent of this report is rather to introduce the subject and indicate some of the more interesting results that are emerging from our initial explorations into this rather complex and extremely interesting field.

The focus of this report is a series of sensitivity and phenomenological studies each of which illustrates a different aspect of integrated containment analysis. However, to put the analysis into perspective, we start with two sections that serve as introductions to the computational tools which are to be used. Section 2 is a brief review of the phenomena which are important in containment analysis, with particular emphasis on the interfaces, or couplings, between phenomena which have often been created separately in the past. Section 3 is a short summary of the models implemented in the CONTAIN 1.0 computer code, with an emphasis on those models actually exercised in the calculations to follow. In Section 4, we present the results of a series of studies with CONTAIN that examine closely a number of specific synergistic effects. Some of these effects were not predicted in advance, but were "discovered" as a result of performing calculations with an integrated tool. They illustrate how a complex computer code can be a teaching tool for qualitative phenomena, as well as for quantitative predictions. (See the paper "Computational Synergetics" by N. J. Zabusky for more on this interesting subject.[9]) Finally Section 5 is a summary of salient results.

2. MODELING REQUIREMENTS FOR SEVERE ACCIDENT CONTAINMENT ANALYSIS

2.1 Severe Accident Containment Phenomenology

It is useful to think of a reactor containment as a gas-filled geometrical volume, bounded on the inside by the surface of the reactor pressure vessel (RPV) and other parts of the primary system and bounded on the outside by the containment wall (typically a steel-lined concrete shell designed to withstand internal pressures of up to ten atmospheres). During a severe reactor accident, various materials will pass through the inner boundary from the primary system to the containment. These sources may occur at a variety of locations, and may consist of steam, liquid water, hydrogen, molten (or partially molten) core debris, and radioactive gases and aerosols.

Inside the containment are a number of structures and systems which, along with the containment atmosphere, respond to the primary system sources in a variety of ways. In some cases, the loads imposed may be sufficient to fail the outer containment boundary, resulting in the release of radioactive materials. The general goal of severe accident containment analysis is to evaluate the response of containment systems and structures to the primary system sources, predict the subsequent events and loads thereby imposed, and calculate the amount and form of the released radioactive inventory should the containment leak or fail. The radioactive inventory passing through the outer boundary of containment is conventionally known as the "source term."

In this section, we will present an overview of the key events and phenomena which could occur in containment during a severe accident. A detailed treatment of all phenomena will not be attempted here. As we will see in Section 2.2, different aspects of the problem are important for different categories of severe accident questions. Since the focus of this report is source term calculations, not all aspects of containment phenomenology need to be discussed in detail. The purpose of this overview is to provide a perspective for the more detailed discussions of selected phenomena to be presented in the remainder of the paper.

For concreteness, let us follow in rough chronological order the course of events that might occur during a particular accident sequence for a particular type of plant. Later we can discuss variations that might occur for other sequences and plants, but a good starting point is (using the terminology of WASH-1400[10]) the TMLB' sequence in a large dry PWR containment. This sequence is often found in Probabilistic Risk Assessments to be a risk-dominant sequence for large dry PWRs.

The TMLB' sequence is typically initiated by simultaneous loss of off-site and on-site AC electrical power, and is therefore sometimes called a Station Blackout sequence. All active core cooling systems are postulated to be inoperative, so the RPV water begins to boil (due to residual decay heat in the core), relieving steam through a safety relief valve.

From the containment viewpoint, then, the first primary system source is a two-phase jet of superheated steam and water. The large volume of the containment and the effective transfer of heat (through condensation) to the walls and other heat sinks limit the pressure and temperature rise to values well within the design capabilities of the containment.

As the water in the RPV boils away, the core becomes uncovered and the steam sources to containment diminish. More important, however, is the fact that sources characteristic of degraded core accidents begin to appear. As the temperature of the exposed Zircalloy cladding rises in the steam-rich core region, hydrogen is produced by reaction of H_2O with Zr. Shortly thereafter, the integrity of the cladding around the fuel is breached, and gaseous fission products which were trapped within this seal escape into the hydrogen-steam mixture, which is then released through the relief valve into containment. As temperatures continue to increase, other volatile fission products are vaporized, then recondense to form aerosols, which can then be transported via gas flow to the containment. Eventually, most of the primary system water inventory will have boiled away, and temperatures inside the RPV will increase above the melting point of the structural and fuel materials. If recovery of core cooling does not occur in sufficient time, the core will melt and slump to the bottom of the RPV. At this point, it is probably only a matter of time before the vessel fails and additional sources of hydrogen, steam, gaseous fission products, aerosols, and molten debris are injected into the containment.

A number of new types of models for containment analysis are needed at this point. For example, the hydrogen source raises the possibility of combustion events of which there are three basic types: deflagrations, detonations, and diffusion flames.

A deflagration is a self-propagating hydrogen-oxygen recombination event that propagates with a combustion front moving at a velocity below the speed of sound. Its principal effect is to raise the temperature and pressure of the gas (more or less uniformly throughout the volume) due to the heat generated from the exothermic chemical reaction. Deflagrations occur typically at relatively low hydrogen concentrations (typically less than about 14%, but greater than 8% mole fraction). Since the atmosphere is partially transparent to thermal radiation from such events, a fraction of the burn energy is transmitted radiatively to exposed surfaces. Low thermal conductivity materials may achieve very high surface

temperatures in this way, so a second concern is the effect of hydrogen burns on exposed equipment and electrical cables. For example, melting of plastic materials due to hydrogen burns occurred during the TMI-2 incident.

At higher hydrogen concentrations detonations may occur; i.e., the combustion front can propagate at or above the speed of sound, and a shock wave results. Dynamic loading of walls and structures due to detonations can be considerably larger than static loads imposed by heating the atmosphere alone. Most hydrogen burns are expected to occur at concentrations below the value needed for a detonation, but since the transition to detonation can be influenced by obstructions in the flame front propagation path, and by atmospheric turbulence induced by fans or containment sprays, the possibility of detonation in containment cannot be precluded.

The third type of burn is a diffusion flame, which can occur if there is a steady, localized source of hydrogen into an oxygen-rich atmosphere, where size and temperature is limited by diffusion of oxygen into the flame zone. This is the familiar flame of the kitchen stove or candle, and it can occur, for example, above the pressure suppression pool of a BWR. It differs in effect from deflagration principally in that the energy source is highly localized in space but greatly extended in time, so that nearby structures and systems can receive excessive thermal loads.

The appearance of radioactive gases and aerosols from the primary system creates the need for other models not needed for DBA analysis. First, the transport of radioactive gases must be considered. The noble gases are the easiest--all that is needed is an accounting for the heat they generate due to radioactive decay, and, in some cases, an accounting for the accumulation of daughter isotopes and diminishment of the parent inventories, as radioactive decay proceeds.

The non-noble gases may require more attention. In particular, the concentration of soluble gases is affected by absorption onto and desorption from wet surfaces, and sumps. In addition, containment sprays can enhance the removal rate of soluble radioactive gases.

The presence of radioactive aerosols complicates the problem even further. Small aerosol particles can remain suspended for hours or days. Removal from the atmosphere through deposition on surfaces takes place via a number of distinct mechanisms that are, in general, quite sensitive to particle size. However, the particle size can increase through agglomeration. Hence, accurate modeling of suspended radioisotopic inventory in containment requires the analysis of aerosols as a particle size distribution which evolves in time through agglomeration and deposition.

Subsequent events in containment are strongly influenced by the mode of RPV failure, about which there is considerable uncertainty. In particular, there is some question concerning whether the pressure is relieved prior to gross failure and melt release, or whether bottom head failure occurs at high pressure. If the vessel fails at low pressure, the molten debris will fall or pour into the reactor cavity at low velocity. If there is a large water inventory in the cavity at this time, a steam explosion (or fuel-coolant interaction) may then quench some or all of the debris, generate a large steam pressure "spike," and possibly eject the debris/water mixture out of the cavity into the rest of the containment.

If the failure occurs at high pressure (e.g., near the relief valve set point) other scenarios may occur. Of particular concern is the possibility that the melt will be ejected first (perhaps out of a failed instrument penetration), followed by a high velocity gas jet (hydrogen and steam) which could have sufficient velocity to entrain the melt, fragment it into small droplets, and eject it out of the reactor cavity to other parts of the containment.[11] There are many potential effects of such a process, but one of the most serious is the possibility that the unoxidized metals (zirconium and steel) in the melt could react chemically with the oxygen in the atmosphere, and the resulting heat, added to the sensible heat of the melt, could be transferred to the atmosphere gas. The result would be pressure and temperature loads on the containment, which could potentially severely challenge the containment integrity.[12]

Debris that is not quenched or ejected from the cavity will probably form a molten layer on the cavity floor, where ablation of the concrete will take place as soon as it is heated to its melting point. This debris-concrete interaction is important for a number of reasons. First, steam generated from the boiling of water overlying the melt and gases produced by the decomposition of the concrete can contribute to the pressurization of the containment. Slowly, the failure pressure of the structure may be approached, then exceeded. Second, some of these gases may be combustible (e.g., hydrogen and carbon monoxide). These will add to the existing combustible gas inventory, increasing the threat of containment failure from burns. Third, radioactive aerosols can be generated and injected into the containment atmosphere, contributing to the source term, but also affecting the transport and deposition of the aerosols that were released earlier in the accident from the primary system. Finally, if enough time passes, the erosion of the concrete may become very extensive, resulting in penetration of interior walls (leading, for example to ingress of water into a dry cavity) or penetration of the concrete basemat, which could result in a release of fission products into the groundwater beneath the plant.

The principal concern from a risk standpoint, however, is not concrete basemat penetration, but failure or leakage of the containment to the outside atmosphere. It is possible that there are pre-existing leakage paths at the time of accident initiation; these failure-to-isolate sequences can result, for example, from neglecting to close valves or hatches following routine maintenance or testing. Loss of containment integrity can also occur as a result of the temperature or pressure loads imposed by the containment atmosphere. As these loads increase, failure may occur gradually, through a leak which depressurizes the containment slowly, or through a catastrophic failure of a large section of the containment external shell. There are two key processes governing the loading of the containment structure; first, decay heat is removed from the debris by ablating concrete, boiling water, or heating gas: second, heat is removed from the atmosphere by condensation and convection heat transfer to the walls, floors, roof, and internal structures (or heat sinks) of the containment building.

Since the TMLB' sequence is predicated on the absence of any electrical power in a large dry containment, this brief chronology of key containment phenomenology includes no discussion of the effect of Engineered Safety Features (ESFs). In other sequences or plants, these systems can play a key role, not only in reducing pressures and temperatures, but also in reducing the concentration of suspended radionuclides. As an example, we can consider the S_2D sequence, which is characterized by a small break LOCA with a failure of Emergency Core Cooling, but with containment ESFs generally available. Containment sprays will have much the same effect for the severe accident as for the design basis accident--that is, the cold water droplets in intimate contact with the atmospheric gas will cool the gas, condense steam, and reduce the pressure. One difference is that in severe accident situations, superheated (rather than saturated) conditions are expected during much of the accident sequence, so spray models must be able to deal with such conditions. More important, the sprays can have a dramatic effect on the suspended radionuclide concentration, since the falling droplets can collect the aerosol particles as they sweep through the gas, and can also absorb soluble gaseous fission products (e.g., elemental iodine). The contaminated water from these sprays will collect in the containment sumps, along with other fission-product-laden water which has condensed on heat sinks and drained down. The heat from these fission products can be sufficient to boil the water in these sumps, adding to the steam concentration in the atmosphere. Fan coolers can have effects on gas temperature and pressures similar to those of sprays, and there is also a related fission product decontaminating effect (principally through the condensation of steam) though it is generally not as dramatic as for containment sprays. Ice condensers are extremely effective pressure reduction systems that also work on the principle of condensation of steam, in this case onto the surface of ice which is held in large baskets suspended in the

gas flow between the lower plenum and upper containment dome. Again, fission product decontamination occurs primarily as an accompaniment to steam condensation (the aerosols are swept into the ice surface by the mass flux of condensing steam).

This narrative summary is not a complete survey of severe accident phenomenology, but it should provide some perspective concerning the types of calculational tools needed for analysis. But in addition to understanding the relevant phenomena, it is also necessary to define what questions need to be answered, before the requirements of calculational tools can be defined. This is the subject of the next section.

2.2 Categories of Severe Accident Questions

It should be apparent from the description above that severe accident containment phenomena are highly complex, and moreover, a great deal of uncertainty exists concerning them. In delineating the needs of calculational tools, it is important to understand the difference between this type of analysis and more conventional engineering computational work (e.g., for design studies). The severe reactor accident is intrinsically a hypothetical and improbable event. Unlike many other safety engineering disciplines, there is virtually no historical record of vessel failure accidents from which to learn. Consequently a wide range of event sequences and alternative phenomenological scenarios is possible, and the experimental and modeling data base is often extremely limited. Furthermore, the reactor and its containment are extremely complex systems, and their designs vary substantially from one plant to another. In addition, the fuel debris and the materials it contacts are expected to be subject to extreme conditions; consequently, the behavior of even small sub-elements of these complex systems is not easy to predict. Laboratory-scale experiments improve our understanding, but it is difficult to circumvent the fundamental difficulty in severe accident analysis: extrapolation, both in physical scale and system complexity.

These difficulties should be recognized as intrinsic to the problem, and should not diminish the incentive to develop adequate analysis tools. The key question is what is "adequate." To answer this it is necessary first to define what questions the analysis tools are intended for. In this section, we will identify a number of broad categories of severe accident analysis questions, hoping to be complete enough to cover all, or almost all specific types of questions which are currently encountered in reactor safety analysis. These categories are:

1. Containment loading and response.

2. Source term calculations.

3. Probabilistic risk assessment.

4. Equipment survival/accident management analysis.

Below, we will briefly discuss the types of issue encountered in each of these categories, with an emphasis on the implications for modeling approaches. This discussion will then serve as an introduction to subsequent sections in which the focus will be narrowed to include only those types of analysis which can be treated with the CONTAIN code.

Containment Loading and Response

There are a number of scenarios for the mechanism by which containment might fail. Some analyses are concerned with failure due to excessive global pressure or temperature in the containment. These loads could be due to long-term pressurization (resulting from a combination of steam and debris-concrete interaction gases). They could also result from the combustion of hydrogen and/or carbon monoxide superimposed on the existing pressure. This type of analysis does not require detailed information about local conditions inside the containment, and, assuming that mixing processes are sufficient, it is likely that a "control volume" or "lumped parameter" treatment will be adequate. In such an analysis, the containment atmosphere is divided into a relatively small number of cells whose boundaries correspond to real physical partitions (walls, floors, etc.) in the building. These cells are considered to be well-mixed repositories of gas mass and energy, and flow between cells occurs through flow paths which are typically modeled with orifice flow correlations. Since combustion of gases is of concern, the fluid model must track a number of different gases as well as steam (which must be treated as a two-phase material). There must also be a model for combustion which is based on the global concentrations of the various gases, and which predicts the energy and duration of the burn. Since decay heating due to suspended fission products is an important contributor to pressurization, some way of modeling a volumetric heat source to the atmosphere is also needed. The power of this heat source changes in time due to the change in radioisotopic composition of the suspended inventory, and because the aerosols and gaseous fission products are removed from the atmosphere by a variety of mechanisms. Some way of modeling this power history is needed, either with a mechanistic aerosol behavior model, or by more *ad hoc* methods. Clearly, models are also needed for the internal sources of mass and energy, e.g., gas from debris-concrete interactions and steam from boiling sumps. The debris-concrete model also should provide for radiant heat transfer from the surface of the molten pool to the atmosphere or internal structures.

These sources of pressure are counteracted by heat and mass transfer to the heat sinks. Condensation heat transfer is the dominant passive heat transfer process, and a model for it must

deal with a variety of thermodynamic conditions in containment (e.g., superheated conditions). Because the heat conduction process is highly nonlinear, provision must be made for transient heat conduction into a number of heat sink structures of different compositions and sizes. One dimensional heat conduction modeling is usually considered sufficient. This model must also take account of the heating due to fission products deposited on the structure surfaces. Finally, the effects of engineered safety features on global containment pressure and temperature and on radionuclide location must be modeled.

All of these features are compatible with a lumped parameter code. However, there are some containment loading questions which require a more detailed analysis of local conditions in the containment. For example, if the mixing forces are not sufficient, it is possible for there to be substantial variations in combustible gas concentration throughout the containment atmosphere. Of particular concern is the possibility of local hydrogen concentrations exceeding the criterion for detonation, even though, based on global concentration, one would predict only a deflagration. Such a problem would require a multi-dimensional analysis of gas flow. Similarly, local sources of heat (e.g., a diffusion flame at the location of a hydrogen source) could cause leakage due to intense heating of a seal or penetration, which would not be predicted on the basis of globally averaged conditions.

Another distinct analysis area is the prediction of containment performance under these pressure and temperature loadings. In particular, it is important to be able to calculate the maximum pressure the containment can support without loss of function (e.g., leakage or catastrophic failure). For such questions, attention must be focused on the deformation of the outer shell of the containment at pressures well in excess of the design pressure. Except when impact of missiles or the effects of detonations are being considered, the loads increase on time scales which are long compared to characteristic response times for the containment structure, so that only static loads usually need to be considered. However, prediction of the containment performance is complicated by non-uniformities of the structural shell, e.g., electrical penetrations and hatches, which tend to concentrate stresses and are often the initial failure points. Another concern is failure of seals in the vicinity of penetrations without gross failure of the structure. Degradation of seal performance is most often considered to be a result of high pressure, but excessive temperatures in the vicinity of the seal is also a potential cause. The result is slow leakage as opposed to massive failure.

The prediction of containment performance under severe accident conditions has generally been accomplished with specialized calculational tools which treat the containment loads as boundary conditions. Neglecting feedback between

containment loading and containment performance is no doubt an acceptable assumption for the catastrophic failure scenario, since the expansion of the containment volume prior to failure is negligible for the loading analysis and, moreover, the failure itself would occur on time scales very short compared to characteristic times for thermal-hydraulic response. For the slow leakage scenario, however, the situation is not so simple. At a minimum, the feedback between containment pressure and leakage must be included in the calculation. One approach is to incorporate parametric models for effective leak path area as a function of pressure or temperature in the containment loading codes. Such models could be developed from detailed analysis of seal response performed independently of the loading analysis. However, additional complications arise when the effect of aerosols on leak paths is considered, since deposited aerosols may actually change the flow characteristics of the leak path. The extent to which such aerosol deposits could quantitatively affect the leak rate is uncertain, but it is likely that the aerosol particle size distribution exiting the leak path would be affected (a phenomenon of more importance to source term issues than containment loading).

Source Term Calculations

Here, the goal is to predict the released inventory of radioactive material in the event of containment failure or leakage. As in the case of containment loading calculations, it is necessary to predict the global thermodynamic conditions in the atmosphere, but there are other requirements as well. Because of their importance to off-site consequence analysis, it is important to provide more detail about the radioisotopes than would be necessary if only loading were of concern. Quantitative prediction of the radioisotope release to the environment (the source term) requires detailed modeling of the aerosol particle size distribution in containment and the radioisotopic composition of each particle size class (though it is common to consolidate the hundreds of possible isotopes into a smaller number of groups). Again, control volume treatments for aerosol behavior are adequate, if it can be assumed that adequate mixing forces exist.

The source term to the environment is essentially determined by the concentration of suspended radionuclides at the time of containment failure and/or by the history of the suspended concentration over the period during which leakage from the containment occurs. The aerosol component of this concentration may vary over five or more orders of magnitude during the course of the accident sequence (several days). In considering the accuracy requirements for integrated containment models, it is necessary to consider this fact in conjunction with another fact: early containment failures are expected to be much less probable than late failures, so the difference in source terms between early and late failures may

be compensated by the difference in probabilities. Moreover, considerable uncertainty exists concerning these probabilities. These considerations result in one of the most difficult challenges to integrated containment analysis: predicting the aerosol and radionuclide concentration with reasonable accuracy at both the low and the high end of the concentration range--that is, at both early and late times.

Models for engineered safety features must be considerably more sophisticated for source term calculations, because the decontaminating effect of the sprays, fan coolers, pressure suppression pools, and ice condensers must be modeled. Some treatments separate the analysis of thermal-hydraulic and decontamination effects of ESFs completely, greatly simplifying the analysis, but there is evidence that a coupled analysis is needed for some cases (e.g., see Section 4.4).

Probabilistic Risk Assessment

The principal difference for this type of application is that a large number of calculations are typically required for any given study, and that accuracy requirements are considerably relaxed, since uncertainty is inherent in the analysis method. The emphasis for modeling therefore becomes speed, and also user access to uncertain parameters, so that estimates of uncertainties in risk can be made. It is also more important to be able to perform complete calculations involving the primary system, containment, and ex-plant consequences in the same computational run, so that large numbers of calculations can be performed without close monitoring of interfaces by the analyst. These are some of the goals of NRC's MELCOR code,[8] which also has specialized features allowing automatic statistical analyses of the results of large numbers of runs. More detailed models can be used to benchmark the simpler treatments of the PRA code.

Equipment Survival/Accident Management Analysis

The principal concern for this type of problem is the successful performance of equipment in containment for control, instrumentation and accident mitigation. In the past, a convenient assumption for risk studies has been either that there is no operator intervention, or that the operator actions assumed to occur are unrelated to conditions or perceived conditions in the reactor or the containment. More recently, this simplification has been questioned, and more realistic analyses are needed of what information might be available to the operator during an accident, what actions might be possible, and what effect these actions might have. One reason such analyses are difficult is that human factors must be taken into account. Of more interest to the present discussion, however, is the effect of extreme conditions on instruments, cables, and control devices. The principal difference between this problem and the global containment loading problem above is that the

conditions in the vicinity of the equipment may not be properly approximated by globally averaged conditions. It is unclear how fine a nodalization is needed for such analyses, and what the appropriate calculational technique should be.

For the remainder of this report, we will be narrowing our focus of attention to deal only with those types of analysis for which the CONTAIN code was developed. These are primarily the containment loading and source term problems. In particular, the broad range of phenomena treated (including aerosol and fission product behavior as well as thermal-hydraulics) make CONTAIN particularly suited to best-estimate source term calculations. (By "best-estimate" code, we mean that state-of-the-art models are used and that there is no intentional bias towards "conservative" results.) However, in its publicly released configuration (version 1.0), it is a lumped parameter code, and the explicit numerical solution technique used is not well suited to nodalization of open containment volumes into many small calculational cells.* Hence, analysis of multi-dimensional effects are not easily performed, and when these effects are a dominant part of the problem, the use of CONTAIN 1.0 is not advisable. Fortunately, there is a broad class of analysis problems for which these assumptions are acceptable.

---

* Developmental versions of (e.g., 1.04 and beyond) CONTAIN have relaxed these restrictions.

3. THE CONTAIN CODE FOR SEVERE ACCIDENT CONTAINMENT ANALYSIS: SURVEY OF MODELS

3.1 General Approach--Integrated Analysis

It should be clear from the preceding discussions that the range of phenomena of importance to severe accident containment analysis is very broad, and that, although the state of the art of modeling these phenomena is evolving rapidly, there are still many areas for which adequate models do not exist, or for which existing models remain unproven. A full discussion of the status and needs of analytical methods for all of the types of questions described in Section 2.2 would be beyond the scope of this report. Therefore, we will now narrow the focus of the discussion to a subset of these questions, namely, the source term and containment loads issues which can be addressed with a code utilizing the well-mixed atmosphere assumption in a network of one to, perhaps, twenty control volumes. In particular, we will consider a series of calculational studies performed with the CONTAIN 1.0 computer code.

CONTAIN is unique among containment analysis tools in that it simultaneously models thermal-hydraulics, aerosol behavior, and fission product decay, heating and transport. Because of the breadth of range of these phenomena, it is sometimes necessary to use simplifications in the modeling (e.g., the well-mixed assumption). However, CONTAIN is the only tool available to analyze some of the synergistic effects which can occur when feedback loops among many disparate phenomena are taken into account. Figure 3-1 indicates some of the couplings among these phenomena. In some cases, analysis with CONTAIN indicates that the coupling effects are not important, and that the use of separate-effects codes linked together through one-way data transfers is justified. In other cases, it is found that the feedback effects are significant, and that it is not possible to obtain accurate results without an integrated analysis approach. Examples of both types of findings will be given in Section 4.

The purpose of the present section is not to give a complete introduction to the CONTAIN computer code, but only to provide enough information that the results to be presented in Section 4 will be meaningful to the reader who is unfamiliar with the code. Mathematical details will be given only when needed to clarify the discussion of the calculations to follow, and only concerning those features of the code which were activated for those calculations (e. g., models for Liquid Metal Reactors will not be discussed). A more complete description of the code's features and models can be found in the User's Manual.[1]

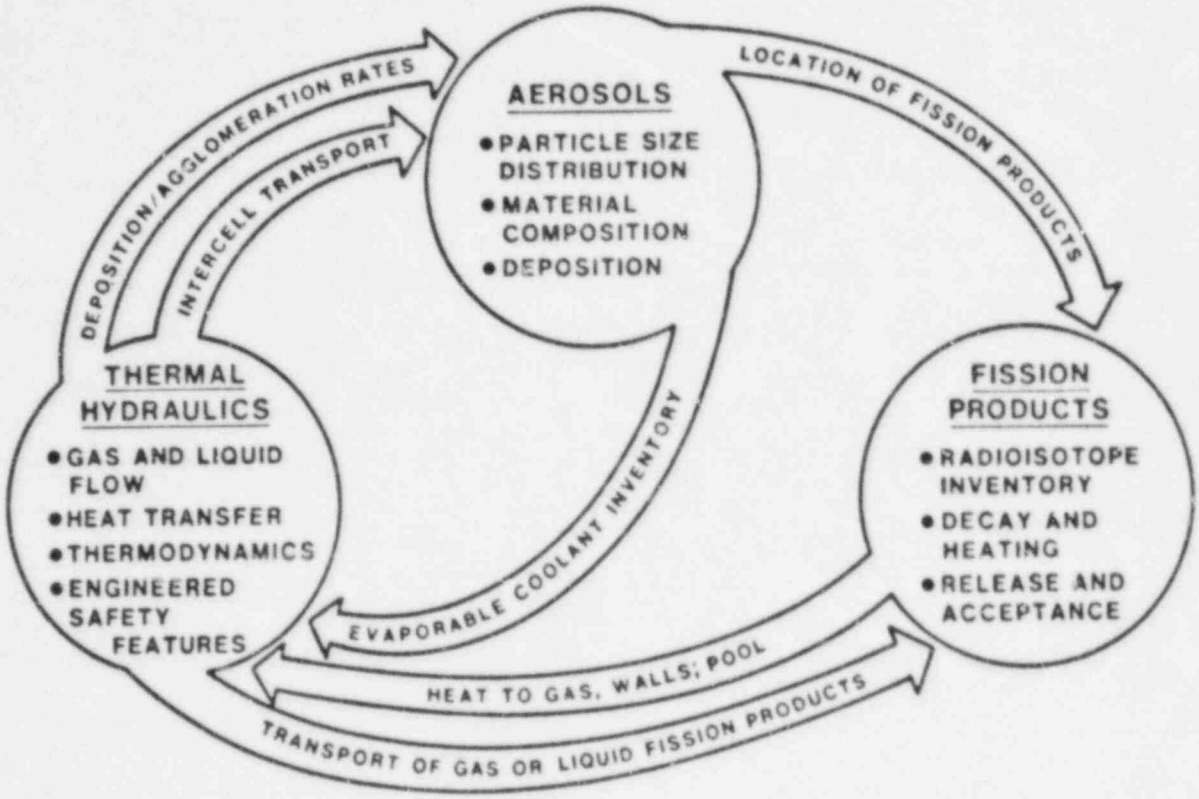

Figure 3-1. Potentially important coupling effects among aerosol behavior, thermal-hydraulics, and fission product decay, heating and transport.

3.2 Atmosphere Thermodynamics and Inter-cell Flow

Figure 3-2 shows a typical reactor containment building reduced to a network of interconnected compartments or "cells". The cells represent the internal subdivisions of the reactor containment building, and one of the principal modeling assumptions in CONTAIN is that gases and aerosols are "well-mixed" within each of the cells. Because the numerical solution technique in CONTAIN 1.0 is explicit, each calculational cell is usually chosen to correspond to a portion of the containment volume which is relatively distinctly bounded by physical partitions (e.g., walls, floors). (Future versions of CONTAIN, using implicit solution techniques, will not have this restriction.) The cells communicate with each other by means of gas flow resulting from pressure differences and/or heat flow (thermal conduction through intervening structures). The environment outside of the containment building can be considered as one of the cells, so that a radiological release to the environment appears as a flow into that cell.

The general inter-compartment flow equation is a simple temporal acceleration equation, including the effect of the flow path as a friction effect.

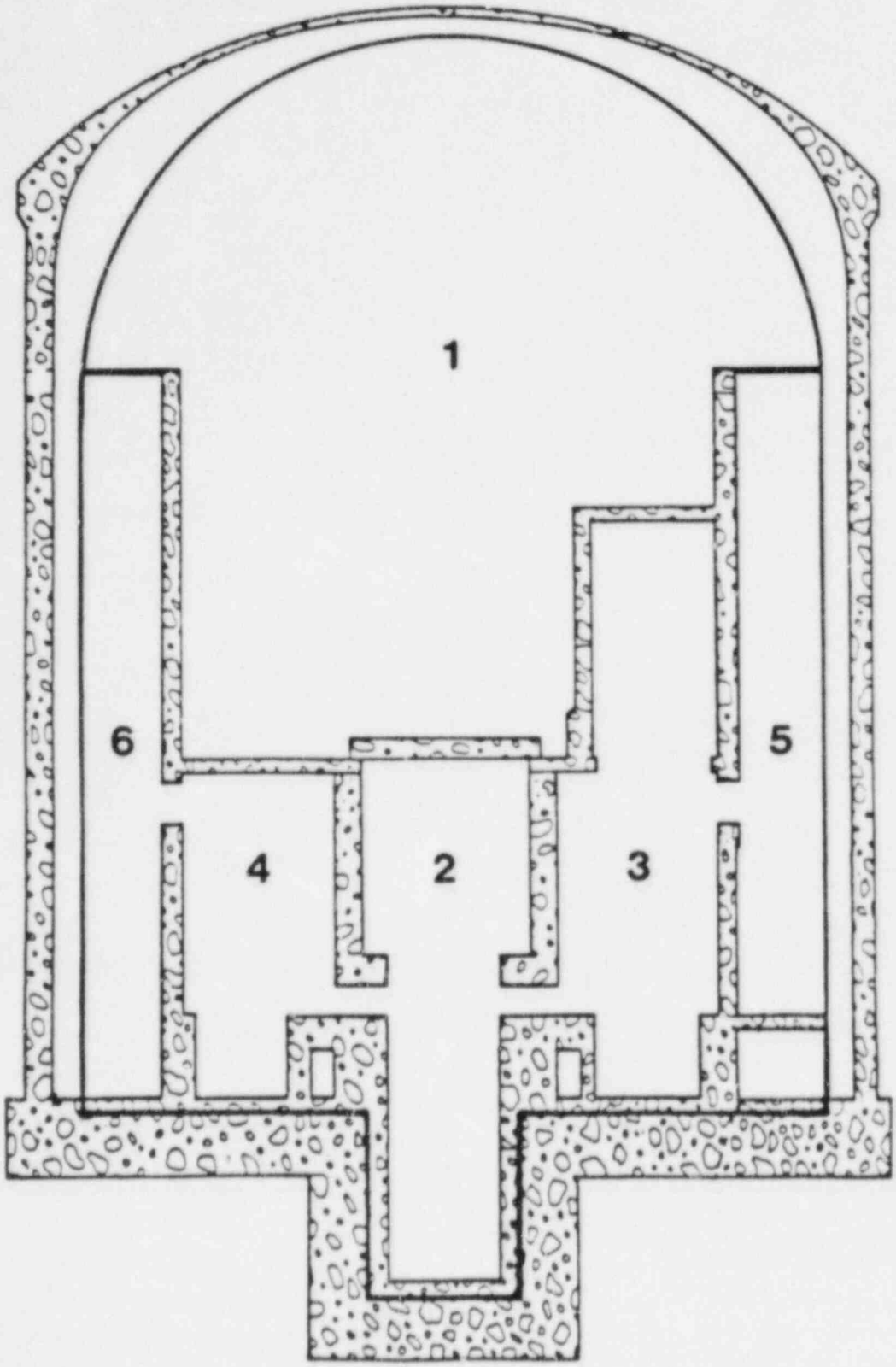

Figure 3-2. Reactor containment building reduced to a configuration of interconnected compartments.

$$\frac{dW_{ij}}{dt} = \left((\Delta P_{ij} - \frac{|W_{ij}|W_{ij}}{2\rho C^2 A_{ij}^2}) \right) \frac{A_{ij}}{L_{ij}} \qquad (3.1)$$

where W_{ij} is the mass flow rate (kg/sec) between cells i and j, P_{ij} is the pressure difference between them, A_{ij} is the flow path area, ρ is the gas density, L_{ij} is the effective length of the flow path and C is the discharge coefficient.[13] For many calculations, the effect of the inertia of the material in the flow path is negligible, so the left side of Eq. (3.1) can be set to zero. This gives the quasi-steady flow option, which is a simpler equation to solve.

The atmosphere not only is a repository for the masses of steam, water, and noncondensible gases, but it also exchanges heat with a number of other components in contact with it. In particular, heat sinks typically absorb heat from the atmosphere through condensation and convective heat transfer. Also, heat from the decay of gaseous or aerosol-borne fission products is added to the gas mixture. Finally, combustion of hydrogen adds additional heat.

An arbitrary number of heat sink structures within each compartment can be treated, and each structure can be composed of an arbitrary combination of layers of different materials. The floors, walls, roof, as well as the surfaces of enclosed objects such as pumps or other machinery, are approximated in the input by choosing shapes that most closely resemble the objects to be modeled. Slabs, hemispheres, and cylinders are used as a standard set of shapes from which the choice can be made, and the heat conduction equation is solved in one dimension for the appropriate geometry. The heat released by fission products deposited on surfaces by condensation or aerosol deposition is taken into account in the heat conduction calculation.

Under most circumstances, the dominant mechanism for heat transfer is condensation of water on the heat sinks. Because CONTAIN must deal with a broader range of conditions than DBA codes, its model for condensation and evaporation mass and heat transfer is more general and mechanistic than what is usually found in such codes. A boundary layer in the atmosphere contributes the principal thermal resistance under condensing conditions. This is because the coolant vapor must diffuse through a region of enhanced noncondensible concentration and depleted condensible vapor concentration. This resistance is considered to be in series with smaller resistances of a condensate film and a layer of oxide or paint at the structure surface. Condensation and convection (i.e., conduction through the turbulent boundary layer) are treated as occurring simultaneously. To obtain a condensation rate, it is necessary to have a mass transfer coefficient. Since appropriate correlations for such coefficients are not

generally available, use is made of a mass transfer/heat transfer analogy which provides a mass transfer coefficient in terms of a Nusselt number (dimensionless heat transfer coefficient). The Nusselt number is then calculated through a variety of correlations which depend on wall and atmosphere conditions, and the type, dimensions and orientation of the structure. This method of calculating condensation heat and mass transfer is similar to the one outlined in Reference 14.

The condensate film which accumulates on the cold surfaces plays a minor role in the heat transfer process, but it can be relatively important in accounting for water inventory in the overall containment calculation. To account for it CONTAIN calculates a film thickness which varies in time according to a simple model for the accumulated condensate mass on each exposed surface. When the thickness builds up beyond a specified amount, any additional condensate is assumed to flow off to the containment sump.

Hydrogen burns are assumed to occur whenever the levels of oxygen, hydrogen, and water vapor are within certain concentration ranges. In particular, if the oxygen mole fraction exceeds 5%, the hydrogen mole fraction exceeds 8%, and the steam mole fraction is less than 55%, a hydrogen burn ignition is assumed to occur. These ignition criteria are taken from the HECTR code for hydrogen combustion analyses.[15] A number of other burn characteristics are also treated with HECTR correlations (which are experimentally based). These include the degree of completeness, burn duration,, and criteria for propagating from one cell to the next. In CONTAIN, the burn is always treated as deflagration, and all of the heat released is deposited in the atmosphere.

State variables (such as temperature, pressure, and enthalpy) are calculated according to equilibrium thermodynamics. The pressure of the noncondensible gases and the condensible vapor under superheated conditions is given by the ideal gas relation. Under saturated conditions the pressure of the condensible gas is equal to the saturation vapor pressure. Analytic expressions for the saturation vapor pressure and for the specific enthalpies of the noncondensible and condensible gases are stored internally.

3.3 Aerosol Behavior (MAEROS)

One of the principal purposes of CONTAIN is to characterize the radiological source term in the event of containment failure. Aerosols are one of the principal mechanisms for transport of radioactive materials within the containment and to the external environment, should containment failure occur. The MAEROS module in CONTAIN allows for a multi-sectional, multi-component treatment of aerosols.[16] This means that the particle size distribution is discrete ("multi-sectional") and can therefore have an arbitrary shape, and that each particle

size class can have a different composition among several component materials ("multi-component"). One of the unique features of CONTAIN is that condensation/evaporation of coolant onto aerosols is modeled in a manner consistent with the atmosphere-thermodynamics calculation. Moreover, these processes can occur simultaneously with condensation or evaporation from heat sinks.

The evolution of the aerosol particle size distribution proceeds under the influence of four general processes:

(a) agglomeration (or coagulation), whereby two particles collide and form a larger particle

(b) deposition onto surfaces

(c) size change through condensation or evaporation of water

(d) sources of aerosols.

Figure 3-3 illustrates the effect each of these four processes has on a typical particle size distribution.

The evolution of the aerosol particle size distribution is governed by a complex integro-differential equation. Gelbard and Seinfeld[17] have developed a method of discretizing this equation into a form which can be solved numerically. The full range of particle diameters is divided into m "sections", and the equations are integrated over each of these sections, resulting in a set of "sectional equations". If the subdivision of the particle size range is chosen such that each section corresponds to particle masses which are at least twice the mass of the previous size class, these equations can be written:

$$\frac{dQ_\ell^k}{dt} = \sum_{i=1}^{\ell-1} \{\beta_{i\ell}^{(1)} Q_i^k Q_\ell + \beta_{i\ell}^{(2)} Q_i^k Q_{\ell-1} + \beta_{i\ell}^{(3)} Q_{\ell-1}^k Q_i\}$$

$$- \sum_{i=1}^{m} \beta_{i\ell}^{(4)} Q_\ell^k Q_i + S_\ell^k - R_\ell^k + G_\ell^k \qquad (3.2)$$

Here, Q_ℓ^k is the mass of material k in size section ℓ, and

$$Q_i = \sum_k Q_i^k \, . \qquad (3.3)$$

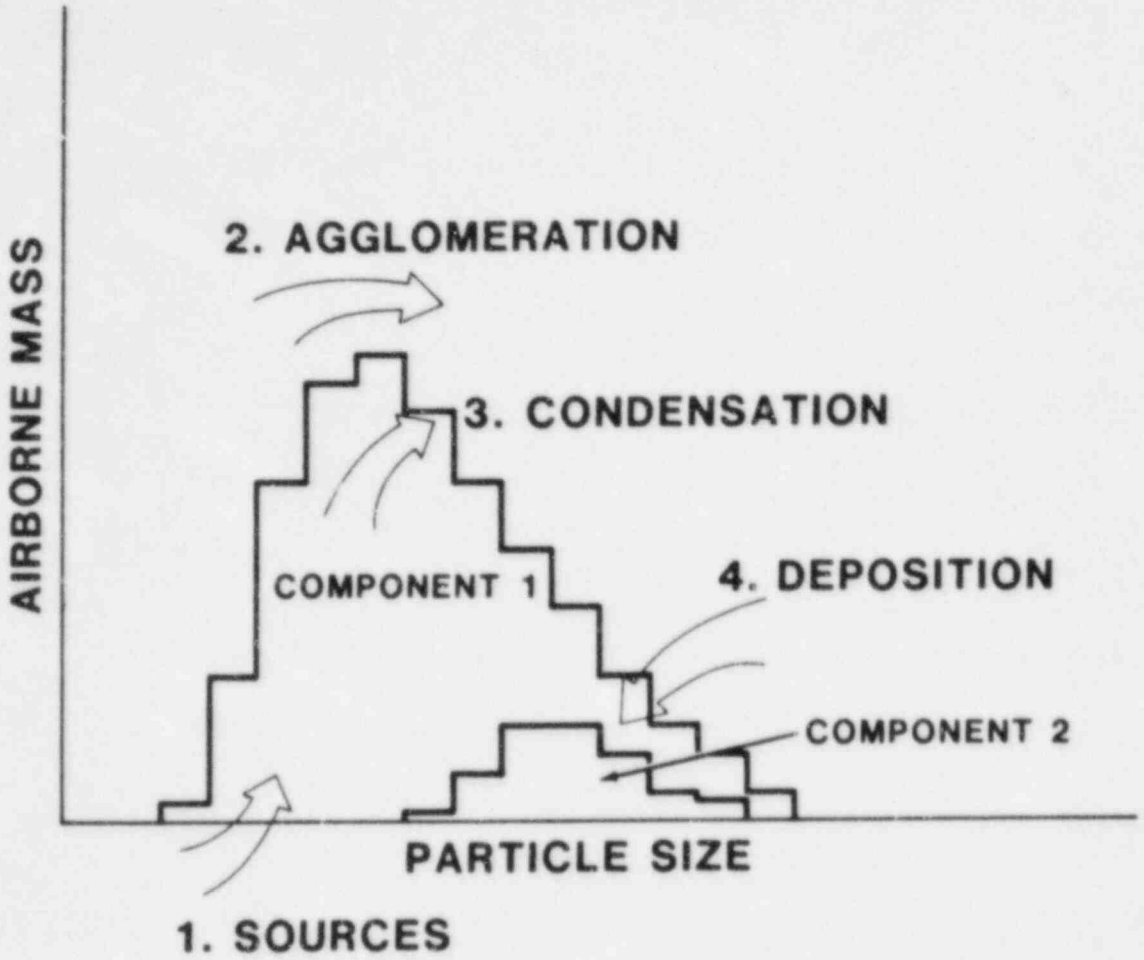

Figure 3-3. Schematic illustration of the typical effects of the four aerosol processes discussed in the text. (1) the source shown adds small particles; (2) agglomeration increases the population of larger particles at the expense of smaller ones; (3) condensation accomplishes the same horizontal effect on the distribution, but it also adds mass at the same time; (4) deposition processes remove mass, particularly the larger particles (if gravitational effects dominate).

Each term in Equation (3.2) represents a distinct mechanism for changes in mass of material k in a particular size class. The first three represent growth through agglomeration. The first involves addition of mass from smaller particles without enough addition to move the agglomerated particle into the next higher size class. The next two terms account for movement of particles into the ℓ size class from the next lower one through agglomeration with a still smaller particle. The fourth term represents losses from the ℓ class resulting from movement into the next higher one due to agglomeration with other particles.

The B_{ij} are called sectional coefficients, and they can be evaluated by using a variety of formulas which incorporate the effects of the different physical processes operating. These include gravitational agglomeration (a larger particle overtakes a smaller one as they both fall) and agglomeration through diffusion (either Brownian or turbulent).

The S_ℓ^k, R_ℓ^k and G_ℓ^k are mass change rates from sources, deposition, and growth, respectively. In CONTAIN 1.0, sources appear either through intercell flow or via user-specified input tables. (Future versions of CONTAIN will include sources from release processes such as debris-concrete interaction phenomena.)

Deposition occurs through a number of processes, including gravitational settling, diffusion to surfaces, thermophoresis (a Brownian process causing migration of particles towards higher temperatures), and diffusiophoresis (deposition induced by condensation of water vapor onto surfaces). For some ESF decontamination calculations, a fifth process, inertial impaction, is included. Again, these processes are accounted for in CONTAIN through formulas for the R_ℓ^k in terms of various state variables. These expressions are given in Reference 16, except for impaction, which is given in Reference 18.

The condensation term, G_ℓ^k used in CONTAIN is taken from Reference 19. Both condensation and evaporation may take place on aerosols, and either process can occur simultaneously with condensation or evaporation from heat sink surfaces. Condensation on and evaporation from aerosols is one of the principal couplings between thermal-hydraulics and aerosol behavior (see Figure 3-1).

These equations describe the evolution of the particle size distribution within each computational cell. Each cell has its own distribution, and the aerosols are carried from one cell to the next by the gas flow (assuming zero slip). As we will see below, the aerosols may be associated with fission products, resulting in decay heating of the gas, heat sinks or water pools, depending on what aerosol transport or deposition processes have taken place.

3.4 Fission Product Transport, Heating and Decay

The composition of the fission-product inventory in the reactor core at the time of scram can be determined with reasonable accuracy through a knowledge of the power history and the application of any one of several well-documented "burn-up" codes. During a core-melt accident, however, the physical disposition of the radioisotopes is highly uncertain. Because CONTAIN does not analyze in-vessel phenomena, it

depends on inputs from the user or other codes to specify the initial locations and time-dependent sources of the fission product inventory. From that point on, CONTAIN models three aspects of fission product behavior: transport (which determines the locations), decay (which determines inventories of each isotope), and heating (which couples back to the thermal-hydraulic behavior).

To determine the location of the radioisotopes being studied, CONTAIN tracks them as if they were physically attached to a "host" material or structure. Each fission product can be "released" from one host and "accepted" by another at rates which are specified by the user.

The reason for this flexible system of fission product transport is that the masses of fission products involved are usually very small compared to the masses of the hosts, whose transport is modeled in the thermal-hydraulics analysis. Thus, the movement of the radioactive material is controlled by the movement of the nonradioactive materials, which is modeled mechanistically. The principal uncertainty is in the physical and chemical forms of the fission products and their affinities for the various host materials. The experimental and modeling data base for the release of fission products from fuel, and for subsequent chemical changes in the various isotopes, is currently inadequate to provide reliable mechanistic models for a code like CONTAIN. The release-and-acceptance formalism is therefore used to allow the analyst to evaluate the consequences of different modeling assumptions.

The decay of each radioisotope is modeled according to user-specified decay chains, half-lives, and decay powers. This accomplishes two things: first, the daughter products may be a different element, and may be released and accepted among hosts at different rates; second, the heat of the radioactive decay is deposited at the location of the host material. (This is a simplifying assumption.) However, it is usually undesirable to specify in detail all of the radioisotopes that would contribute to decay heating, since this would require a large amount of input. Normally, only a selected subset of radioisotopes is of interest for health physics reasons, and it is these radioisotopes that are typically specified by species or, if desired, by fission product groups. The remaining decay heat from the reactor fuel can be handled in a different way. A standard decay power curve is used to calculate total decay power as a function of time since shutdown. The power associated with the specified individual fission products is subtracted from this total power, and the remaining power is then deposited in a number of locations (coolant pool, atmosphere, etc.) according to fractions specified in the user input. This greatly simplifies many calculations.

3.5 Lower Cell Models

Each cell in CONTAIN is divided, for computational purposes, into an upper cell, dealing with the atmosphere and solid structures in thermal contact with it, and an (optional) lower-cell, dealing with liquids and fuel debris on the floor. Core-melt accident scenarios generally lead to a breach of the primary system and the development of some kind of "bed" or "pool" of core debris and coolant in the bottom of the reactor cavity. Ablation of the concrete floor and walls threaten basemat penetration while simultaneously producing water vapor, other gases, and aerosols, all of which carry fission products, heat, and reaction products into the upper containment atmosphere. The lower-cell model deals with these phenomena. In some cells, not all of these processes will occur; for example, the lower-cell system may serve simply as a sump for collecting coolant.

The lower-cell model is a system of layers of different materials which communicate with each other primarily through heat conduction. These layers may include a concrete layer, intermediate layers, and a coolant pool layer. The intermediate layers allow for further breakdown into other layers such as molten metal and oxide by-products of core/concrete interactions. Because a high level of phenomenological uncertainty prevails concerning the configuration of debris, coolant, and other materials, CONTAIN allows the user to override the default configuration and analyze other systems of layers.

The principal interaction among the various layers is heat transfer. Generally, each layer is treated as a single lumped thermal mass, with heat-transfer coefficients between layers that are selected from a variety of correlations (or are supplied through input). Two layers, however, are treated in special ways. First, the concrete layer is separately nodalized, and one-dimensional transient heat conduction is modeled. The concrete layer can also be ablated if the temperature of the overlying material is sufficiently high. Second, the pool layer is unique in that it can boil if the temperature exceeds the pressure-dependent boiling temperature. Coolant can also evaporate from or condense onto the pool surface.

As heat flows from the core debris into the concrete, temperatures rise and the concrete suffers thermal ablation. The material becomes molten and begins to decompose. The vaporized and liquefied materials mix with the core debris where further chemical reactions take place. The chemical reactions generate hydrogen, carbon monoxide, and other products. The CORCON code, a detailed mechanistic code, models these processes.[20] CONTAIN has its own one-dimensional model for making these calculations, but it draws heavily from the CORCON code (which is two-dimensional). Because CONTAIN's treatment is relatively simplistic, any problem in which core/concrete interactions are critical should probably use CORCON-Mod2, or an equivalent phenomenological code, for this part of the analysis. Many of the calculations described in Section 4 make use of CORCON via mass and energy tables.

3.6 Engineered Safety Features

Virtually all nuclear power plants include Engineered Safety Features (ESFs), designed to reduce pressure, temperature, and fission-product concentrations in order to assure containment integrity and limit fission product release should leakage occur. CONTAIN 1.0 has detailed models for three major ESFs: containment sprays, fan coolers, and ice condensers. Associated with these models is a framework for constructing systems that provide sources and sinks for the liquids connected with the ESFs. The components available for such systems include tanks, pumps, orifices, pipes, valves, and heat exchangers, as well as user-specified external liquid sources.

The ESF models are generally mechanistic in nature so that their range of applicability is greater than would be possible with more empirical models. Because of the integrated treatment of fission products, aerosols, and thermal-hydraulics, it is possible to analyze the redistribution of fission products and aerosols effected by the ESFs.

The containment spray system represents a nearly universal safety feature in PWR plants. This system provides a high-pressure, water spray to the containment atmosphere. Heat transfer to the droplets and subsequent condensation of atmospheric steam provide a rapid reduction in temperature, pressure, and fission product concentrations. The sprayed water, as well as much of the condensate, collects in a sump at the bottom of the containment. Generally, the initial spray source is the refueling-water-storage tank. When that source is exhausted, water is pumped from the sump, through a heat exchanger, and back to the spray nozzles. A model has been developed for CONTAIN that determines the heat transfer between the droplets and atmosphere and the resulting evaporation from or condensation onto the droplets.

The containment spray model allows for the removal of fission products and aerosols as a result of the sprays. At present the model allows for elemental iodine removal from the containment atmosphere, as well as spray washout of airborne aerosols. Models are included for diffusional deposition, thermophoresis, diffusiophoresis, inertial impaction, and interception. These mechanisms and their relative importance are discussed further in Section 4.4.

Fan coolers are included in dry PWR containments to provide non-emergency cooling and to augment the heat removal capabilities of the water sprays in the event of a LOCA. These coolers consist of banks of finned, service-water-cooled coils across which large-capacity fans circulate the containment atmosphere. CONTAIN has two fan cooler models, available at the user's option, that provide reasonably mechanistic treatments of fan cooler performance. The first model is similar to that developed for the MARCH code.[6] It is simple

and fast and reproduces the cooling capacity of actual plant equipment under normal conditions adequately. It can be used whenever the effects of non-condensible gases or superheated conditions are expected to be relatively minor.

A second, more mechanistic fan-cooler model is based on the condensation heat transfer formulations used throughout the CONTAIN code. The model calculates condensation and convective heat transfer coefficients which depend on the cell atmospheric conditions. This model can treat the effects of non-condensible gases and superheated conditions. However, it requires a more detailed knowledge of fan-cooler characteristics than the simpler model described above.

Because of the relatively cool surfaces and high condensation rates provided by fan coolers, substantial amounts of aerosol fission products will be removed from the atmosphere. This process is included in the more detailed CONTAIN fan cooler model.

Ice condensers are used in some PWR containment systems to condense steam released from the primary system during a LOCA. In so doing they reduce containment pressure and temperature. The CONTAIN ice-condenser model uses the atmospheric flow model to determine the dynamic and thermodynamic condition of the air-steam mixture through the ice compartment. Flow through the ice condenser can be initiated by pressure-differential criteria specified by the user. Heat transfer to and condensation on the ice structures is treated by the forced convection/condensation wall-heat-transfer model that is used throughout CONTAIN. As with the other ESFs discussed above, the code models the effects of aerosol removal by the ice condenser.

3.7 Modeling Limitations in CONTAIN 1.0

The preceding brief description of the CONTAIN code has focused on the capabilities and features of the models. It is also important to be aware of the limitations of those models, so that the significance of the calculations for any particular application can be properly understood. There are many reasons for such limitations. Clearly, the modeling system is very complex, and there are limitations of resources, not only computational time and memory, but also code development time. Hence an element of judgment is required concerning what simplifications to make, and what phenomena to neglect. Moreover, perceptions change about what is important, often because of understanding gained from experimental research. Thus, model limitations result from a combination of inadequacies in the experimental data base, the unavoidable time lag required to develop and implement models incorporating the latest phenomenological understanding, and simple pragmatic considerations of the limitations of human and computer resources.

An issue which is closely related to model limitations is code validation. On one hand, successful validation (i.e., comparison of code predictions against experimental results) can allay doubts which stem from simplifications inherent in the models. On the other hand, even the most detailed analytic methods must be considered somewhat speculative in the absence of experimental validation. Considerable effort has been expended in the validation of CONTAIN, particularly through blind code prediction exercises.[21,22] However, there are still numerous aspects of the code for which validation is inadequate, partly because appropriate experimental data is often lacking. This problem is not unique to CONTAIN, which is probably better validated than most codes used in severe accident analysis. However, the need for additional validation must be kept in mind in evaluating the significance of the predictions of CONTAIN.

In the remainder of this section, we will briefly identify a number of key simplifications and assumptions which are made in CONTAIN, so that the results to be presented in Section 4 can be understood in their proper context. We will discuss these limitations in two categories, though the distinction between them is not precise. The first category involves simplifying assumptions or other sources of uncertainty in existing models. The second involves the actual neglect of phenomena. The discussions will be very brief, since they are intended only to be warning flags, not assessments of the importance of the limitations for any specific application.

Simplifying Assumptions and Uncertainties in the Models

We have already referred, in Section 2.2, to the importance of the well-mixed atmosphere assumption. Clearly, any situation in which spatial inhomogeneities within a single calculational cell are important cannot be adequately modeled with a lumped parameter code in which the cells are constrained to correspond more or less with compartments having real physical boundaries. Such a limitation does exist in the released version (1.0) of the code because the explicit numerical solver used suffers from severe stiffness problems when cells are connected by large-area flow paths. An implicit solver for CONTAIN is under development, which will allow a finer nodalization of the atmosphere, but it is not clear whether or not some gas transport problems will require a true finite difference treatment of the hydrodynamic partial differential equations.

There are other limitations in the flow models as well. For example, intercell transport of aerosols or spray droplets by diffusion or settling through flow paths is not treated. These two limitations are related to the explicit solution technique, since any practical calculation will generally have flow path areas which are small compared to the cross sectional area of any cell. Similarly, buoyant forces are generally neglected for intercell gas transport because the explicit

solver cannot handle them. Thus, natural convection processes cannot be modeled in CONTAIN until the implicit solver is implemented.

Another difficulty is that the treatment of blowdown jets assumes spatially homogeneous condensation on aerosols, neglecting the localized nature of such plumes or jets, and probably underestimating the amount of liquid that falls out of the jet immediately. (As discussed in Section 4.5, however, this error is probably transitory.)

The hydrogen burn model is based on correlations developed from experiments, and it can play a key role for many accident scenarios. However, there are several parts of the parameter space for which the existing data base is quite sparse, and the correlations somewhat questionable. This is true, for example, of the criteria for burn initiation, burn time, and burn completeness, under conditions of relatively high steam concentration. Other important deficiencies in the combustion models are the absence of a model for burning carbon monoxide and the neglect of thermal radiation in the calculation of heat transfer from the gas to the heat sinks. (These problems will be remedied in the near future.)

The decay energy of radioisotopes is also treated in a simple way; generally the host material receives all the decay heat. In addition, heat from radioisotopes deposited on heat sinks goes entirely into the first heat conduction node of the structure. This treatment ignores the ability of gamma radiation to penetrate materials (gases, liquids in the pool, and the structural solids) and it also neglects the ability of radioisotopes deposited on structural surfaces to heat the gas. Section 4.1 discusses some calculational results which shed some light on the magnitude of the resulting uncertainty.

Finally, there is a general category of limitations of CONTAIN 1.0 models which involves nonmechanistic treatments of various transport phenomena. In building the code, cognizance has been taken of the existence of these phenomena, but the current state of phenomenological understanding has been inadequate to implement a validated, predictive model. Instead, features have been implemented in the code to allow the user to transfer conserved quantities at rates that are consistent with his understanding of the problem under consideration. For example, the fission product release and acceptance formalism allows the user a great deal of flexibility in changing the host assignments of the various radioisotopes as a function of time. The structure of the formalism is not inconsistent with many of the physico-chemical processes governing the migration of radioisotopes from one location to another, but the code lacks a data base of release and acceptance coefficients derived from experiment or theory. The principal reason for this deficiency is that such a reduction of the knowledge base would be a very large undertaking, and would necessarily be

incomplete, since there is much about fission product chemistry that is still not known.

Another example of nonmechanistic treatment of uncertain phenomena involves interactions between molten debris and water in the reactor cavity. When melt pours into the water pool, it is likely that a steam explosion will occur, though the amount of debris and water participating in it are quite uncertain. This process is not modeled explicitly in CONTAIN, but it is possible to simulate the quenching effect (with the user controlling the timing and the extent of participation of the melt) with the lower-cell model. More mechanistic treatments of such phenomena will be included in future versions of the code.

Neglected Phenomena

There are a number of phenomena or systems that may be important in some applications but which are not modeled in CONTAIN. In some cases, models are feasible and under consideration for future improvements of the code. It is also possible in many (but not all) cases to simulate the effect of the phenomenon with the source tables or the other nonmechanistic features of the code (as discussed above). Below, we will identify a number of these neglected phenomena, without attempting to discuss in detail the consequences of the neglect, or to provide a complete list of such phenomena.

One area of concern is the possible feedback between the primary system and the containment. It is possible that the pressure and temperature in containment will affect the rate of heat or mass transfer from the primary system. However, since the containment atmospheric conditions will be confined to a range (e.g., 1-10 atmospheres of pressure) which is fairly narrow compared to the primary system range, this neglect is not expected to be important except in special circumstances, e.g., release of revolatilized fission products from the failed RPV. Another issue is the treatment of the failed RPV when it is exposed to the reactor cavity atmosphere through a large opening (e.g., following massive circumferential failure of the lower head). With the remaining core and molten pool in thermal contact (mediated either by radiation heat transfer or by convection through the intervening gas), it would be difficult to analyze this configuration without a coupled treatment.

Another general area that is lacking in the code involves the generation of aerosols. The most important mechanism in containment occurs at the molten pool surface during melt-concrete interactions. In BMI-2104,[5] the VANESA model, coupled with CORCON, was utilized (see Figure 1-1). A two-way link between CONTAIN and VANESA/CORCON is planned, but in the meantime, these aerosol and radioisotope sources can be input to CONTAIN through source tables (as is done in many of the calculations discussed in Section 4). Other potential aerosol sources to containment include those due to high pressure melt

ejection from the RPV, and resuspension events (e.g., following hydrogen burns and containment failure). At present, these must also be supplied to the code in the form of source tables.

We have discussed the fact that CONTAIN provides a number of two-way coupling mechanisms between aerosol behavior and thermal-hydraulics. There are also some potential couplings which have been neglected. For example, the possibility that aerosols may plug narrow leak paths, thereby affecting the pressure and temperature histories has sometimes been suggested. CONTAIN has no mechanistic models for this process. Another, more important coupling is the transport of fission products within containment via liquid pathways. Of particular importance is the possibility that aerosols deposited on walls will be washed down by condensing steam, and be redeposited in containment sumps. This process can be simulated, to some extent, by the release and acceptance machinery, but a realistic model would be preferable. Similarly, water that is transferred from one cell to another (e.g., by means of engineered safety features) does not carry dissolved or suspended fission products with it.

A number of phenomena involving interactions between the molten debris and concrete should be mentioned. The debris-concrete interaction model in CONTAIN does not treat two-dimensional effects. Thus, radial ablation does not occur, and it is not possible to predict penetration of interior walls (leading, for example, to ingress of water to a previously dry cavity). This deficiency can be remedied by replacing the CONTAIN model with the CONTAIN/CORCON link. However, there are a number of potential phenomena that cannot be so easily handled. In particular, the effects of radiant heating of concrete, which is not in direct contact with the melt, are not modeled in CONTAIN or CORCON. These include ablation (perhaps by spallation) and outgassing of steam or carbon dioxide.

The removal of molten debris or water from the cavity because of high velocity gas entrainment at the time of vessel failure, or because of steam explosions, is another process not modeled in CONTAIN. It may be important to consider not only the transport of this material to the upper containment, but also the heat transfer and possible chemical reactions between the gas and the hot debris. Future versions of CONTAIN, incorporating models taken from the MEDICI code[23] will improve this situation.

It should not be inferred from this brief summary of modeling limitations that calculations performed with CONTAIN 1.0 will not be realistic. Many of the deficiencies are simply a consequence of inadequacies in our current understanding of severe accident phenomena. Furthermore, the potential impact of most of the limitations can be assessed through the use of the user-controlled features in the code (e.g., source tables, user overrides, etc.). The ways this can be accomplished have been

noted in numerous places above, but the best way to understand how the flexibility of the code can be exploited is to consider a number of detailed accident sequence calculations. This is the subject of the next section.

4. INTEGRATED CONTAINMENT ANALYSIS SENSITIVITY STUDIES

In this section, we will describe a number of sensitivity studies performed with CONTAIN 1.0. The purpose of the studies is to identify or illuminate one or another aspect of integrated containment analysis. These calculations are based on realistic accident sequences at actual power plants, though in some cases parameters have been chosen to emphasize particular effects. However, in all cases, the inputs and parameters chosen are believed to reside within the uncertainty ranges for each plant/sequence combination.

4.1 Aerosol Deposition and Decay Heating

The effect of containment thermal-hydraulics on aerosols is widely understood to be important for source term calculations, but what is less widely appreciated is the fact that feedback from aerosol physics to thermal-hydraulics can be an important consideration when assessing containment loads and, ultimately, the likelihood of containment failure. Containment pressure and temperature histories are required in such an assessment, and these depend on a proper treatment of all energy sources, including fission product decay heat. The CONTAIN code has the capability to evaluate the feedback between heat sources and the conditions that the sources are affecting within the containment. An example of such a situation is the effect of aerosol processes on the location, and hence the effects, of decay heat sources (see Figure 1-1). In this section we will focus on this coupling by means of a series of TMLB' accident sequence calculations that differ only in the manner in which fission product decay heat is treated. (The general event sequence in a TMLB' accident was reviewed in Section 2.1.)

A useful simplification for analyzing the effects of decay heating is to organize the major isotopes contributing to the decay heat into a few radionuclide groups. The approximate breakdown of the decay power of a PWR for times greater than about an hour after shutdown is the following: 70% refractories, 20% iodine, 5% tellurium, and 5% noble gases. For a TMLB' sequence, the noble gases are slowly released through the pressure relief valve opening to the containment atmosphere before reactor vessel failure, and then in large amounts at the time of failure. These gases remain in the atmosphere as a continuous source of heat diminished only by radioactive decay. Other decay sources are released to the atmosphere primarily as aerosols both at the time of vessel failure (puff release) and during core-concrete interactions (continuous release) that occur later. There are also significant quantities of inert aerosols released at vessel failure and

during core-concrete interactions that, while they do not generate heat, are an important part of the decay heat analysis within the containment because they affect the deposition rate of the radioactive aerosols.

Nonintegrated containment codes (e.g., MARCH) cannot mechanistically treat decay heat sources to containment when these sources are in the form of aerosols which undergo natural depletion. For such purely thermal-hydraulic codes, decay heat from sources other than noble gases are often modeled as continuous heat sources to the containment gas throughout the accident. However, for many species this treatment is inaccurate. For example, there is evidence[5] that the dominant iodine species for most accident conditions is cesium iodide, CsI, which would be in aerosol form in the containment. The calculations to be discussed in this section address the sensitivity of containment conditions to aerosol heat sources.

As discussed in Section 2.2, there is considerable flexibility in CONTAIN regarding the treatment of decay heating; each fission product can be input to the containment atmosphere either as a gas or aerosol, and either as an individual isotope or as part of a fission product group with a specified decay power curve. Once in the atmosphere, all decay heat is deposited into the gas. When the aerosol is deposited on structures, the heat is deposited in the surface node of the structure. (In reality, the decay power has a gamma radiation component, which is absorbed partially in the gas and partially in the structures. We will return to this point at the end of this section.)

For the TMLB' sequence to be discussed here, the containment is that of a large dry PWR, generally resembling the Bellefonte plant. The containment phenomena occurring during this sequence were outlined in Section 2.1. For the CONTAIN calculations, a one-cell representation of the containment was used, the gas sources from the RCS are taken from MARCH 2.0 output, and the gas sources from core-concrete interactions are obtained from CORCON-Mod2. Only two aerosol sources are included, in order to simplify the problem. The fission product decay source is input as one aerosol material, named "CsI," while the inert aerosols are named "Other." The "CsI" is released as a 40 kg puff at vessel failure. "Other" is released as a 1200 kg puff, followed by an additional continuous source which simulates the core-concrete aerosols. The aerosol sources are similar to those used in the QUEST study[2] of the Surry plant, but are scaled here to the 3,800 MWt Bellefonte plant.

To simplify the analysis of aerosol effects on decay heating in the atmosphere, all the released decay power is

assumed to be in the form of CsI. To be more accurate, one would partition this heat between noble gases and a number of aerosol groupings. However, since the noble gases represent a relatively small fraction of the decay heat for a scenario with maximum decay heat release, the noble gas contribution is neglected here. The concern for the refractory contribution is met by noting that only small fractions of the refractory inventories are released from the fuel, and it is unlikely that this source will make a large contribution compared to products (such as iodine) with high release fractions.

Figure 4-1 shows the containment pressure histories for four different treatments of decay heat within containment. The bottom curve (Case 1) is a baseline calculation showing the history calculated without any decay heat source. The initial pressure rise is due to the steam and water sources released to containment through the pressure relief valve. The next pressure spike at about 6300 seconds is a result of the RPV

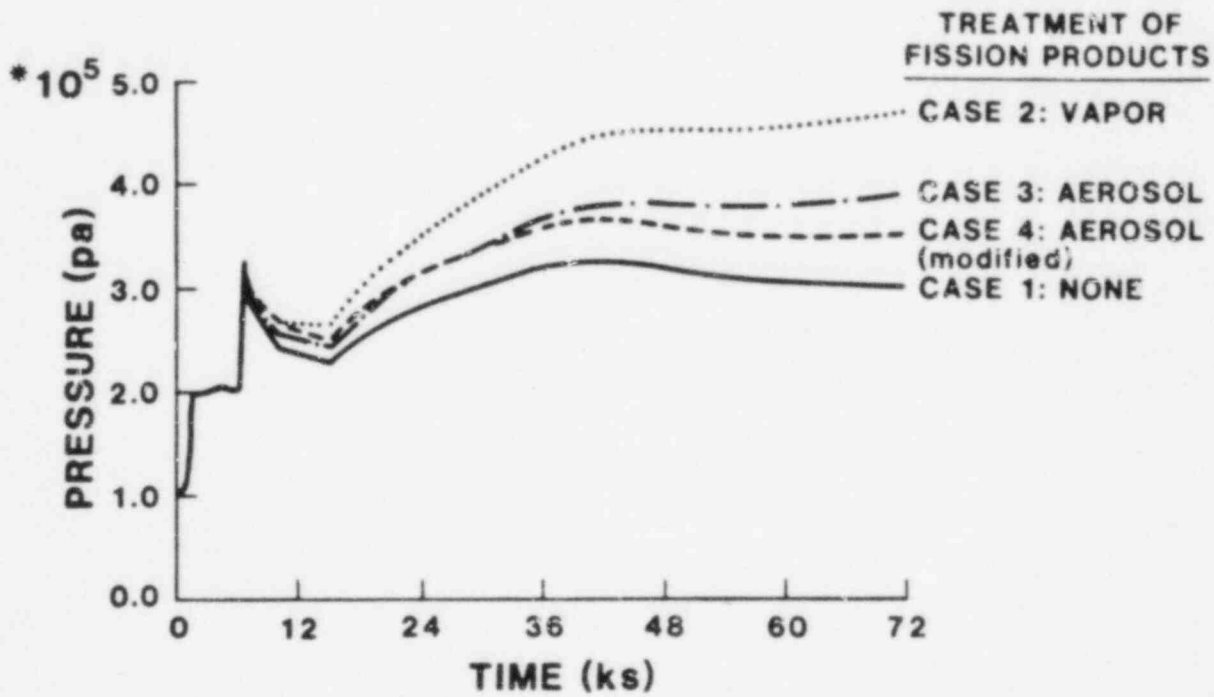

Figure 4-1. Containment pressure for a TMLB' accident showing the effect of various treatments of fission product decay heating.

failure. The late time increase is due to H_2, CO_2, CO and steam, from the core-concrete interaction. The top curve (Case 2) shows the effect of placing all the decay heat into the gas, while Case 3 shows the effect of putting the decay heat on the CsI aerosol. The span of nearly two atmospheres in pressure at late time between Case 1 and Case 2 clearly shows the

importance of including decay heating when late time containment integrity is an issue. When suspended fission products are treated as aerosols (Case 3), the pressure history tracks a path that is about midway between the two bounding calculations.

These first three calculations (Case 4 will be discussed later) indicate that late time atmospheric pressure can be significantly reduced when decay products are considered as aerosols rather than as gases. As an aerosol, the energy source to the atmosphere is reduced not only by decay, but also through rapid natural deposition processes. Some of the heat-carrying aerosols are deposited on wall structures, and some on floors; as a consequence, the location of the decay power source is altered, as shown in Figure 4-2. Initially, the heat load in the gas is reduced, as steam released from the failed vessel rapidly condenses on the cool containment walls, taking with it suspended aerosols (the effect of diffusiophoresis). Later, agglomeration of the suspended aerosols (primarily "Others") increases the mass median diameter enough that gravitational settling dominates, and floors become the principal deposition surface. As the inert

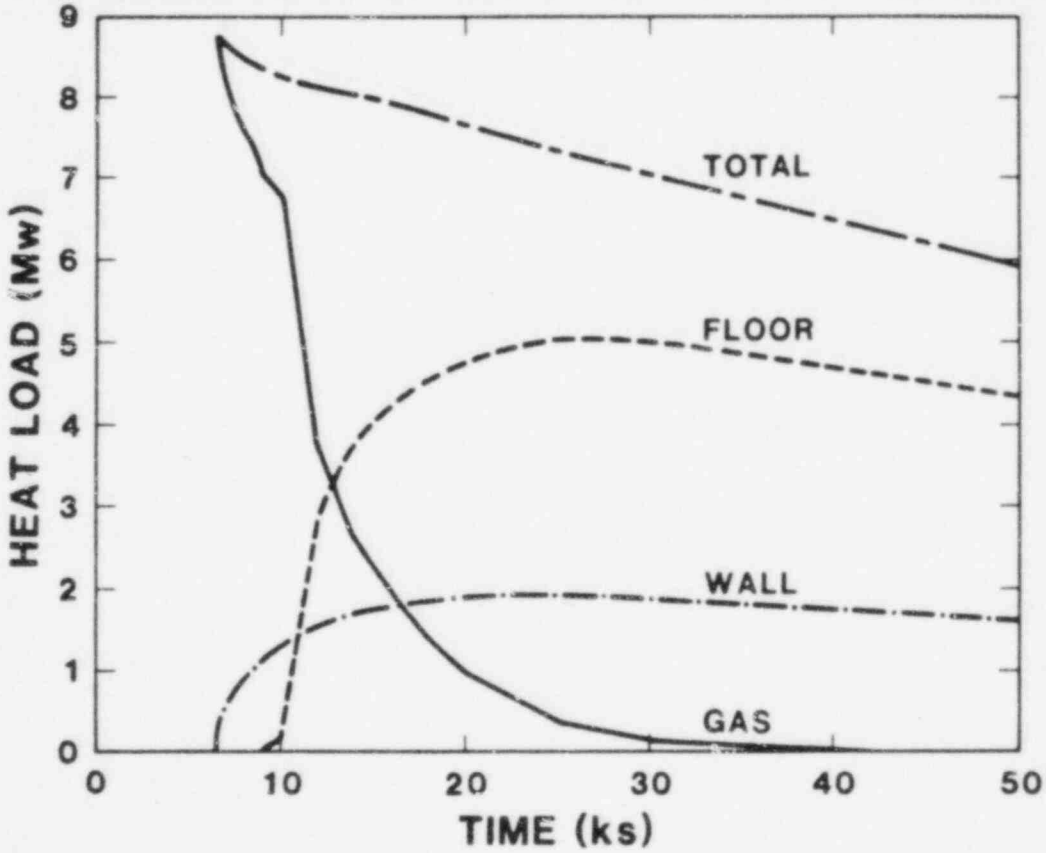

Figure 4-2. Partitioning of decay energy between structures and the containment atmosphere when the decay energy is introduced as fission product aerosols.

aerosols settle out, they also sweep out the CsI aerosols, carrying the decay heat to the containment floor. The sweepout process is quite rapid, illustrating the importance of including inert aerosols for decay heat analysis. At times greater than about 30,000 seconds, virtually all of the nearly 7.0 MW of total decay energy is removed from the atmosphere and deposited on structures, 30% going to walls and 70% going to the floor.

Thus far, we have discussed the location of the sources of decay heat. Another concern is the proper treatment of the absorption of this energy. This is the purpose of Case 4 in Figure 4-1, which is a variation on Case 3. To understand it, it is necessary to review some simplifying assumptions in CONTAIN's treatment of absorption of fission product decay power. As discussed in Section 2.3, all decay heat in the atmosphere is assumed to be deposited in the gas, while fission products deposited on heat sinks deliver their energy to the surface node of the heat sink. In reality, most of the gamma radiation energy will be deposited at some depth in the heat sink structures (e.g., up to 10 cm or more in concrete) almost independently of whether the radionuclides are airborne or deposited. On the other hand, significant fractions of the beta energy from deposited radionuclides may be emitted into, and absorbed by, the atmosphere.

There are two opposing effects of these simplifications. Since CONTAIN deposits all structure heating in the first node, instead of at some depth, there is a tendency for the surface temperatures to be too high, and hence the heat transferred from the structure back to the atmosphere through normal convection or evaporation of water films on the surface is overestimated (or else there is an underestimate of heat flow in the opposite direction, which amounts to the same thing for the present discussion). This effect by itself would lead to overpredictions of temperatures and pressures by the code. However, the heating of the gas due to gamma and beta radiation from deposited fission products (which CONTAIN neglects) has an effect in the opposite direction. Hence it is difficult to predict whether CONTAIN's calculations would be too high or too low as a result of these simplifications. However, a simple variation of the CONTAIN input for Case 3 provides some insight concerning the lower bound of the variation due to these simplifications. This is achieved simply by deleting the floor as a heat sink from the problem (but retaining it as a deposition surface). This variation is Case 4 in Figure 4-1. The result of deleting all floor heat sinks from CONTAIN is the loss from the analysis of all the decay power associated with fission products deposited on the floor. Since this is essentially equivalent to depositing the heat at an infinite depth, and since the floor is the major repository of decay

power at late times (see Figure 4-2), it is reasonable to conclude that a proper treatment of gamma radiation deposition would result in late time pressures higher than those obtained in Case 4. Obtaining a reasonable upper bound on the pressure (other than Case 2, which is extreme) is not so simple, and further progress in this assessment will probably require actual implementation of improved models in the code, an effort beyond the scope of the present review, but one which is actively being pursued as part of the continuing development of CONTAIN.

We have focused on containment pressure, but other quantities are also of importance to the accident analysis, and can be affected by the treatment of decay heating. One such quantity is relative humidity, which may be important to aerosol behavior (a point to be discussed in more detail in

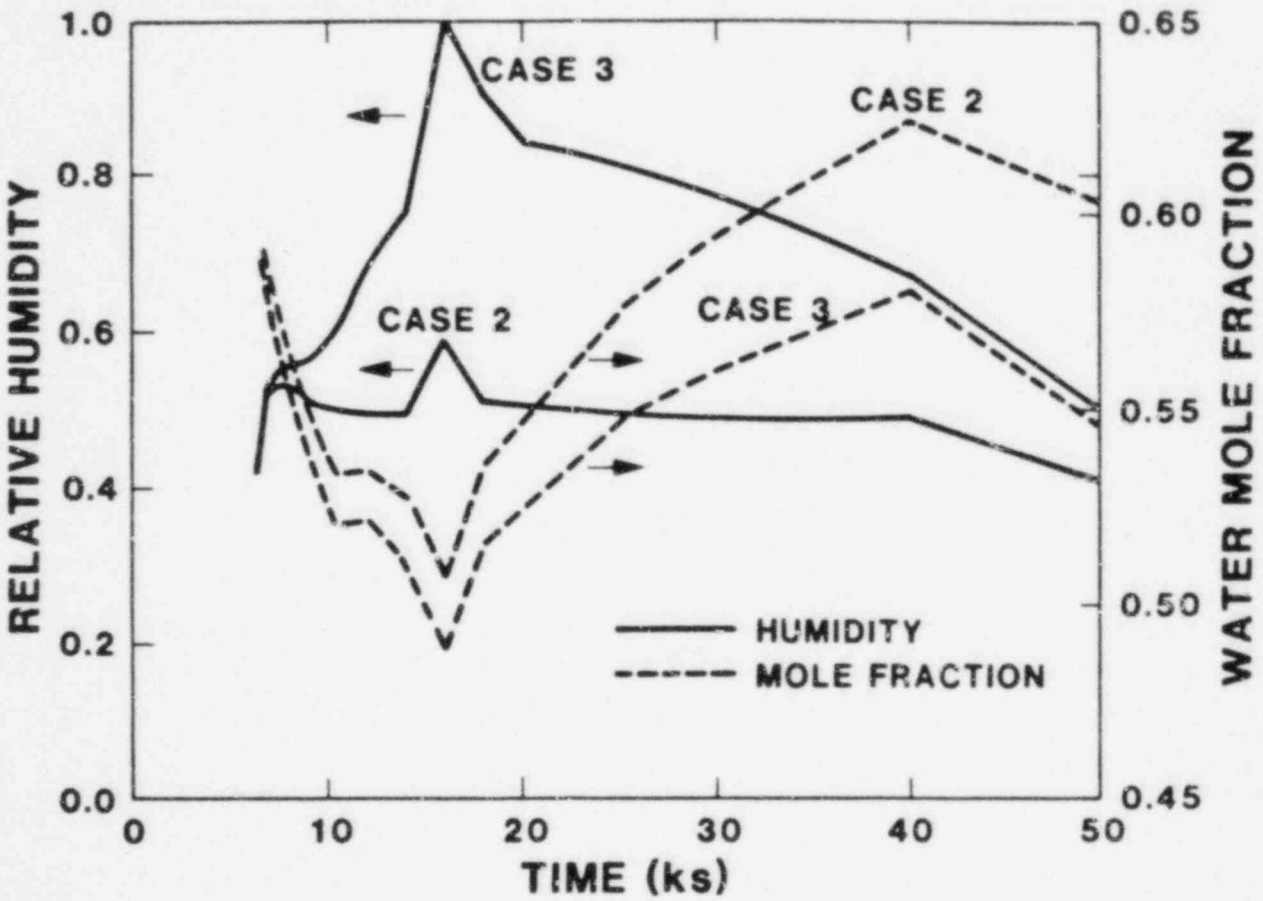

Figure 4-3. Containment atmospheric relative humidity and water mole fraction for decay energy introduced either as a vapor (Case 2) or an aerosol (Case 3).

later sections), and as a consequence, represents a link between aerosols and thermal-hydraulics which is a true two-way feedback loop. Figure 4-3 shows the relative humidity and water mole fractions predicted for Cases 2 and 3 as described above. Clearly, the treatment which gives the higher pressures (Case 2) also gives significantly more superheated conditions as well as higher mole fractions of water. In subsequent sections it will be shown that such differences in relative humidity and water mole fractions can have significant consequences on the nature of hydrogen burns, atmospheric turbulence, and aerosol shape factors.

4.2 Depressurization Condensation on Aerosols

The Nuclear Regulatory Commission (NRC) and the American Nuclear Society (ANS) have recently published source term studies which predict the leakage of radionuclides from a reactor containment building as a result of a containment failure during overpressurization.[5,3] In the case of early failure, the overpressurization occurs coincident with reactor pressure vessel (RPV) melt-through when large quantities of high temperature steam and hydrogen are released from the RPV. The primary component of the total containment pressure is the water vapor partial pressure. Unless the containment atmosphere is superheated to a substantial degree, depressurization will cause substantial condensation of water in the atmosphere, similar to what occurs in a Wilson cloud chamber. For source term prediction, an interesting aspect of the depressurization is that atmospheric condensation can enhance aerosol settling, and can therefore partially decontaminate the containment atmosphere during the release phase. The resulting natural depletion may be significant in reducing source terms for certain accident sequences and rates of depressurization. Failure to include condensation may therefore result in source terms which are overly conservative.

When containment thermal-hydraulics are decoupled from an aerosol transport calculation, as has been the case in both the NRC and ANS studies, there is a tendency to neglect certain coupling phenomena which are difficult to interface between two dissimilar codes. Condensation of water on aerosols is such a coupling, and since it has been neglected in previous source term calculations, it seems worthwhile to investigate the sensitivity of atmospheric condensation for a selected accident scenario.

In the following calculations for the TMLB' accident sequence, the quantitative effect of condensation during depressurization for two containment failure hole sizes, 0.8 m^2 and 0.02 m^2, is analyzed using CONTAIN input options

to selectively turn off atmospheric condensation for times following containment failure. The calculation makes use of the containment description (passive heat sinks and volume) of the Zion nuclear plant. The steam and gas sources into containment during the accident sequence are obtained from MARCH calculations. Two aerosol sources are included: an RPV source that is a puff release of 100 kg at the time of vessel failure (13000 seconds), and a continuous release of aerosol in the cavity that simulates the core/concrete source, beginning at the time of RPV failure. For brevity, only the cavity aerosols are considered here.

The containment pressure histories for the two failure hole sizes are shown in Figure 4-4. The containment failure time (19000 seconds) was chosen arbitrarily to occur slightly after the time of maximum overpressure so that there is no suspended water aerosol present at the time of depressurization. The containment atmosphere is approximately 6 degrees superheated at the time of containment failure. Fission product heating is neglected in the calculation for simplificity. It should be pointed out that the analysis is not based upon actual failure pressures for the Zion containment, which are much higher than the pressures calculated here. However, the purpose of the calculation is to provide insight that may be used to judge the relative importance of a selected phenomenon that may be occurring during a severe accident.

As the containment depressurizes, atmospheric water vapor condenses on suspended solid aerosols. The mass of water condensed on the aerosols is dependent on the rate of depressurization, i.e., the containment hole size. For the example problem, Figure 4-5 shows that the slow depressurization results in a peak suspended water aerosol mass of ~ 1100 kg, while the more rapid depressurization produces three times that amount. These water aerosol masses can be compared to the more than 140,000 kg of water vapor present in the atmosphere at the time of containment failure. The relatively small condensed fraction implies that the atmospheric thermal-hydraulics within the containment are insensitive to the condensation process. The depressurization curves of Figure 4-4 therefore apply whether condensation is accounted for or not.

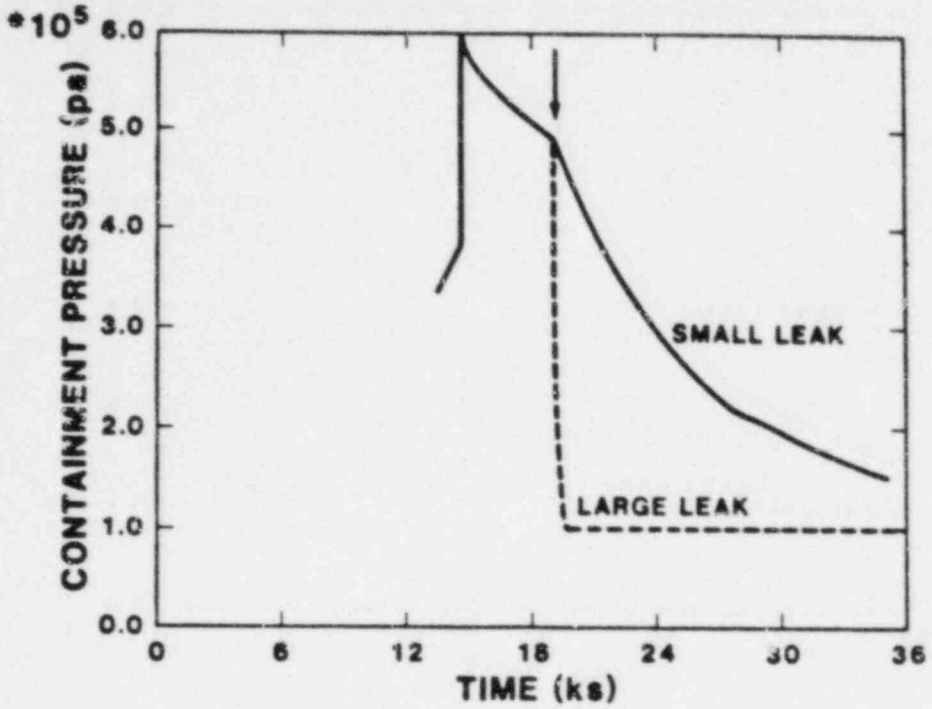

Figure 4-4. Containment pressure showing depressurization rates for two containment hole sizes, 0.8m^2 and 0.02 m^2, representing both a large and small leak rate. The arrow indicates containment failure time.

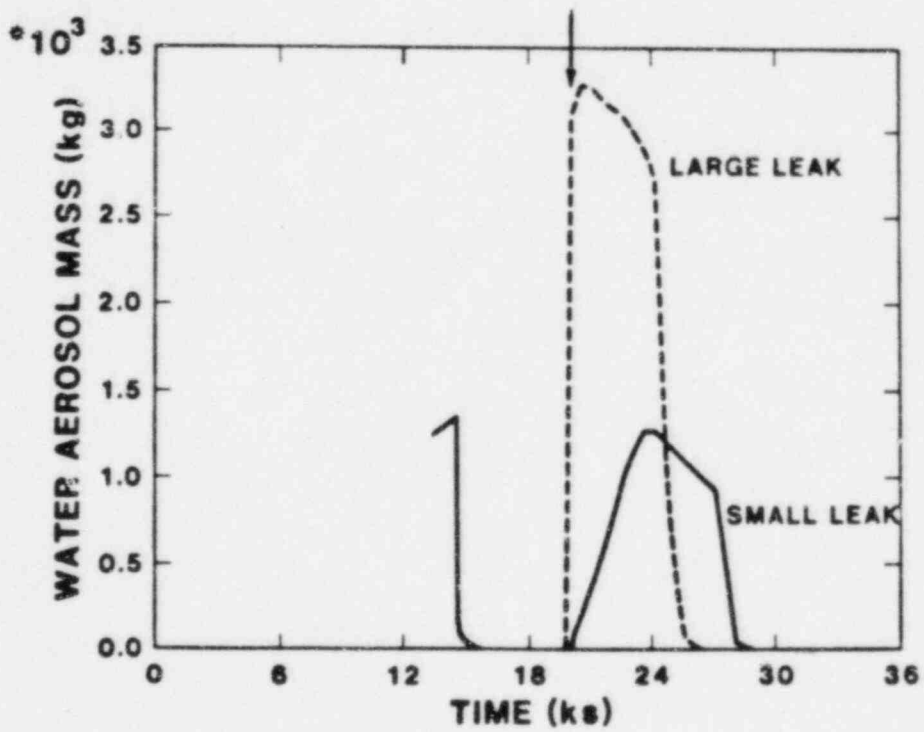

Figure 4-5. Airborne water aerosols within containment following containment depressurization. The arrow indicates containment failure time.

In the CONTAIN code, aerosols are assumed to flow between cells (e.g., from the containment to the environment) without slip along with the atmospheric gases. The rate of aerosol transport out of the containment is therefore proportional to both the aerosol concentration within containment and the gas flow rates out of the containment. The rate of deposition of the suspended aerosols onto surfaces is dependent mainly on mechanisms involving condensation, aerosol agglomeration, and gravitational settling, all of which take time to have an effect. If the leakage of solids is to be significantly reduced by the condensation effects, the aerosol processes must have time to act before containment depressurization is complete, since it is during containment depressurization that most of the release of gases and aerosol will take place.

For the slow depressurization case (0.02 m^2 leak size), Figure 4-6 presents the suspended masses of the cavity aerosols within containment as calculated with and without condensation, starting at the time of containment failure. It is apparent that condensation effects eventually reduce the concentration of solid aerosols by large factors, but the effect is not immediate. Condensation begins about 1000 seconds after containment failure, but another 3000 seconds are required before the combined effects of condensation and enhanced water aerosol agglomeration substantially enhance the settling rates of the latter. During the first 4000 seconds following a containment failure, therefore, leakage of solid aerosol from containment is almost independent of whether condensation has been occurring. However, depressurization of the containment is incomplete at this time, and the subsequent release is substantially reduced by the condensation effects. Overall, the effect upon the total time-integrated release is significant, as can be seen in Figure 4-7.

In the case of the rapid containment depressurization (0.8 m^2 leak size), gas flow rapidly transports the aerosol out of the containment. The amount of condensation is actually larger in this case than in the slow depressurization case, and the delay in the effects of condensation upon the amount of airborne solids is somewhat shorter. However, containment depressurization is so much faster that it is complete before condensation has any effect. Hence, the impact of condensation upon the amount of aerosol released is insignificant.

In summary, atmospheric condensation during containment depressurization can have a significant decontamination effect

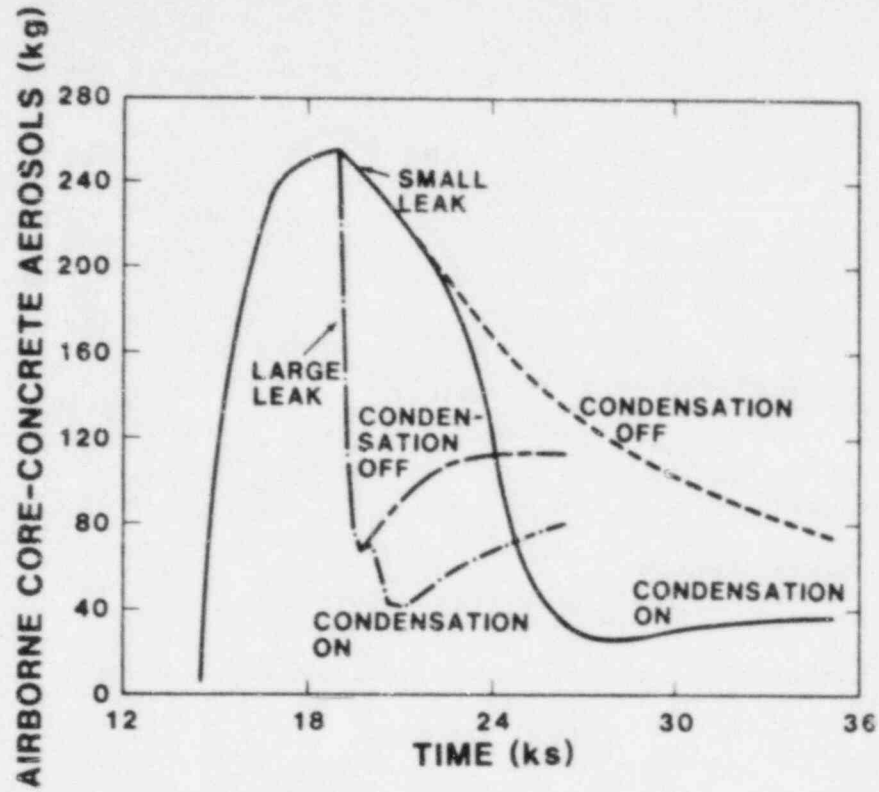

Figure 4-6. Suspended masses of cavity aerosols within containment showing the partial decontamination effect caused by water condensation following the depressurization.

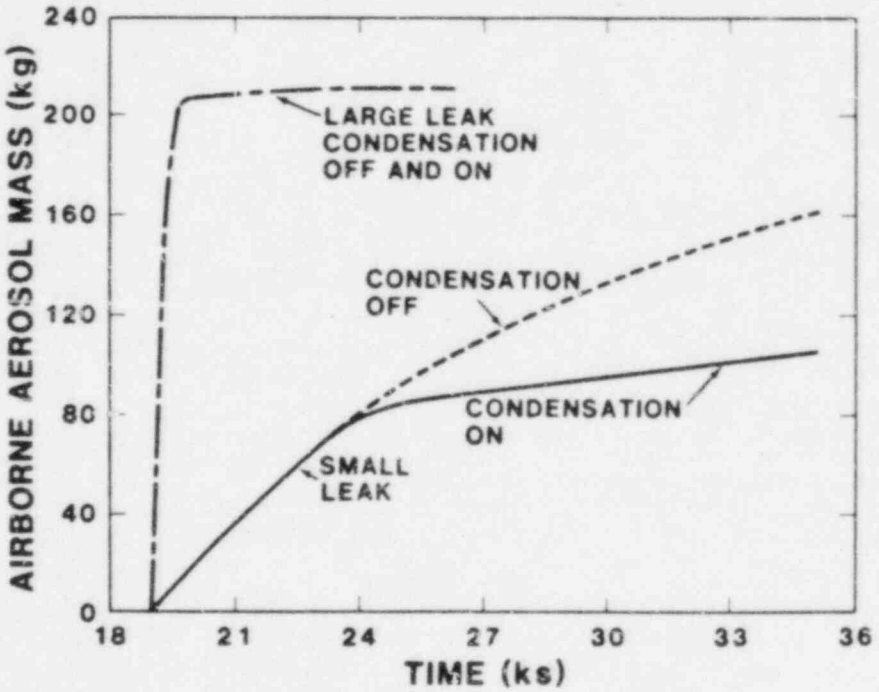

Figure 4-7. Reductions in leaked cavity aerosols when water condensation within containment is modeled for two widely varying depressurization rates.

that will reduce leaked radionuclide aerosols. The depressurization must, however, be slow enough to allow the processes of condensation, agglomeration and gravitational settling to reduce the aerosol density during the time when the driving pressure within containment is still high. The reduction factor of 0.6, obtained in the example calculation for a slow depressurization, is not large compared to some other uncertainties in the source term, but it is also not insignificant. In other sequences or scenarios, the effect may be larger.

This analysis is not intended to be an exhaustive study of this effect; the point to be made here is simply that there are many potentially important phenomena that couple thermal-hydraulics to aerosol transport. For some accident scenarios, the coupling is weak, but for others it can be quite strong. To evaluate the magnitude of such effects, it is generally necessary to use an integrated aerosol/thermal-hydraulic analysis.

4.3 Effects of Steam and Heat Sources in the Station Blackout Sequence

Once the reactor vessel has failed, important sources to the containment include noncondensible gases, steam (e.g., from debris concrete interactions), aerosols, radionuclides, and thermal energy. The influence of aerosol and radionuclide sources was considered in Section 4.1. In this section the effects of steam and energy sources is considered. The impact of these sources upon possible hydrogen burns, containment thermal-hydraulic conditions, and certain parameters that affect aerosol behavior will be discussed.

The containment to be studied for this analysis is that of the Surry plant, a Westinghouse large dry PWR in which the containment is held at a subatmospheric pressure (typically 0.7 bar). The sequence to be used as an example is basically the Surry TMLB' sequence used as a base case in the QUEST study discussed in some detail in Reference 2, except that the releases of radionuclides and aerosols from the RCS when the vessel fails were reduced by factors of three to five, in order to better conform with the final results of BMI-2104, volume 5. The parameter variations chosen are illustrative rather than intended to represent best estimates for specific accident scenarios, though the values are taken from the range thought to be credible for these parameters. A single-cell representation of containment was used.

In the base case for the Surry TMLB' analyses considered here, the only long-term sources to the containment were those from core-concrete interactions as calculated by the CORCON code. These involved a small amount (typically ~0.1 kg/sec) of very hot steam plus noncondensible gases with a total enthalpy input corresponding to roughly 0.5-1 MW of sensible heat. In addition, decay heat from airborne radionuclides ranged from about 1.5 MW immediately after vessel failure to less than 0.5 MW at late times (> 10 hr) into the accident. Though the noncondensible gases generated were not very significant as a source of containment pressurization, a major component of the gas was hydrogen in amounts sufficient to be important in terms of potential hydrogen burns. In the TMLB' sequence, steam inerting is expected to prevent this hydrogen from burning until some substantial time after vessel failure, but sufficient condensation may eventually occur to permit combustible gas compositions to develop (a process referred to as "de-inerting"). Since inerting permits large amounts of hydrogen to accumulate without burning, the burns that result when de-inerting finally does occur can be especially severe. The calculations to be described below illustrate that the occurrence and timing of de-inerting burns in the TMLB' sequence is quite sensitive to the steam and energy sources to the containment.

It is entirely possible that there are additional sources of steam not properly accounted for in the base case source term calculations. Radionuclides released from the fuel can be transported to the sump or other water pools where the resulting decay heating can generate steam. Steam generation rates of up to 1 kg/sec, or somewhat more, could result from these processes. Larger steam sources are possible if water can flow to the cavity and interact with the melt. Though this may be unlikely for the Surry TMLB' sequence, it could occur in TMLB' events at other PWR plants and might be important for other sequences at Surry. Still other steam sources that may exist include steam released from concrete heated by radiant energy and hot gases originating from the melt in the reactor cavity.

Many of these various steam sources are not modeled mechanistically in CONTAIN. Though progress is being made, inadequate understanding of some of the phenomena involved have limited the capability to develop mechanistic modeling. For example, modeling of transport of radionuclides within containment via liquid pathways would require information as to the detailed physical and chemical properties of the radionuclides involved, and this information is not presently available. Despite the lack of mechanistic models for these processes, CONTAIN can be used to simulate their effects in various ways, and the code can therefore be used to investigate the consequences of postulated steam sources that might result from these effects.

In addition to steam sources, there exist other potentially important sources of thermal energy to the containment. In particular, core-concrete interaction calculations for the Surry TMLB' sequence employing the CORCON Mod2 code indicate that radiant heat loss from the upper surface of the melt is of the order of 10 MW, assuming a high effective emissivity for the melt. The fate of the radiated energy is quite uncertain. It is not known whether this radiant energy heats the gas or heats the adjacent structures or is simply reradiated back to the melt surface. The opacity of the aerosol-laden atmosphere above the melt is one of a number of contributors to this uncertainty. As in the case of the additional steam sources, it is possible to use the CONTAIN code to explore the sensitivity of the containment response to the additional heat sources.

Calculations were run for the Surry TMLB' base case (which does not include the sources discussed above) and for variations with the following additional sources specified:

A. A source of 1 kg/sec saturated steam (enthalpy = 2.73 MJ/kg), relative to water at 273°K,

B. A source of 2.24 MW of thermal energy, without additional steam,

C. Both (A) and (B) together,

D. A source of 10 MW of thermal energy, without additional steam,

E. Both (A) and (D) together.

All these sources were assumed to start at vessel failure time and continue until the end of the calculation, 20 hours after accident initiation. The thermal energy input in case B is equal to the latent heat of the steam input in case A. The thermal energy input in the last two cases is intended to represent approximate upper limits to the energy that might be radiated from the melt to the overlying atmosphere, and may well be larger than is realistic.

Effects on Hydrogen Burns

The pressure-time histories for all six cases are shown in Figure 4-8. In all cases, there is an initial pressure rise to about 5.4 bars due to vessel failure and steam generation when the accumulators dump onto the melt. Strong hydrogen burns occur in the base case and in cases A and B, while the other three cases remain steam-inerted throughout the calculation (and would probably remain so indefinitely if the late time sources continued indefinitely).

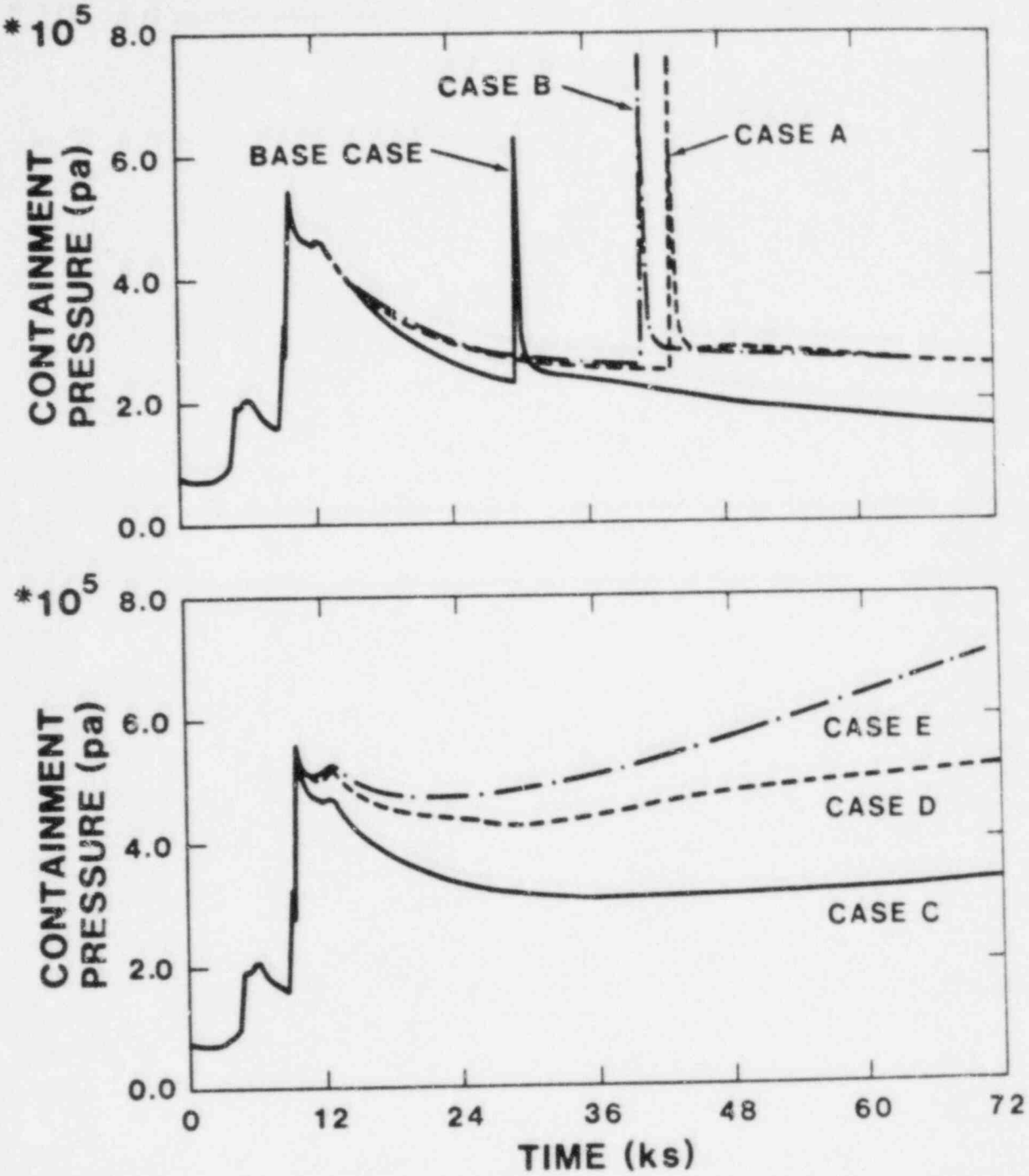

Figure 4-8. Pressure-time history for the Surry TMLB' ("Station Blackout") sequence. Sources of steam and/or heat to the containment, in addition to the base case sources, are postulated to exists as follows: Case A, 1 kg/sec steam; Case B, 2.24 MW heat; Case C, 1 kg/sec steam + 2.24 MW heat; Case D, 10 MW heat; and Case E, 1 kg/sec steam + 10 MW heat.

Table 4-1

Effect of Steam and Heat Sources on Hydrogen Burns

Case	Additional Sources[a]		Burn			
	Steam (kg/s)	Heat (MW)	Initiation (s)	Duration (s)	Maximum Pressure (bars)	Maximum Temp. (K)
Base	0	0	28266	88.1	6.19	1167
A	1.0	0	43154	64.8	7.76	1366
B	0.0	2.24	40550	66.7	7.67	1355

Cases C, D and E: No Burns

[a] In addition to the sources listed, the base case sources were assumed to be present in all cases.

Table 4-1 summarizes key features of the burns for the base case and cases A and B. In all cases, the burn is initiated by de-inerting, which is assumed to occur when the mole fraction of steam in the containment atmosphere falls to 55%. The presence of the steam source (case A) or the heat source (case B) delays the burn by several hours, which permits more hydrogen to accumulate before de-inerting occurs and thus results in a more severe burn. In all cases, the burn duration is relatively long, several tens of seconds. This time is long enough to permit heat transfer during the burn to provide some reduction of the peak pressures and temperatures that would otherwise occur. The long burn durations are characteristic of de-inerting burns because the code employs correlations for the flame speed (taken from the HECTR code) which predict low flame speeds in steam-rich atmospheres. It should be noted, however, that steam-rich hydrogen burn data are somewhat sparse, so there is considerable uncertainty in the correlations. Burn times would be over an order of magnitude shorter in a dry atmosphere.

It is noteworthy that the heat source without steam is almost as effective in delaying the burn as the steam source with the equivalent enthalpy in the form of latent heat. The reason is that de-inerting requires condensation of steam upon the containment structures, and the rate at which this process occurs is governed primarily by the rate at which heat can be conducted into the structures. The latter rate does not depend upon whether the heat is transferred to the structure as sensible heat of hot gases or released at the surface as latent heat of condensation. Hence, increasing the thermal load to the structures from the atmosphere by a given amount delays de-inerting by about the same amount, independently of whether the enthalpy is input to the atmosphere as sensible heat or as latent heat of steam.

With additional delays in de-inerting times, hydrogen accumulation continues, but burn severity does not increase without limit because the supply of oxygen is limited. Additional calculations (not shown) similar to cases A and B, but with slightly greater energy sources, show that the burn becomes oxygen-limited if it is delayed beyond 60000 sec, with peak pressures of about 8.4 bars being the maximum obtainable from a de-inerting burn. In this connection, it should be remembered that the Surry containment is subatmospheric, which reduces the oxygen supply; in an atmospheric containment, larger burns would be possible.

Effects on Thermal-hydraulic Conditions

Additional insight into containment response to steam and energy sources is provided by a more detailed examination of some of the thermal-hydraulic quantities calculated by the code. Some of these results are tabulated in Table 4-2 for a time of 28000 sec after accident initiation, which is before hydrogen burns occur in any of the cases. For cases C - E, which had no hydrogen burns, results are also given at late times (72000 sec).

In Table 4-2, TGAS is the bulk temperature of the containment atmosphere and TSAT is its saturation temperature. TWALL2 is the surface temperature of the wall structure having the largest surface area (several heat transfer structures were included in these calculations, and their temperatures are not all the same). The next two columns give, respectively, the relative humidity and the mole fraction of water vapor in the atmosphere. The last column in the table gives the total atmospheric pressure, PGAS.

The presence of additional steam and heat sources increases TGAS, with the effect of the heat sources being considerably larger, much as one would expect. However, case A and case B have closely similar values of TSAT, mole fraction H_2O, and PGAS. For all these quantities, the most important parameter governing the results is the net balance between steam condensation and steam input. As discussed above in connection with the delay in the hydrogen burns, this balance is expected to be about the same in case A and case B, since the limiting process is conduction into heat sinks. Note, however, that the higher temperature of case B implies a considerably lower value of the relative humidity, even though the absolute quantity of water vapor is about the same.

Except for late times in case D, which had a high heat input and a low steam input, the CONTAIN code calculates that there will be films of condensed water on at least some of the heat transfer surfaces. For these cases, it is seen in Table 4-2 that TWALL2 is very close to TSAT. The reason is that in steam-rich atmospheres condensation and evaporation provide a very efficient heat transfer mechanism between the structure surfaces and the atmosphere whenever the difference between TSAT and TWALL2 is substantial. Hence substantial differences between TSAT and TWALL2 cannot be supported for any length of time, and the two temperatures closely approach one another except when heat sources are sufficiently large that the structures completely dry out, as at late times in case D.

Table 4-2

Response of Containment Conditions to Steam and Heat Sources

Case	Additional Sources:[a] Steam kg/s	Heat MW	Time (s)	TGAS (K)	TSAT (K)	TWALL2 (K)	Rel. Humidity	Mole Frac. H_2O	PGAS (bars)
Base	0	0	28000	390.7	378.8	378.4	0.694	0.553	2.30
A	1.0	0	28000	398.4	387.5	387.0	0.726	0.618	2.75
B	0	2.24	28000	413.8	386.5	386.3	0.466	0.611	2.81
C	1.0	2.24	28000	417.9	392.5	392.2	0.503	0.653	3.17
			72000	416.6	392.2	392.1	0.515	0.615	3.33
D	0	10.0	28000	464.8	402.4	403.9	0.235	0.713	4.28
			72000	482.8	408.1	432.2	0.195	0.713	5.19
E	1.0	10.0	28000	463.7	408.7	408.6	0.284	0.747	4.83
			72000	479.3	424.9	427.4	0.319	0.792	7.10

[a] In addition to the sources listed, the base case sources of steam, gas and energy were assumed to be present in all cases.

For all cases, the relative humidity is significantly less than unity and is much less than unity when there are large heat sources to the containment. This result is quite general in CONTAIN calculations: the code calculates a saturated atmosphere to exist only in rather special circumstances, e.g., during certain containment depressurization events (see Section 4.2) or shortly after containment sprays have been turned on in some scenarios (Section 4.4). This result is in accord with physical expectation. As noted above, TSAT and TWALL2 are usually constrained to lie close together. However, in the presence of heat sources other than saturated steam, maintaining a thermal balance usually requires removal of significant amounts of sensible heat from the containment atmosphere in addition to removal of steam and its associated latent heat. Transfer of sensible heat is relatively inefficient unless TGAS is significantly higher than TWALL2 and, hence, higher than TSAT. The various temperatures and vapor partial pressures involved therefore tend to correspond to significant degrees of superheat.

The heat source in cases D and E is sufficient to substantially reduce condensation on structures during much of the time period of interest. Hence, the high pressures following reactor vessel failure do not decline greatly, and there is a tendency for the pressure to increase at late times. In case D, the increase is slow because the CORCON sources of steam and gas are rather small. The reduction in condensation with the large heat sources means that the additional steam source of 1 kg/sec in case E is more effective in pressurizing the containment at late times, since there is less mitigation by condensation. Thus, the impact of the steam source at late times in going from case D to case E is greater than when heat sources are smaller, i.e., in going from the base case to case A and from case B to case C.

It is worth noting that many earlier analyses of the TMLB' sequence, notably analyses with the widely-used MARCH code, gave results qualitatively resembling cases D and E in Table 4-2 and Figure 4-8 rather than the CONTAIN base case. In particular, those calculations indicated that inerting would prevent hydrogen burns, but that long-term overpressurization of the containment would occur. There were at least two reasons for this difference. First, the INTER module of MARCH, which calculates core-concrete interactions in that code, typically gives gas and steam rates several times as great as those given by CORCON. The second is that MARCH assumes that all of the volatile species will be released from the fuel and will remain suspended indefinitely in the containment atmosphere, with all of the decay heat going to heat the atmosphere. As discussed

in Section 4.1, CONTAIN mechanistically models the aerosol processes which remove much of the radionuclides and their associated decay heat from the atmosphere. Thus, it is entirely reasonable that the MARCH predictions of pressure should resemble the CONTAIN calculations with enhanced steam and energy sources more than they resemble the CONTAIN base case. However, CONTAIN's prediction of significantly superheated conditions are not seen in the MARCH calculations, presumably because of important differences in the models for condensation heat and mass transfer; as discussed in Section 3.2, condensation and dry convective heat transfer are treated as parallel processes in CONTAIN, while MARCH appears to alternate periods of pure condensation with periods of pure dry heat transfer.

The presence of additional heat sources to the atmosphere has two consequences which can affect the rate of agglomeration and settling of aerosols. The first of these is the decrease in relative humidity already discussed in connection with Table 4-2. At low relative humidities, non-spherical particle shapes are more likely to yield aerosol shape factors differing substantially from unity, which may enhance agglomeration rates. In addition, the heat sources increase the difference between the wall temperature and the bulk gas temperature which drives natural convection, and this in turn is expected to increase the degree of turbulence in the containment atmosphere. Turbulence can enhance agglomeration rates, especially when the shape factors are large. Some quantitative examples of the potential impact of these effects are given in Reference 2.

4.4 TMLB' Sequences with ESF Recovery

Background

Analyses of the TMLB' sequence usually assume that AC electric power remains unavailable and that the accident proceeds free of human intervention indefinitely. In the real world, it hardly seems likely that the accident would continue in this "hands off" mode for the many hours or even days required to realize such scenarios as containment failure due to slow overpressurization. It is more likely that power would be restored at some point; even if the normal off-site power and the emergency on-site power sources remain unavailable, it is quite possible that mobile power sources could be brought to the plant in the long times available in such scenarios.

This possibility has inspired some discussion as to how, or even whether, ESFs should be operated if power is recovered. If containment heat-removal systems are recovered, their operation can prevent containment failure due to steam over-

pressurization; however, condensation of sufficient steam may lead to de-inerting of the containment atmosphere and thus permit hydrogen burns, which could challenge containment integrity if sufficient hydrogen has accumulated during a long period of inerted conditions.

In analyzing questions related to ESF recovery, attention has centered more on the containment loads issues than on the effects upon the airborne radionuclide inventory, which determines the potential source term should containment fail. In the present subsection, we shall examine the effects upon airborne radionuclides and upon hydrogen burns which result from spray initiation following power recovery in the TMLB' sequence at the Surry plant (which does not possess fan coolers). We will show that integrated analysis of this scenario provides a particularly rich interplay of phenomena which combine to yield a potentially important practical result, namely, that the sprays are especially effective in bringing about a rapid decontamination of the containment atmosphere in this particular situation. Before examining these results in detail, it will be helpful to provide a brief description of spray modeling in CONTAIN and to discuss a few related issues.

Spray Modeling in CONTAIN

The problem of collection of particles and small drops by larger drops falling through the atmosphere has been studied in many different contexts: nuclear safety, industrial pollution control, phenomena involving natural precipitation, etc. No attempt will be made to review in detail the experimental and theoretical literature here. However, it should be noted that detailed modeling can be quite complex and, even with such modeling, obtaining good agreement between theory and experiment over wide ranges of conditions has proven to be an elusive goal.

Five collection mechanisms are considered in the CONTAIN model for aerosol removal by spray droplets:

1. Inertial impaction, which occurs because the particle has a finite inertia, leading the trajectory of the particle center of mass to cross the flow streamlines around the drop and thus to intersect the surface of the drop.

2. Interception, which arises because the finite size of the particle permits its surface to contact that of the drop, even when the particle center of mass is on a trajectory which does not intersect the drop.

3. Brownian diffusion, which results from molecular diffusion of the particles across the flow boundary layer around the drop.

4. Diffusiophoresis, which arises as a response of the particle to concentration gradients and vapor flow toward (or from) the drop surface when condensation on (or evaporation from) the drop is occurring.

5. Thermophoresis, which results from the migration of a particle down a temperature gradient due to the effect of differential molecular impacts.

These effects are assumed to be additive in CONTAIN. The first three effects are primarily a function of drop and particle size, while the phoretic effects are primarily a function of temperature and humidity of the atmosphere and of the temperature of the drop. The latter changes rapidly at the start of the drop's fall through the atmosphere, and particle collection is therefore integrated over the drop's fall history in CONTAIN. Under evaporating conditions, the diffusiophoretic effect becomes negative, as would the thermophoretic effect in the unlikely circumstance that the drop were hotter than the atmosphere. In such cases, the total collection efficiency is still constrained to be non-negative. Under extreme conditions (e.g., those resulting from hydrogen burns) the drop may completely evaporate during its fall; when this occurs, the solid residue is returned to the appropriate size section of the aerosol distribution.

It is useful to consider the relative importance of the various mechanisms as a function of particle size, but doing so is somewhat complicated by the sensitivity of the phoretic effects to containment conditions and spray temperature. However, when sprays are operating, containment conditions tend to approach a quasi-steady state in which the sprays are removing about as much steam and energy from the containment as the various sources are supplying to the containment. (Important exceptions to this behavior arise during and shortly after major transient inputs of steam or energy to the containment.) Likewise, the drop itself tends to reach a quasi-steady state with respect to the containment atmosphere very early in its fall, with little change in the drop parameters (such as temperature) after the first few tenths of a meter or so of its fall. Over much of the accident history, the spray effectiveness will therefore be dominated by the drop collection efficiencies under these quasi-steady conditions.

Collection efficiencies as a function of particle size as calculated by CONTAIN for a typical set of quasi-steady conditions are shown in Figure 4-9. The collection efficiencies are defined as the ratio of the number of particles collected by the drop to the number present in the atmospheric volume swept out by the drop as it falls. The particular conditions assumed in Figure 4-9 are those that prevailed about five hours into the Surry S_2D sequence analyzed for QUEST and discussed in more detail in Reference 2. A particle material density of 3000 kg/m^3 and a drop size of 1000 μm have been assumed. In interpreting these results, it should be noted that spray intensities are sufficiently high that a unit collection efficiency would correspond to very short particle residence times, typically 1.5 to 7.5 seconds.

It is seen from the figure that impaction gives very efficient collection for particles of a few microns and larger, while the dominant process for smaller particles is interception, down to sizes of about 0.1 micron. For still smaller particles, Brownian diffusion becomes important; however, such small particles are generally calculated to agglomerate rapidly with each other and with larger particles, with or without sprays, and consequently, the size regime dominated by Brownian diffusion usually is not very important to the overall source term.

For all particle sizes, the phoretic effects are small compared with at least one of the other collection mechanisms, under the conditions for which Figure 4-9 was calculated. It also should be noted that the diffusiophoretic effect is negative in the present example, while the thermophoretic effect is positive. This result is typical of quasi-steady conditions, which generally involve a slight amount of superheat (typically of the order of a degree) unless there are essentially no heat sources to the containment. The drop therefore undergoes a slight amount of evaporation as it falls and maintains a temperature slightly below that of the atmosphere. The sign of the net balance between the opposing phoretic effects is sensitive to both modeling uncertainties and various particle parameters, and valid generalizations can not be offered as to whether the net phoretic effect will be positive or negative. On the other hand, the conclusion that the net phoretic effect will be small compared with other effects is valid for most quasi-steady conditions. Phoretic effects may become quite important, however, during transient conditions.

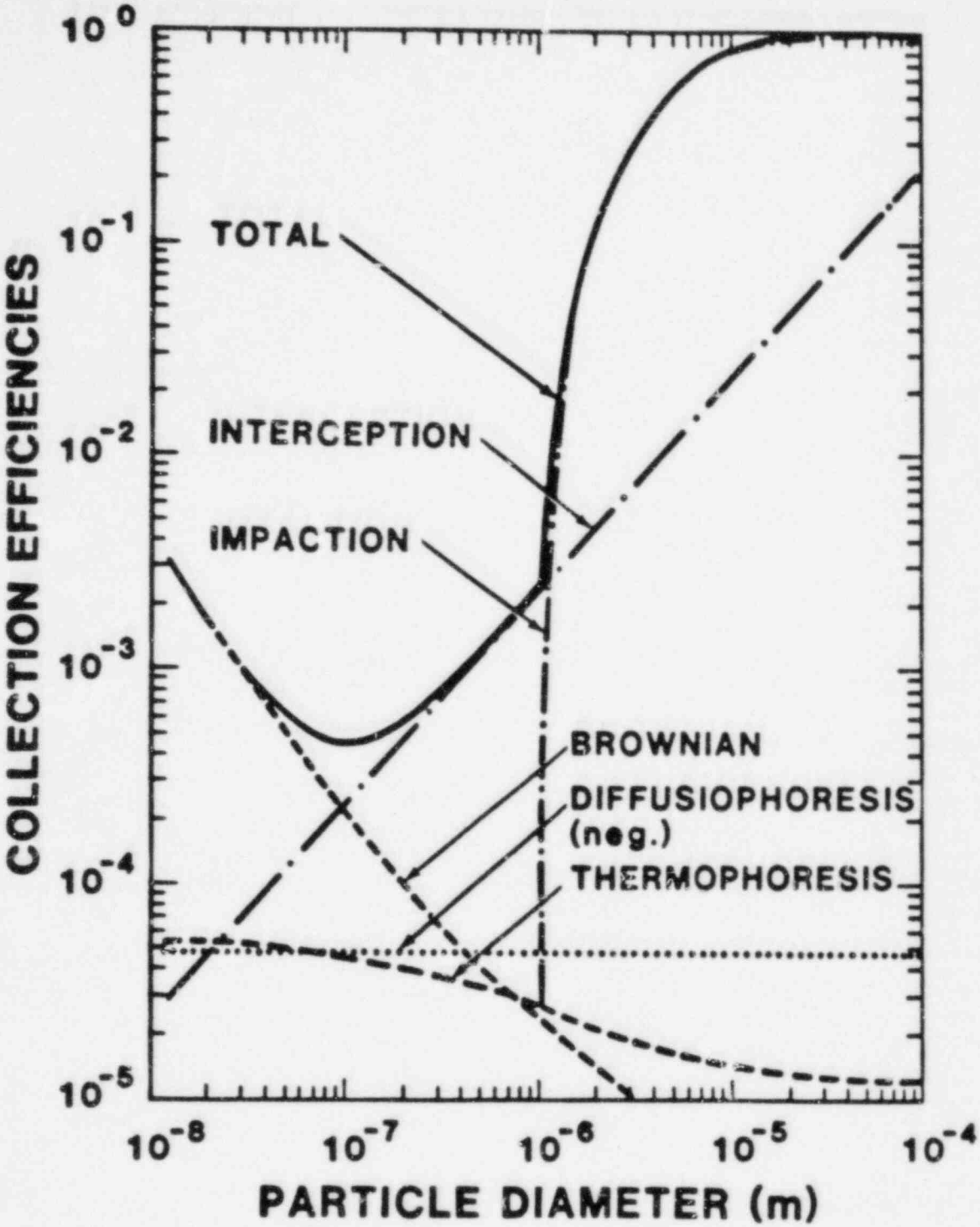

Figure 4-9. Aerosol collection efficiencies for a 1000 μm spray drop as a function of particle size for the collection mechanisms treated in the CONTAIN spray model. The diffusioporetic effect is negative for the containment conditions assumed here.

Containment Phenomena Following Spray Recovery

The sequence to be analyzed here as an example of the effects of spray recovery is essentially the same as the Surry TMLB' sequence analyzed in Section 4.3. However, the hydrogen inventory was increased so that burn severity would be limited only by the oxygen inventory of the Surry containment, not by the amount of hydrogen. The rationale was that the actual hydrogen inventory is quite uncertain, and only hydrogen burns with a severity near this upper bound pose a substantial threat to the Surry containment.

According to the Surry Safety Analysis Report,[24] normal operating procedures for the Surry sprays start with operation of the injection spray at a design flow of 252 kg/sec. After about 90 seconds, the recirculation spray initiates also, with a design flow of 347 kg/sec. The injection spray is supplied from the refueling water storage tank, having a capacity of 2120 m^3, and will shut off when this is exhausted, after a maximum of 8400 seconds. The recirculation spray then continues alone. This sequence of events was assumed in the present calculation, even though it is not clear that it would actually be followed in the TMLB' power recovery scenario. The effects of some alternative assumptions will be explored in the limited sensitivity studies reported later in this section.

Two alternatives were investigated as to the assumed time of spray initiation. In one case, designated the "early" case in the discussion below, a time of 12000 seconds after accident initiation was assumed. This is only 2500 seconds after vessel failure, and radionuclide levels are still high; however, steam concentrations are also high (about 75 mole percent) and the spray systems must operate about 820 seconds before the 55% de-inerting criterion is met. In the second case, designated the "late" case, spray initiation was deferred until 25000 seconds into the accident, when radionuclide concentrations were lower but steam concentrations had also fallen to about 56.5 mole percent. Hence, the de-inerting criterion was met only 80 seconds after spray initiation, and during this short time only the injection sprays were operating to remove radionuclides. In both cases, a hydrogen burn was assumed to initiate as soon as de-inerting took place.

Pressures are plotted as a function of time for the base case (no sprays) and the two spray recovery cases in Figure 4-10. At the time of the hydrogen burns, pressures rise to slightly over six bars, not enough to severely challenge the containment although the pressure combined with high temperatures (in excess of 700 K) might conceivably act to induce leakage, e.g., due to seal failure. In these calculations, the standard CONTAIN flame speed correlations were assumed, which implied a slow burn with a duration of about 55 seconds in the steam-rich atmosphere characteristic of de-inerting burns. This duration is sufficient to permit the

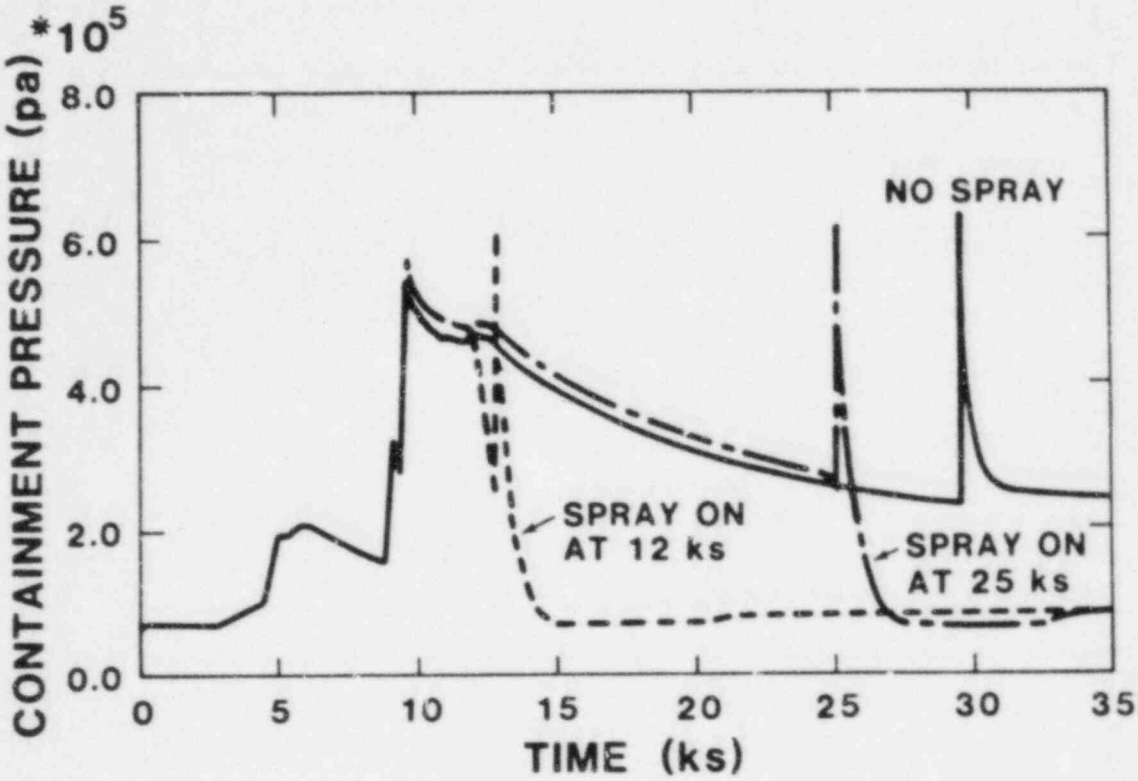

Figure 4-10. Pressure-time histories for the Surry TMLB' base case with no spray recovery and for two scenarios with augmented hydrogen inventories and with spray recovery at 12000 s and 25000 s, respectively.

sprays to substantially mitigate the peak pressures that would otherwise develop. There is, however, little data available to support the flame speed correlations at these high steam fractions and no data at all to support their use in the presence of sprays. Shorter burn times yielding higher pressures cannot be ruled out and the effects of shorter burn times are explored in the sensitivity studies discussed below.

In Figure 4-11, airborne radionuclides, expressed in total curies, are plotted as a function of time for these three cases. Once the sprays initiate, the airborne radioactivity declines very rapidly. Substantial decontamination prior to the hydrogen burn occurs even for the late spray initiation case, where the available time is short. Indeed, airborne radionuclide curves appear to dip to anomalously low levels shortly after the hydrogen burns, and also before the burn in the early spray initiation case.

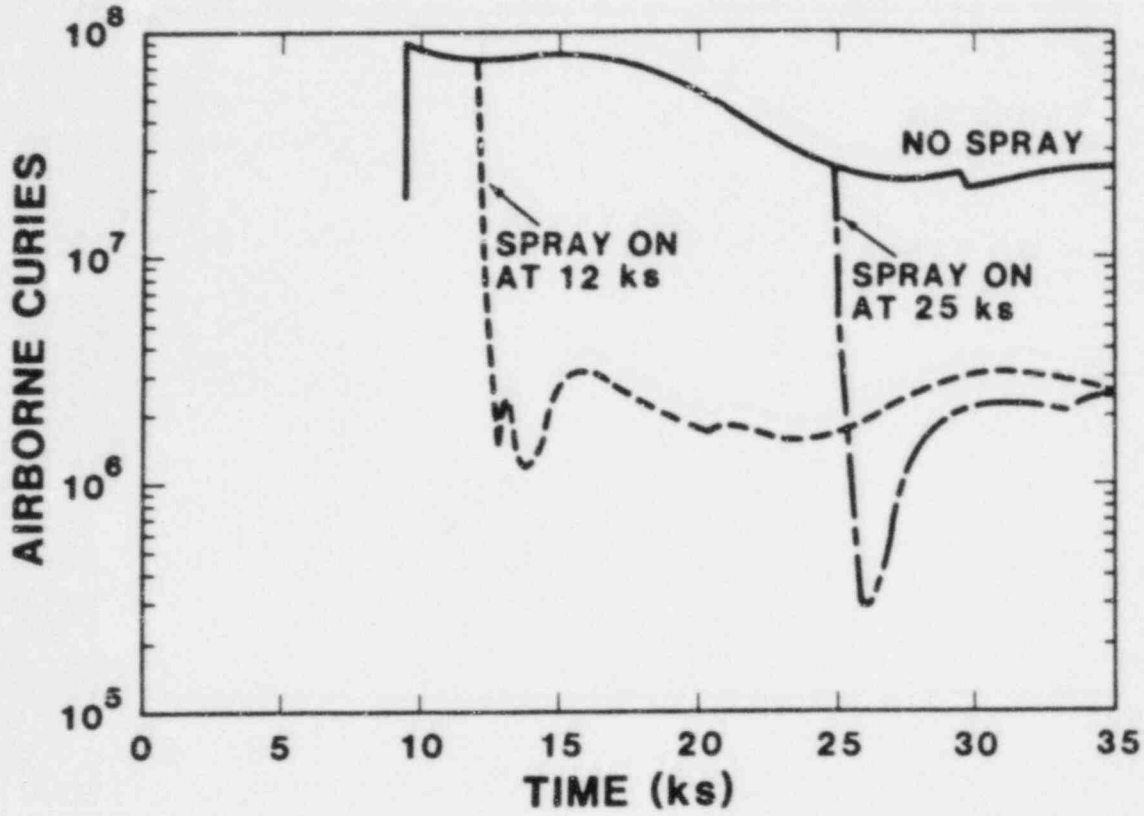

Figure 4-11. Airborne radionuclides as a function of time for the three scenarios of Figure 4-10.

Rapid decontamination by sprays may be in accord with intuitive expectations; however, examination of the parameters of this calculation shows that it is not immediately obvious that such rapid decontamination should be expected and that some explanation is indeed called for. A simple analysis of decontamination rates that might be expected can be performed by noting that the mass median diameter of the aerosol sources in these calculations was 1 μm for all species, except for two minor components of the aerosol released at vessel failure time. For particles of this size and a spray drop size of 1000 μm, as was assumed here, Figure 4-9 indicates that the collection efficiency will be about 0.0025. A simple calculation using the spray parameters assumed in this analysis then indicates that a factor of two decontamination prior to the hydrogen burn would be expected in the early initiation case; allowing for the enhanced phoretic effects characterizing the transient conditions of the present problem would yield another factor of two, for an overall decontamination factor of about four. In the late case, very little decontamination prior to the hydrogen burn is predicted by this kind of simple analysis, even allowing for the phoretic effects.

The actual effects of the sprays as calculated by CONTAIN are dramatically larger. For the early spray initiation case, the sprays reduce airborne radionuclides from 75.5 MCi to 1.65 MCi at the time of the hydrogen burn, a factor of 50. Even for the late initiation case, airborne radionuclides are reduced from 24.6 MCi to 4.2 MCi, a factor of almost 6, in the short interval prior to burn initiation. An investigation into the details of the CONTAIN analysis leads to the conclusion that simplistic calculations are inadequate, and an integrated calculational tool is needed for accurate predictions of aerosol removal by sprays.

There are several reasons for the very rapid decontamination by the sprays. The simplest has to do with the effect of agglomeration, which shifts the actual size distribution of the airborne aerosol toward sizes significantly larger than those of the source. At the time the sprays come on, particles larger than 1.5 μm were calculated to account for about 62% of the airborne mass in the early case and about 85% in the late case. For these particles, Figure 4-9 indicates that scavenging by the inertial impaction mechanism will be very efficient. In the late case, it was found that, at the time of hydrogen burn initiation, the larger aerosol particles had been greatly depleted, while particles of 1 μm diameter and less had undergone very little depletion, much as one might expect from the simple analysis.

The situation is more complex for the early spray initiation case. Here all parts of the size distribution were substantially depleted. Examination of the detailed CONTAIN output shows that cooling of the atmosphere by the spray produced supersaturated conditions within the containment atmosphere during the interval between spray initiation and the hydrogen burn. As a result, water aerosol condensed in the containment atmosphere, with the amount being one to two orders of magnitude greater than the total solid aerosol present. The combined effect of condensation and agglomeration shifts the effective particle size of the solids into the region of higher spray collection efficiencies.

The interplay of key variables over the time interval of interest (11000 - 16000 s) is illustrated in more detail for the early spray initiation case in Figure 4-12. In the figure, plots are given for the pressure, the temperature, the effective collection efficiency for airborne radionuclides (averaged over all particle sizes and averaged over the drop fall history), the total curies airborne, and the concentration of water aerosol. After the sprays initiate, the pressure declines by a factor of

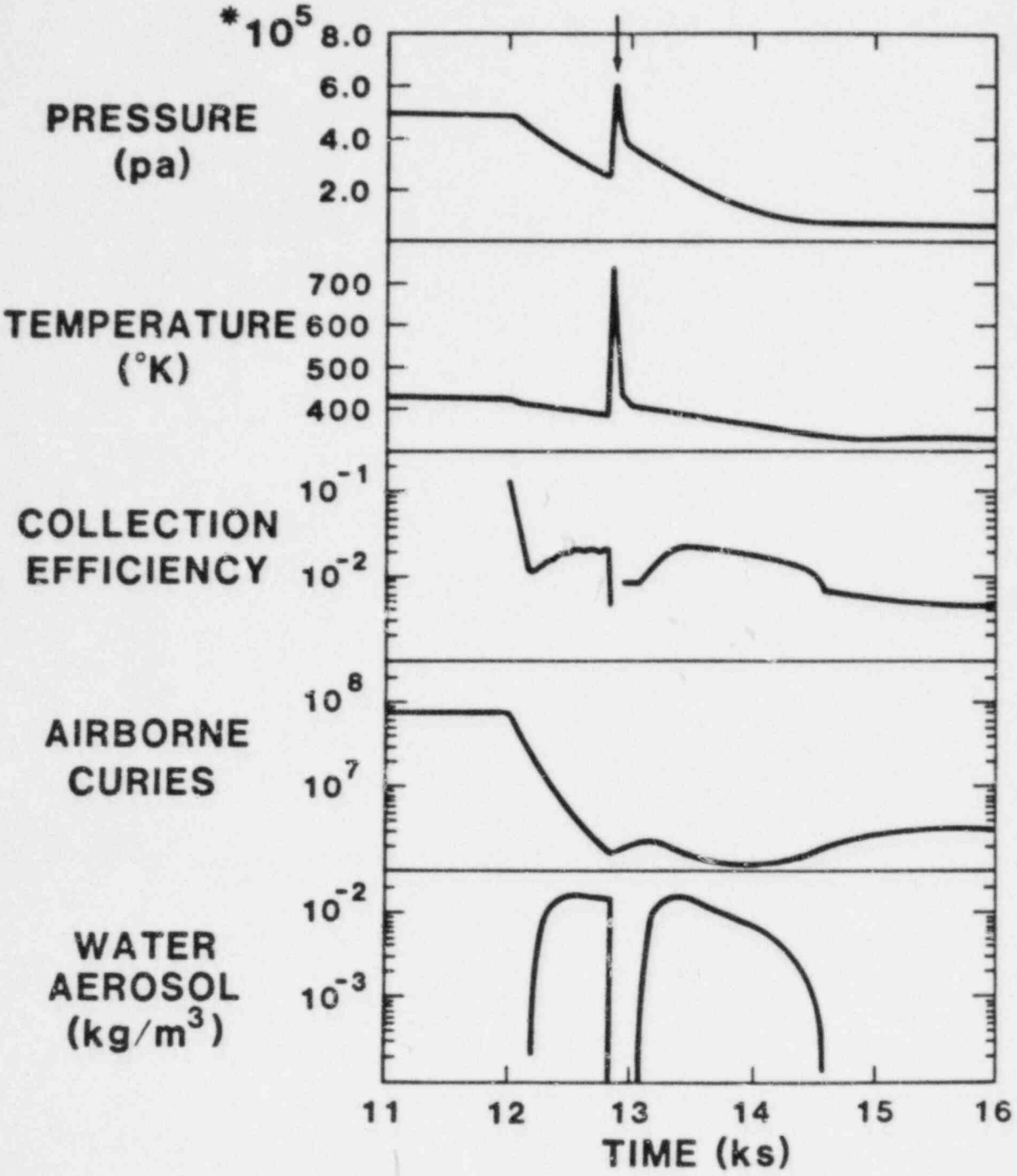

Figure 4-12. Plots of interrelated key parameters during the period shortly after spray recovery for the TMLB' early recovery scenario with augmented hydrogen inventory. The arrow indicates time of hydrogen burn.

two prior to the hydrogen burn and the temperature declines along the saturation curve. The radionuclide collection efficiency is initially very large, corresponding to collection of particles from the large end of the size distribution, but it falls very rapidly as these large particles are depleted until the condensation of water aerosol begins. At this point, the collection efficiency rises significantly. The radionuclide concentration declines steadily until the hydrogen burn occurs, at which point the water aerosol immediately evaporates and the collection efficiency decreases very sharply (it actually becomes undefined during the period of highest temperatures, as the spray drops evaporate completely during their fall). Airborne radionuclides start to increase for a brief period, since radionuclide sources are fairly strong at this time, about 7500 kCi/sec.

Following the hydrogen burn, the temperature recovers almost immediately, but the immediate recovery of the pressure is less complete because most of the hydrogen burn energy initially goes into evaporating spray water, and the resulting steam partially repressurizes the containment. As this steam is recondensed, the course of events following spray initiation is repeated: water aerosol reappears, radionuclide collection efficiencies rise, and airborne radionuclide levels resume their decline. Eventually the containment reaches a quasi-steady state with a small degree of superheat as described in the previous subsection. At this point, the water aerosol disappears, radionuclide collection efficiencies decline, and airborne radionuclide concentrations increase (the increase would be larger were it not for a decline in radionuclide source strengths to the containment at this time). However, by the time the water aerosol disappears, the containment pressure has returned to subatmospheric levels; had damage from the hydrogen burn resulted in a leak, the leakage would have ceased by this time.

In the late spray initiation case, the interval between spray initiation and the hydrogen burn is too short for the condensation of water aerosol to develop and have any significant effect upon the airborne radionuclide concentration. After the burn occurs, however, the sequence of events is essentially the same as in the early spray initiation case. It is the effect of the water aerosol resulting from the atmosphere cooling by the sprays that leads to the deep dip in the radionuclide concentration following the hydrogen burn (Figure 4-11). Once again, the containment has reached subatmospheric pressures by the time the water aerosols and their effects dissipate.

Variations in Spray and Hydrogen Parameters

The Surry injection and recirculation spray systems are both fully redundant with 100% of design capacity and, based upon the SAR descriptions, it appears that operation at 200% of design flow rates is possible. Hence, the consequences of doing so were explored. In addition, calculations were performed for the "normal" or base case hydrogen sources, without the augmentation assumed in the preceding analyses. Finally, calculations were run assuming a substantially shortened (5 sec.) hydrogen burn time with the large hydrogen supply.

In Figure 4-13, the response of total curies airborne to variations in spray flow rate and in hydrogen quantities are illustrated for the case of spray initiation at 12000 sec. Plots are given for the case discussed above, the same case

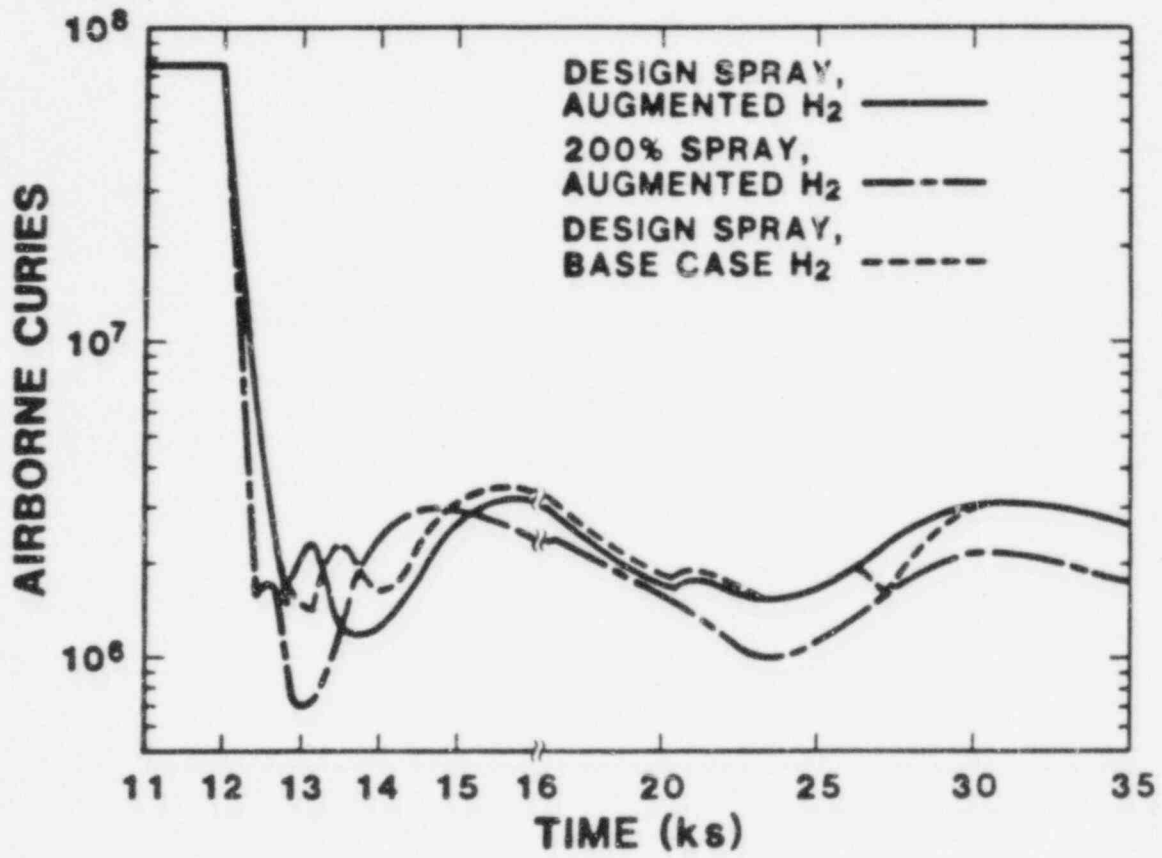

Figure 4-13. Airborne radionuclides as a function of time for three variations on the TMLB' scenario with spray recovery at 12000 S. Burns occur at the top of the first maximum following spray initiation in each curve.

with the spray at 200% of design flow, and the case with 100% of design flow and only the base case hydrogen sources assumed present. Doubling the spray flow rates accelerates the course of events following spray initiation, but otherwise the sequence is quite similar. When containment steady state conditions are reached, concentrations of airborne radionuclides are smaller with the higher flow rates but the difference is slightly less than a factor of two; apparently the reduced residence times at the higher flow rates reduce the degree to which agglomeration can enhance particle size and collection efficiency during spray operation. The times at which total spray flow rates decrease due to shutoff of the injection spray is also reflected in Figure 4-13 (and in Figure 4-11) by small but rather abrupt rises in the airborne radionuclide curves.

For the case with only the base case hydrogen sources, the sequence of events following spray initiation is similar to that found with the augmented source except that the burn is slightly delayed because the hydrogen concentration takes longer to reach 8% (which occurs some time after steam de-inerting has occurred). Following the burn, the effects are still similar to the previous case but not quite as strong. This initial burn does not reduce oxygen levels to a degree sufficient to prevent subsequent burns and, at about 26000 seconds, sufficient hydrogen from core-concrete interactions accumulates that a second burn does occur. This burn is quite mild and leads to the production of only relatively small amounts of steam. Nonetheless, some condensation of water aerosol is calculated to occur, and a noticeable dip in the concentration of airborne radionuclides results.

Some of the more important results of these additional studies are summarized in Table 4-3. The first column gives a run identification number and the next four columns describe the conditions of the run: spray intensity relative to the design basis, spray initiation time (t_{spr}), hydrogen inventory at the time the burn initiates, and the burn duration time. The latter quantity is actually calculated by the CONTAIN default burn correlations for all cases but the last two. The last five columns summarize some results of particular interest: the peak pressures and temperatures resulting from the burn, the time delay between spray initiation and burn initiation, and the radioactivity (curies) airborne at the time the sprays initiate and at the time the burn initiates.

Key results concerning spray recovery for the Surry TMLB' sequence may be summarized as follows:

1. The challenges posed by hydrogen burns with the base case hydrogen sources are all very mild, partly because of the smaller hydrogen inventories but also because reduced hydrogen concentrations lead to longer burn durations in the CONTAIN correlations. Other things being equal, increasing the spray intensity reduced the thermal-hydraulic challenge from the hydrogen burns, as one would expect.

2. If much shorter burn times are hypothesized, the large hydrogen inventory cases yield more severe challenges to the containment (cases 9 and 10), even though spray flow rates at 200% of design basis were specified for these cases. The 5 second burn time assumed here may be overly conservative; however, it should be noted that the actual degree of burn slowing due to high steam fractions is very uncertain, especially with sprays operating. Moreover, the CONTAIN correlations in the case of low steam concentrations would give even shorter burn times, about 2.8 seconds. Moreover, it has been suggested that turbulence resulting from spray operation might accelerate hydrogen burns.

3. In all cases, very substantial decontamination resulted during the interval between spray initiation and burn initiation, even when this interval was short. The degree of decontamination was not very sensitive to the parameters varied in this study.

4. All the cases with sprays exhibited steam condensation, water aerosol production, and enhanced decontamination during the time interval between the hydrogen burn and complete containment depressurization due to the action of the sprays. Again, the occurrence of this behavior was not sensitive to the parameters that were varied in this study.

Table 4-3

Results of Parameter Variations, Spray Recovery Scenario

Case	Sprays: Flow (% of Design)	Sprays: Time On, t_{spr} (s)	Hydrogen: Mass at t_{burn} (kg)	Hydrogen: Burn Duration (s)	Burn: P_{max} bar	Burn: T_{max} (K)	Burn: $t_{burn}-t_{spr}$ (s)	Radionuclides Airborne (MCi): at t_{spr}	Radionuclides Airborne (MCi): at t_{burn}
1	None	--	780[c]	84.4	6.33	1192	b	--	22.9
2	100%	12000	482[c]	113	2.76	467	135	74.3	1.45
3	100%	25000	727[c]	93.1	3.80	513	185	24.5	2.44
4	100%	12000	1155[d]	54.8	6.12	742	820	75.5	1.65
5	100%	25000	1224[d]	53.6	6.25	752	85	24.6	4.10
6	200%	12000	474[c]	112	2.35	424	570	73.5	0.93
7	200%	25000	726[c]	93.7	3.33	458	110	24.5	2.41
8	200%	12000	1150[d]	54.9	4.87	534	425	74.3	1.84
9	200%	12000	1149[d]	5.0	8.57	1320	425	75.5	1.59
10	200%	25000	1224[d]	5.0	9.01	1410	45	24.6	3.99

[a]Burn duration from CONTAIN default correlation for Cases 1-8.

[b]Burn occurred at 29550 sec. for all cases.

[c]Base case hydrogen sources.

[d]Augmented hydrogen sources; burn magnitude oxygen-limited.

Some caveats should be made lest it be concluded that the benefits of these phenomena can be counted upon for all spray recovery scenarios. Even though the time required for substantial decontamination upon spray initiation is very short, it is obvious that no such decontamination can be expected to occur prior to the hydrogen burn if spray initiation also initiates the burn. This event could arise if the atmosphere had actually de-inerted prior to spray initiation and the spray systems provide an ignition source (e.g., electric sparking). It is also possible that the atmosphere composition might be inert while stagnant but support combustion in the presence of spray-induced turbulence. In addition, the strong post-burn decontaminating effects of the sprays will provide little mitigation if the hydrogen burn results in catastrophic containment failure, as might occur in Cases 9 and 10 in Table 4-3. Still another concern would be spray disablement as a result of the burn.

There are a number of parameters whose effects upon these phenomena have not been studied here. These parameters include the inlet spray water temperature. There is some reason to believe that water temperatures higher than those assumed here (324-331 K) could reduce the water aerosol effects, though no detailed studies have yet been made. Another parameter of some significance is the density of the aerosol materials; values lower than the 3000 kg/m^3 assumed here would reduce spray effectiveness somewhat.

On the other hand, one modeling uncertainty should be noted that could mean that CONTAIN is actually underpredicting the decontamination associated with sprays in these scenarios. Many potential aerosol components have at least some affinity for water, even if they are insoluble, and some components (e.g., CsOH) may even be strongly hygroscopic. CONTAIN does not allow for any affinity of the aerosol materials for water, and this effect could increase the amount of condensation upon aerosols. Indeed, it is quite possible that affinity for water could lead to condensation of significant water upon the aerosols even during the quasi-steady conditions, when the atmosphere is generally superheated but typically only by very small margins, with relative humidities in the 90-99% range. Should this be the case, the calculation may be significantly underestimating spray effectiveness under the quasi-steady conditions normally prevailing during spray operation, not just the transient conditions emphasized here.

4.5 Integrated Analysis of Isolation Failure Sequences

Recently, there has been an increasing appreciation of the effectiveness of natural processes in depleting airborne radionuclides within containment during severe accidents. Hence, there has been a corresponding focus of attention upon sequences involving early containment failures, in which the natural processes will have a minimal opportunity to mitigate accident consequences. Unless such sequences can be shown to be especially improbable, they will likely dominate total risk because of their higher consequences.

One important class of such sequences involves containment isolation failure (ß-sequences, in WASH-1400 terminology), such that the containment is impaired from the very start of the accident. Calculations concerning one such sequence, the Surry AB-ß sequence, will be discussed here. Results will be compared with other recent evaluations of this sequence and examined for the purpose of identifying the kind of effects revealed by integrated analysis.

The AB sequence is defined as a large break LOCA with loss of all AC power and thus failure of both emergency core cooling and all containment ESFs. The sequence is of low probability and therefore not thought to be a major risk contributor. However, if it is assumed the break is in the hot leg (as in all analyses to be discussed here), radionuclide transport path lengths and residence times within the primary system are minimized. Hence, AB hot-leg sequences provide maximum opportunity for the radionuclides to escape from the primary system to the containment, which is one reason the sequence has been of interest in source term calculations, despite the low probability believed to be associated with it.

The AB-ß sequence is one of those selected for study in the early Battelle source term analyses reported in Volume I of BMI-2104,[5] and was included when the Surry analysis was repeated using revised models and revised input assumptions as reported in Volume V of BMI-2104. The sequence also was analyzed in some detail in an important study of severe accident source terms performed for the American Nuclear Society (ANS) by Stone and Webster Engineering Corporation.[3] Both the present work and the ANS work were patterned in part after BMI-2104 in order to facilitate comparisons among the various studies; since the more recent version of the Battelle analyses was not available at the time that the ANS and CONTAIN studies were initiated, both the latter employed Volume I of BMI-2104 as a source of needed input data.

In this section, comparisons will be made between CONTAIN calculations and some of the ANS results for this sequence (For some comparisons between CONTAIN and BMI-2104, Vol. I, see Reference 25.). In the ANS study, a number of sensitivity studies were performed, including a study of the release as a function of the the effective area of the leakage path or paths characterizing the isolation failure. The study found that there was a "worst case" hole size of about 0.093 m^2 (1 ft^2), with larger leak areas as well as smaller ones giving lower releases. A similar study has been performed with CONTAIN, and the results obtained will be presented and compared with those of the ANS study.

The AB sequence is characterized by a very rapid blowdown, lasting at most a few tens of seconds. Remaining water in the vessel boils off until the level drops to below the core, after which any further boiloff continues at much reduced rates until hot core material begins to descend into the vessel lower plenum. In typical calculations using the MARCH code, as described in BMI-2104, core melt starts within the first half hour of the accident, core slumping into the lower plenum begins at 40-55 minutes, and vessel failure occurs well over an hour into the accident. Major releases of the relatively volatile species (noble gases, CsI, and CsOH) from the fuel are calculated to begin before core melt, and most of these species are calculated to be released from the fuel by the time of core slump. At this time, substantial amounts of water (20,000 - 25,000 kg) are calculated to remain in the lower plenum, providing an important source of steam and hydrogen to the containment when the core slumps. Steam sources to containment during the period from the start of core degradation to core slump are calculated to be strongly superheated in these analyses.

The total aerosol mass assumed to be released from the RCS was about 435 kg for the CONTAIN calculations, and this material included slightly over half of the core inventory of the volatile species. Since the aerosol released from the RCS was calculated to have a considerably higher specific activity than that of the aerosol generated in core-concrete interactions, the RCS aerosol dominates the potential consequences of an early containment failure. Results to be presented will be discussed in terms of the "containment release fraction," which is defined to be the ratio (RCS aerosol released to the environment)/(total RCS aerosol released to the containment).

In Figure 4-14, the RCS aerosol release fraction is plotted as a function of time for leak sizes of 0.05 m^2 (Case 1) and 1.0 m^2 (Case 2). For the smaller leak, the RCS aerosol released increases smoothly as a function of time, with the rate of increase declining as the driving pressure within containment decreases and as the RCS aerosol remaining airborne within containment decreases. For the larger leak sizes, the release of RCS aerosol is more concentrated around the time of steam and hydrogen sources to containment that are associated with core slump into the lower plenum. With the large leak sizes, the containment fully depressurizes from the initial blowdown before the RCS aerosols are released to the containment and driving forces for expelling these aerosols are small until the steam and hydrogen sources associated with core slump commence. Indeed, in-leakage of outside air is calculated to occur during some intervals, because cooling and steam condensation within the depressurized containment exceed the heat and gas sources at these times. Similar behavior was observed in the ANS study.

For the large leak sizes, the release associated with the steam sources during and shortly after core slump is substantially augmented by pressurization due to simultaneous hydrogen burns. The default assumption in CONTAIN is that a burn initiates whenever the flammability criteria are met, i.e., whenever hydrogen and oxygen concentrations exceed 8 and 5 mole percent, respectively, and the steam concentration is less than 55 mole percent. For the larger hole sizes, steam concentration is calculated to be in the range 45-50 mole percent at the start of core slump and the hydrogen concentration is 7-7.9 mole percent; thus, burns have not occurred up to this time because hydrogen concentrations are insufficient, although the steam concentration is low enough to permit burns. At the time of core slump, metal-water reactions in the lower head produce a burst of hydrogen sufficient to drive the containment hydrogen concentration to values of the order of 9.5 mole percent, thus initiating a burn. It is interesting to note that the "window" for burn initiation is quite short in this calculation; if a burn is hypothesized not to occur at this time (e.g., for lack of an ignition source) the burn criteria would cease to be satisfied after less than ten minutes because of steam inerting and/or dilution of hydrogen by steam.

For the smaller leak sizes, containment depressurization from the initial blowdown is not complete at the time of core slump, and the gas density is, therefore, higher. Hence, the hydrogen is diluted to a greater extent than with the large leak sizes and concentrations in excess of the burn initiation criterion do not arise during this period.

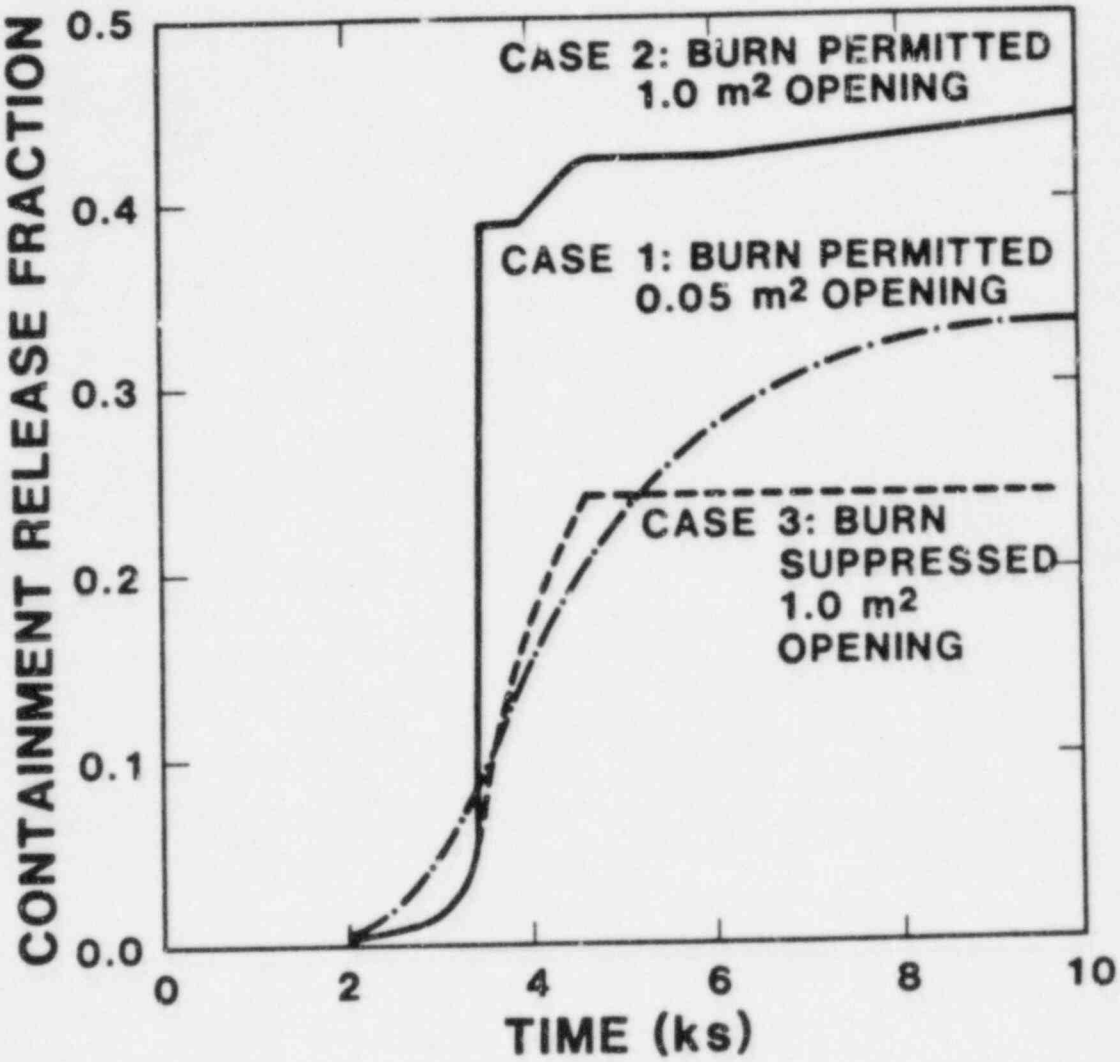

Figure 4-14. Containment release fraction of RCS aerosols as a function of time for the Surry AB-β (isolation failure) sequence for a 0.05 m^2 leak area and for a 1.0 m^2 leak area with and without hydrogen burns.

The margins by which the burn criteria are satisfied or not satisfied are often rather small in these calculations. Whether the burn criteria are met is relatively sensitive to the thermal-hydraulic conditions at the time of interest, as well as to the exact timing and magnitude of the hydrogen sources. Furthermore, it is not obvious that an ignition source will be available during the relatively brief period that the burn criteria were calculated to be satisfied. Hence, it is plausible to assume that no burns will occur at the time of core slump, even for the large leak size. Case 3 in Figure 4-14 shows the containment release fraction as a function of time for the 1 m^2 leak size with hydrogen burns deleted from the calculation. Much of the release is still concentrated during the time of boiloff following core slump, but the total release is significantly smaller than when the hydrogen burn was permitted to occur.

To understand the similarities and differences between these results and the ANS study results, it is necessary to compare the ANS calculational method to the CONTAIN work. In both the ANS study and the present work, all sources of radionuclides and aerosols to the containment were taken from Volume I of BMI-2104, as were all sources of gas, steam, and energy to the containment following vessel failure. Prior to vessel failure, the ANS study used steam sources to containment calculated by the RELAP-4 code for the blowdown phase of the accident and sources were calculated using hand calculations for the boiloff and core slump phases. In the CONTAIN work, steam and hydrogen sources were those of BMI-2104 Volume I (calculated using MARCH 1.1) except that the sources during and after core slump were modified to correspond more closely to the sources used as input in the ANS study, which also were considerably closer to the corresponding sources in Volume V of BMI-2104 than to those of Volume I. Although the steam and hydrogen sources assumed in the present work are not identical to those of the ANS study, it is thought that the remaining differences in these sources are not sufficient to cause major discrepancies in the calculated radionuclide release.

In the ANS study, aerosol and radionuclide transport and deposition were performed using the NAUA aerosol code,[26] and containment thermal-hydraulic analyses were performed using the THREED code.[3] In the present work, the CONTAIN integrated thermal-hydraulics and aerosol analyses were used for all phases of the in-containment analyses. For both studies, the results to be discussed below were obtained using single-cell representations of the containment, although the ANS study also included some multi-compartment analyses.

In Figure 4-15, the containment release fraction is plotted as a function of effective leak area for both the CONTAIN and the ANS studies. Results are given at a time of three hours into the accident; leakage of RCS aerosols is largely complete at this time and results at much later times would not be significantly different. For the CONTAIN calculations, the complete series was run both with and without hyd ogen burns being permitted whenever the burn criteria were met.

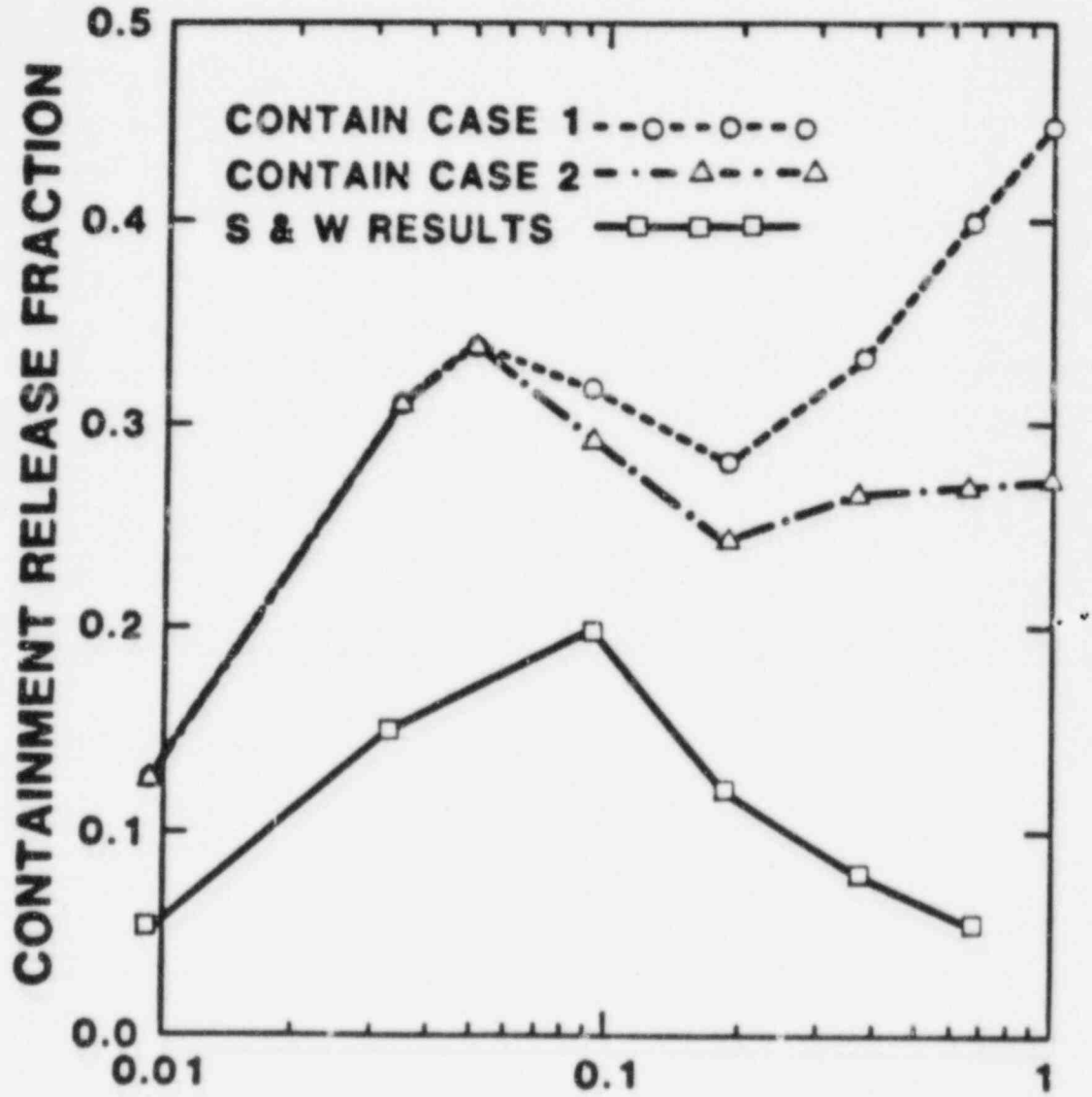

Figure 4-15. Time-integrated containment release fraction of RCS aerosols as a function of leak area as calculated by the American Nuclear Society study (S&W)and as calculated by CONTAIN with (Case 1) and without (Case 2) hydrogen burns being permitted.

Qualitatively, there are important similarities between the two sets of CONTAIN results and the ANS results. For the smallest leak sizes, the amount of leakage is limited by the amount of material that can flow out the leak before natural processes deplete the airborne RCS aerosol within containment; the containment remains substantially pressurized in these cases. For the smaller leak sizes, the release therefore increases as the leak size increases. In all three series of calculations, there is a maximum in the release fraction for leak sizes of the order of 0.05-0.1 m^2, with the release fraction tending to decline when the leak size is increased to somewhat larger values. The reason is that larger leak sizes permit the initial pressurization of the containment to completely dissipate before the radionuclides are released from the RCS.

For the CONTAIN results with hydrogen burns, after a slight dip, the release fraction as a function of leak size again turns upward. Hydrogen burns occur at the time of core slump in these calculations for all cases with leak areas of 0.093 m^2 or larger, but the leak area must be significantly greater than this for the burn to be very effective in increasing the containment release fraction. One reason is that the pressure pulse due to hydrogen burns is quite short, considerably shorter than that due to bursts of steam, and large leak sizes are required if this brief pressure pulse is to drive large amounts of material out of the containment.

For leak sizes of 0.05 m^2 or smaller, no burns occur until much later in the accident, roughly three hours after initiation. The effects of these burns upon the RCS aerosol release fraction is totally insignificant.

Despite the qualitative similarities, there are significant quantitative differences between the results of the ANS study and the CONTAIN results, even when hydrogen burns are suppressed in the latter (the ANS study did not predict burns to occur at this time). The CONTAIN calculations tend to give higher containment release fractions, especially for the larger leak areas. The reasons for these differences have not been fully identified. However, some possible effects related to integrated analysis have been identified, and it is instructive to consider them.

The effects of interest are related to the difficulty of giving a proper account of the liquid water content in the containment atmosphere in a conventional thermal-hydraulic code which, like THREED, does not treat aerosol processes. The conditions of the initial blowdown are such that somewhat less than half the primary system water actually flashes to steam,

and the remainder is introduced into the containment as liquid. In CONTAIN, this liquid is introduced by condensation as a water aerosol uniformly throughout the volume. In reality, a localized two-phase jet occurs so CONTAIN's treatment of this source would tend to overpredict the amount of liquid water in the form of fine particles, as opposed to larger droplets. However, the treatment of the subsequent agglomeration and settling of the water aerosol is mechanistic. The initial aerosol density is extremely high by normal aerosol standards, about 2 kg/m^3, and it is therefore very rapidly depleted by agglomeration and settling. It is characteristic of calculations involving initially dense aerosols that the system quickly loses "memory" of the initial conditions, and the amount airborne at later times is insensitive to these initial conditions. Hence, the CONTAIN description of the liquid water content of the atmosphere at later times (i.e., after a few minutes) is expected to be reasonably realistic.

In THREED, as in CONTAIN, the blowdown is assumed to result in a steam-water mixture, but THREED has no means of mechanistically modeling the behavior of the liquid water in the atmosphere. In the ANS study, the liquid was left in the atmosphere by modeling it as steam with a quality of less than one.[27] Since precipitation of the liquid fraction by aerosol processes is not modeled, the calculation can substantially overestimate the containment atmosphere liquid water content at later times.

In the CONTAIN calculation, agglomeration and settling reduced the liquid content of the atmosphere to less than 0.1 kg/m^3 by the time superheated steam and gas associated with core degradation began to flow into the containment. By the time any solid aerosols were introduced, evaporation due to the superheated steam, plus continued settling, had essentially totally eliminated the water aerosol from the atmosphere, and the water aerosol initially present actually played no role in the subsequent solid aerosol and radionuclide behavior. Indeed, the flow of hot gases into the containment resulted in substantial superheat developing, of the order of 50 K, and steam fractions fell to levels sufficiently low to permit hydrogen burns, as noted previously.

In the ANS study, superheated conditions did not develop because the superheat of the steam and gas sources from the core went to evaporating part of the liquid water fraction assumed to be still present in the atmosphere. One possible consequence involves the occurrence of hydrogen burns. While the ANS study did not treat the effects of hydrogen burns upon aerosol release, it was found that the THREED calculations

indicated steam fractions in excess of 60% at the time of core slump,[27] probably too high to permit hydrogen burns in any case. It is likely that the evaporation of the atmospheric liquid water fraction assumed to be still present played a significant role in maintaining the calculated steam fractions at these high levels.

In the ANS study, it was recognized that liquid water aerosol could affect the behavior of the solid aerosols, and that THREED could not give an adequate accounting of the amount of liquid airborne. Hence, NAUA calculations were performed to address the water aerosol behavior. In the calculations referred to in Figure 4-15, it was assumed that 25% of the total blowdown liquid, or about 28000 kg, was initially introduced as a water aerosol. As in CONTAIN, NAUA calculated agglomeration and settling to reduce this water by large factors before solid aerosols are released to the containment. However, the codes were decoupled, and in the absence of evaporation due to superheat, substantial (~1000 kg) water aerosol did remain airborne at the time release of solid aerosols began. Although this amount of water aerosol is not very significant in terms of thermal-hydraulics, it is quite significant in terms of aerosol physics, and agglomeration of the liquid aerosol with the solid aerosol would be expected to significantly enhance the settling rate of the latter and thereby reduce the release fractions.

In the ANS study, it was recognized that the amount of water aerosol injected at the time of the initial blowdown was quite uncertain. A sensitivity study was therefore performed for the 0.093 m^2 leak case, in which the water aerosol assumed to be initially present was varied from 0 to 28000 kg. It is the results with no water aerosol that would be analogous to the CONTAIN calculation, since the latter evaporated all its water aerosol. For this case, the ANS study calculated a release fraction of 0.33, which is in very good agreement with the release fraction of 0.29 calculated by CONTAIN for this leak size, without hydrogen burns. It would probably be an over-simplification to attribute all the differences between the CONTAIN calculations and the ANS results to these effects, but this agreement is certainly suggestive.

To summarize, it appears that the analyses of the AB-ß sequence illustrate the interplay of phenomena in an integrated analysis in the manner suggested in Figure 3-1. In the CONTAIN integrated analysis, aerosol processes rapidly deplete the great majority of the liquid water initially airborne; the small remainder is quickly evaporated following the onset of sources of superheated steam and gas from the RCS. Hence,

liquid water plays no role in the transport and deposition of the solid aerosols and associated radionuclides, and steam fractions fall to sufficiently low levels to permit hydrogen burns to add to the driving forces available to expel radionuclides from the containment. In the thermal-hydraulic calculation without an integrated model for water aerosol, the liquid water assumed to remain in the atmosphere is large enough to keep the atmosphere saturated and probably at least contributes to keeping steam fractions high enough to prevent hydrogen burns until much later in the accident; the non-integrated aerosol calculation predicts sufficient water aerosol to remain airborne to significantly affect the behavior of the solid aerosols.

5. CONCLUSIONS

A number of general conclusions can be made on the basis of the calculations and analyses discussed in this report. It is clear that severe accident containment analysis involves complex interactions among many disparate phenomena, and that simple or intuitive analyses are likely to be inadequate (and may be completely misleading). The calculational studies presented here indicate (among other things) that severe accident containment codes need to take account of two-way couplings among aerosol, thermal-hydraulic, and fission product phenomena. These feedback effects may not always be important, but in many cases they are, and it is difficult to even assess their importance without an integrated analysis tool.

In this regard, one important point must be stressed. It should not be supposed that the effects of integrated analysis described here (especially in Section 4.4), were fully anticipated in advance and the calculations run to demonstrate them. On the contrary, considerable scrutiny of the detailed CONTAIN output, as well as some amount of physical understanding, were required in order to reconstruct the interplay of phenomena described here. Experience has shown that it is extremely difficult to intuitively predict the net effects that arise in integrated analyses of this type, even in a qualitative sense. Indeed, it is difficult to predict in advance whether integrated analysis will yield results exhibiting any significant differences from results of more traditional approaches. It is for precisely this reason that integrated analysis tools are expected to play increasingly important roles as the technology for severe accident assessment matures.

For containment analysis, CONTAIN is unique among present-generation computer codes in its ability to couple these areas of phenomenology, and for that reason it has been used for the studies presented in this report. However, the results presented should be considered to be only the first steps towards understanding integrated severe accident containment phenomenology. As continuing experimental research provides better understanding of individual phenomena and as calculational tools become more sophisticated and better validated against experiment, further reductions in uncertainty concerning severe accidents can be expected, so that decisions made by industry, regulators, and the public can be made on a more rational and consistent basis.

REFERENCES

1. Bergeron, K. D., Clauser, M. J., Harrison, B. D., Murata, K. K., Rexroth, P. E., Schelling, F. J., Sciacca, F. W., Senglaub, M. E., Shire, P. R., Trebilcock, W., and Williams, D. C. (1985), User's Manual for CONTAIN 1.0, A Computer Code for Severe Nuclear Reactor Accident Containment Analysis, NUREG/CR-4085, SAND84-1204, Sandia National Laboratories, Albuquerque, New Mexico 87185.

2. Lipinski, R. J., et al.,(1984). Uncertainty in Radionuclide Release under Specific LWR Accident Conditions, SAND84-0410, Sandia National Laboratories.

3. Report of the Special Committee on Source Terms, (1984). American Nuclear Society, Lagrange Park, Ill.

4. Kanzleiter, T., ed. (1984). Investigation of Reactor Containment Behavior During and After Blowdown (Water and Steam Line Break), PHDR 49-84, Kernforschungzentrum, Karlsruhe (Kfk, W. Germany).

5. Gieseke, J. A., Cybulskis, P., Denning, R. S., Kuhlman, M. R., Lee, K. W., and Chen, H., (1984). Radionuclide Release Under Specific LWR Accident Conditions -- BMI-2104, Volumes I-VI, Battelle Columbus Laboratories Report.

6. Wooton, R. O., Cybulskis, P. and Quayle, S. F. (1984). MARCH 2 Code Description and User's Manual, NUREG/CR-3988, BMI-2115, Battelle Columbus Laboratories.

7. Young, M. F., Tomkins, J. L., and Camp, W. J. (1983). "MELPROG Code Development and Methods," International Meeting on Light Water Reactor Severe Accident Evaluation, Cambridge, MA, August 28 to September 1.

8. Sprung, J. L., et al., (1983). "Overview of the MELCOR Risk Code Development Program," in International Meeting On Light Water Reactor Severe Accident Evaluation, Cambridge, MA, August 28-September 1.

9. Zabusky, N. J. (1984). "Computational Synergetics," Physics Today 37, 36.

10. Reactor Safety Study - An Assessment of Accident Risks in U.S. Commercial Nuclear Power Plants, (1975), (NUREG-75/014) WASH-1400, U.S. Nuclear Regulatory Commission.

11. Zion Probabilistic Safety Study, (1982), Commonwealth Edison, Chicago, Ill.

12. Bergeron, K. D., and Williams, D. C. (1984). "CONTAIN Calculations of Containment Loading of Dry PWR's," Proceedings of the Second Workshop on Containment Integrity, NUREG/CR-0056, SAND84-1514, Sandia National Laboratories.

13. Baumeister, T., ed. (1978). Marks' Standard Handbook for Mechanical Engineering, McGraw-Hill, New York, New York.

14. Collier, J. G. (1972). Convective Boiling and Condensation, McGraw-Hill (U.K.).

15. Camp, A. L., Wester, M. J., and Dingman, S. E., (1985). HECTR Version 1.0 User's Manual, NUREG/CR-3913, SAND84-1522, Sandia National Laboratories.

16. Gelbard, F., MAEROS User Manual, (1982), NUREG/CR-1391, SAND80-0822, Sandia National Laboratories.

17. Gelbard, F. and Seinfeld, J. H. (1980). J. Colloid and Interface Science 78, 485.

18. Fuchs, N. A. (1964). The Mechanics of Aerosols, The MacMillan Co., New York.

19. Byer, H. R. (1965). Elements of Cloud Physics, U. Chicago Press.

20. Cole, R. K., Jr., Kelly, D. P., and Ellis, M. A. (1984) CORCON-Mod2: A Computer Code for Analysis of Molten Core-Concrete Interactions, NUREG/CR-3920, SAND84-1246, Sandia National Laboratories.

21. Murata, K. K., et al., (1983). "CONTAIN: Recent Highlights in Code Testing and Validation," International Meeting on Light Water Reactor Severe Accident Evaluation, Cambridge, MA, August 28-September 1.

22. Bergeron, K. D. and Tills, J. L. (1983). Results of Blind Predictions of the HDR Steam Blowdown Experiments Using the CONTAIN Code, Winter Meeting of the American Nuclear Society, San Francisco, CA, Oct. 30-Nov. 4.

23. Bergeron, K. D. and Trebilcock, W. (1983). "The MEDICI Reactor Cavity Model," International Meeting on Light Water Reactor Severe Accident Evaluation, Cambridge, MA, August 28-September 1.

24. Surry Power Station Units 1 and 2 - Final Safety Analysis Report, Vepco, (1969), Virginia Electric and Power Company.

25. Tills, J. L., Murata, K. K., and Williams, D. C. (1983). "CONTAIN Calculations of Severe Accident Sequences at the Surry Nuclear Power Plant," Eleventh Water Reactor Safety Research Information Meeting, Gaithersburg, MD, October 24-28.

26. Bunz, H., Koyro, M., and Schoeck, W. (1983). NAUA Mod 4, Kfk-3554, Kernforschungzentrum Karlsruhe (Kfk, W. Germany).

27. Warman, E. A., Stone and Webster Engineering Corp., personal communication.

APPENDIX A

SAMPLE CONTAIN INPUT FILE

The following is the input file with which the station blackout with spray recovery at 25000 seconds case (see Fig. 4-10) was performed. The reader will note that this series of calculations used numerous and extensive tables to describe the sources of gas, fission products, and aerosols to the atmosphere These were obtained from other computer codes (MARCH, CORCON, VANESA) used in the source term studies described in References 2 and 5. This large amount of source data is not representative
tive of all CONTAIN calculations.

```
CRAY
&& ---------------------- PNE11 ----------------------------
&& ------- SURRY TMLB SEQUENCE --- SPRAYS ON AT 25000 S --
&& --------- AUGMENTED H2 AND DESIGN BASIS SPRAY --------
&& ------4APR84----PER---------
&& ---ADDITION OF LIQUID WATER FROM RCS
&& ---FINER SOURCE TABLE AT VESSEL FAILURE TIME
&& ---RADIOACTIVE CHAINS TE132 AND TE131M
&& ---INCLUDE TC IN REFRACTORY AEROSOLS
&& -----EXTENDED AER AND FISSION TABLES
&& -----EXTENDED CORCON GAS TABLES
&& -------RELEASES FROM RPV UPDATED 9/25/84 AS PER DCW--
&& ----------------AEROSOL/FISSION PRODUCT MATCH-------------
&&          DESCRIPTION         AEROSOL                FISSION
SPECIES(CONTAIN)
&&          CSI                 UO2                      CS AND I
&&          CSOH                PU                       CS2
&&          TE                  U                        TE
&&          REFRACTORY          MNO                      RF
&&          OTHER               MGO                      OTH
&&          HP EJECTION(1)      TIO2                  NOT PRESENT
&&          HP EJECTION(2)      CAO                   NOT PRESENT
&&          PHOTON CLOUD        NONE                    CURIES
CONTROL=9 2 2 8 15 11 20 8 1 0
MATERIAL
COMPOUND H2 O2 CO CO2 H2OL H2OV FE N2 CONC UO2 PU
  U MNO MGO TIO2 CAO K2O
FISSION
  TE
  I
  CS
  RF
  XE
  KR
  OTH
  CS2
  TE132 I132 XE132
  TE131M I131 XE131
  CURIES
```

```
TIMES 720.0  0.0
&& ---------TIME ZONES-------
  20.    40.     200.
  25.   100.    1000.
  25.   500.   25000.
   5.    15.   25090.
   5.    10.   25100.
   5.    50.   27000.
   5.   100.   30000.
  10.  1000.   40000.
&& ---------------------------
 1.  1.
THERMAL
FLOWS
 AREA(1,2)=0.01 AVL(1,2)=0.1 CFC(1,2)=2. TOPEN(1,2)=1.E8 QUASI
PRHEAT PRFISS PR:ER PRFLOW PRH-BURN PR-USERO PRENGSYS
FISSION  1 K2O C
  1 1 1 1 1 1 1 1 3 3 1
  TE
  I
  CS
  RF
  XE
  KR
  OTH
  CS2
  TE132 I132 XE132
  TE131M I131 XE131
  CURIES
  1.0E20
  1.E20
  1.E20
  1.E20
  1.E20
  1.E20
  1.E20
  1.E20
  2.808E5 8.280E3 1.0E20
  1.08E5 6.945E5 1.0E20
  1.E20
FGPPWR=4
  1.77E5 3.861E-04 1.714E4 1.25E-05  && --------TE
  3.33E5 1.194E-05 5.03E5 2.525E-04  && --------I
  6.48E4 4.528E-04 817.5 8.889E-06   && --------CS
  0.5 0.0 0.5 0.0                    && --------RF
  1.97E4 8.861E-04 1.29E3 2.342E-07  && --------XE
  2.231E5 5.75E-04 8.891E4 7.389E-05 && --------KR
  0.5 0.0 0.5 0.0                    && --------OTH
  6.48E4 4.528E-04 817.5 8.889E-06   && --------CS2
  0.0 0.0 0.0 0.0                    && --------TE132
  0.0 0.0 0.0 0.0                    && --------I132
  0.0 0.0 0.0 0.0                    && --------XE132
  0.0 0.0 0.0 0.0                    && --------TE131M
  0.0 0.0 0.0 0.0                    && --------I131
  0.0 0.0 0.0 0.0                    && --------X131
  0.0 0.0 0.0 0.0                    && --------CURIES
```

```
 FPM-CELL=1
   HOST=GAS 0. 0. 0. 0. 0. 0. 0. 0. 0. 0. 0. 0. 0. 0. 0. 0.

 RELEASE
   CS=0.1
   I=0.1
   RF=0.1
   OTH=0.1
   TE=0.1
   I=0.1
   CS2=0.1
 EOI
   HOST=K2O 0. 0. 0. 0. 0. 0. 0. 0. 0. 0. 0. 0. 0. 0. 0. 0.
 RELEASE
   TE132= 1.419E-05
   I132= 1.0E-03
   TE131M= 1.419E-05
   I131= 1.0E-03
 EOI
 ACCEPT
   CS= 0. 1. 0. 0. 0. 0. 0. 0. 0. 0. 0. 0. 0.
   I=  0. 1. 0. 0. 0. 0. 0. 0. 0. 0. 0. 0. 0.
   RF= 0. 0. 0. 0. 1. 0. 0. 0. 0. 0. 0. 0. 0.
   TE= 0. 0. 0. 1. 0. 0. 0. 0. 0. 0. 0. 0. 0.
   OTH= 0. 0. 0. 0. 0. 1. 0. 0. 0. 0. 0. 0. 0.
   CS2= 0. 0. 1. 0. 0. 0. 0. 0. 0. 0. 0. 0. 0.
   TE132= 0. 0. 0. 1. 0. 0. 0. 0. 0. 0. 0. 0. 0.
   TE131M= 0. 0. 0. 1. 0. 0. 0. 0. 0. 0. 0. 0. 0.
   I132= 0. 0. 0. 0. 0. 1. 0. 0. 0. 0. 0. 0. 0.
   I131= 0. 0. 0. 0. 0. 1. 0. 0. 0. 0. 0. 0. 0.
 EOI
 EOI
 TITLE
          SURRY TMLB' WITH SPRAYS AT 25000 S
  RUN NO. PNE11, AUGMENTED H2 & DESIGN BASIS SPRAY
 AEROSOL 1 1.E-7 2.5E-4 0. 0. 0. 0.
  RHO=3000.0
  UO2=  1.0E-6  0.7
  PU=  1.0E-6  0.7
  U= 1.0E-6 0.7
  MNO= 1.0E-6 0.7
  MGO= 1.0E-6 0.7
  TIO2= 0.7E-6 0.47
  CAO= 30.0E-6 0.693
  H2OV= 1.E-8 .405
 && --------END OF GLOBAL INPUT-------
 CELL=1
 CONTROL=20
  0 0 5 11
  0 0 8 224
  0 0 12 26
  16 26 0 1
  0 0 1 5
```

```
GEOMETRY 5.097E4 53.39
ATMOS=3  6.85E4  310.9
 H2OV=0.010
 O2=0.23
 N2=0.76
CONDENSE
SOURCE 8

&& --------------RPV SOURCE-----------------------------------
&& ------------------BASE CASE  14DEC-----------------------
&& ------------------REVISION 17FEB84-----------------------
&& -------------------------------------------------------------

&& ------------------ AUGMENTED HYDROGEN ------------------

H2 4 IFLAG=1

T
0.0     9438.   9498.   60000.
MASS
0.0       8.3    0.0     0.0
TEMP
0.0    420.     420.     420.
EOI

&& --------------------LIQUID WATER----------------------

H2OV       224   IFLAG = 1
  T
   .0000E+00  6.0000E-02  3.0060E+01  6.0060E+01  9.0060E+01
  1.2006E+02  1.5006E+02  1.8006E+02  2.1006E+02  6.9006E+02
  1.2001E+03  1.7101E+03  2.1901E+03  2.7001E+03  3.2101E+03
  3.2401E+03  3.2701E+03  3.3001E+03  3.3301E+03  3.3601E+03
  3.3901E+03  3.4201E+03  3.4501E+03  3.4801E+03  3.5101E+03
  3.5401E+03  3.5701E+03  3.6001E+03  3.6301E+03  3.6601E+03
  3.6901E+03  3.7201E+03  3.7501E+03  3.7801E+03  3.8101E+03
  3.8401E+03  3.8701E+03  3.9001E+03  3.9301E+03  3.9601E+03
  3.9901E+03  4.0201E+03  4.0501E+03  4.0801E+03  4.1101E+03
  4.1401E+03  4.1701E+03  4.2001E+03  4.2301E+03  4.2601E+03
  4.2901E+03  4.3201E+03  4.3501E+03  4.3801E+03  4.4701E+03
  4.5601E+03  4.6801E+03  4.7701E+03  4.8601E+03  4.9801E+03
  5.0701E+03  5.1601E+03  5.2801E+03  5.3701E+03  5.4601E+03
  5.5801E+03  5.6701E+03  5.7751E+03  5.8801E+03  5.9701E+03
  6.0751E+03  6.1801E+03  6.2701E+03  6.3751E+03  6.4801E+03
  6.5701E+03  6.6751E+03  6.7801E+03  6.8701E+03  6.9751E+03
  7.0801E+03  7.1701E+03  7.2751E+03  7.3801E+03  7.4701E+03
  7.5751E+03  7.6801E+03  7.7701E+03  7.8751E+03  7.9801E+03
  8.0701E+03  8.1751E+03  8.2801E+03  8.3701E+03  8.3851E+03
  8.4001E+03  8.4301E+03  8.4451E+03  8.4601E+03  8.4901E+03
  8.5051E+03  8.5201E+03  8.5501E+03  8.5651E+03  8.5801E+03
  8.6101E+03  8.6251E+03  8.6401E+03  8.6551E+03  8.6701E+03
  8.6851E+03  8.7001E+03  8.7151E+03  8.7301E+03  8.7451E+03
  8.7601E+03  8.7751E+03  8.7901E+03  8.8051E+03  8.8201E+03
  8.8351E+03  8.8501E+03  8.8651E+03  8.8801E+03  8.8951E+03
```

8.9101E+03	8.9251E+03	8.9401E+03	8.9551E+03	8.9701E+03
8.9851E+03	9.0001E+03	9.0151E+03	9.0301E+03	9.0451E+03
9.0601E+03	9.0751E+03	9.0901E+03	9.1051E+03	9.1201E+03
9.1351E+03	9.1501E+03	9.1651E+03	9.1801E+03	9.1951E+03
9.2101E+03	9.2251E+03	9.2401E+03	9.2551E+03	9.2701E+03
9.2851E+03	9.3001E+03	9.3151E+03	9.3301E+03	9.3451E+03
9.3601E+03	9.3751E+03	9.3901E+03	9.4046E+03	9.4142E+03
9.4252E+03	9.4472E+03	9.4581E+03	9.4784E+03	9.4877E+03
9.5051E+03	9.5208E+03	9.5348E+03	9.5533E+03	9.5691E+03
9.5825E+03	9.5974E+03	9.6147E+03	9.6273E+03	9.6383E+03
9.6825E+03	9.7413E+03	9.7792E+03	9.8392E+03	9.9956E+03
1.0029E+04	1.0089E+04	1.0209E+04	1.0296E+04	1.0356E+04
1.0476E+04	1.0536E+04	1.0595E+04	1.0655E+04	1.0713E+04
1.0768E+04	1.0803E+04	1.0863E+04	1.1017E+04	1.1048E+04
1.1108E+04	1.1228E+04	1.1276E+04	1.1319E+04	1.1379E+04
1.1499E+04	1.1619E+04	1.1899E+04	1.1970E+04	1.2018E+04
1.2078E+04	1.2136E+04	1.2193E+04	1.2256E+04	1.2316E+04
1.2378E+04	1.2436E+04	1.2501E+04	1.2561E+04	1.2623E+04
1.2682E+04	1.2716E+04	1.2776E+04	1.2896E+04	2.3097E+04
3.2963E+04	4.2985E+04	5.3008E+04	6.0024E+04	

MASS

.0000E+00	.0000E+00	.0000E+00	.0000E+00	5.5651E+01
1.1535E+01	.0000E+00	.0000E+00	.0000E+00	.0000E+00
.0000E+00	.0000E+00	.0000E+00	4.8069E+00	1.8534E+01
1.8522E+01	1.8520E+01	1.8530E+01	1.8476E+01	1.8230E+01
1.8299E+01	1.8304E+01	1.8320E+01	1.8337E+01	1.9363E+01
1.9698E+01	1.9695E+01	1.9717E+01	1.9758E+01	1.9819E+01
1.9892E+01	1.9970E+01	2.0050E+01	2.0132E+01	2.0215E+01
2.0298E+01	2.0382E+01	2.0467E+01	2.0475E+01	2.2038E+01
2.2050E+01	2.2107E+01	2.2189E+01	2.2284E+01	2.2385E+01
2.2489E+01	2.2596E+01	2.2705E+01	2.2814E+01	2.2925E+01
2.3036E+01	2.3149E+01	2.3406E+01	5.8248E+01	1.4867E+02
1.4581E+02	1.4656E+02	1.4567E+02	1.4569E+02	.0000E+00
.0000E+00	.0000E+00	.0000E+00	.0000E+00	.0000E+00
.0000E+00	.0000E+00	.0000E+00	.0000E+00	.0000E+00
.0000E+00	.0000E+00	.0000E+00	.0000E+00	.0000E+00
.0000E+00	.0000E+00	.0000E+00	.0000E+00	.0000E+00
.0000E+00	.0000E+00	.0000E+00	.0000E+00	.0000E+00
.0000E+00	.0000E+00	.0000E+00	.0000E+00	.0000E+00
.0000E+00	.0000E+00	.0000E+00	.0000E+00	.0000E+00
.0000E+00	.0000E+00	.0000E+00	.0000E+00	.0000E+00
.0000E+00	.0000E+00	.0000E+00	.0000E+00	.0000E+00
.0000E+00	.0000E+00	.0000E+00	.0000E+00	.0000E+00
.0000E+00	.0000E+00	.0000E+00	.0000E+00	.0000E+00
.0000E+00	.0000E+00	.0000E+00	.0000E+00	.0000E+00
.0000E+00	.0000E+00	.0000E+00	.0000E+00	.0000E+00
.0000E+00	.0000E+00	.0000E+00	.0000E+00	.0000E+00
.0000E+00	.0000E+00	.0000E+00	.0000E+00	.0000E+00
.0000E+00	.0000E+00	.0000E+00	.0000E+00	.0000E+00
.0000E+00	.0000E+00	.0000E+00	.0000E+00	.0000E+00
.0000E+00	.0000E+00	.0000E+00	.0000E+00	.0000E+00
.0000E+00	.0000E+00	.0000E+00	.0000E+00	.0000E+00
.0000E+00	5.8956E+02	.0000E+00	.0000E+00	.0000E+00
.0000E+00	.0000E+00	.0000E+00	.0000E+00	.0000E+00

.0000E+00	.0000E+00	.0000E+00	.0000E+00	.0000E+00
.0000E+00	.0000E+00	.0000E+00	.0000E+00	.0000E+00
.0000E+00	.0000E+00	.0000E+00	.0000E+00	.0000E+00
.0000E+00	.0000E+00	.0000E+00	.0000E+00	.0000E+00
.0000E+00	.0000E+00	.0000E+00	.0000E+00	.0000E+00
.0000E+00	.0000E+00	.0000E+00	.0000E+00	.0000E+00
.0000E+00	.0000E+00	.0000E+00	.0000E+00	.0000E+00
.0000E+00	.0000E+00	.0000E+00	.0000E+00	.0000E+00
.0000E+00	.0000E+00	.0000E+00	.0000E+00	.0000E+00
.0000E+00	.0000E+00	.0000E+00	.0000E+00	.0000E+00
.0000E+00	.0000E+00	.0000E+00	.0000E+00	.0000E+00
.0000E+00	.0000E+00	.0000E+00	.0000E+00	

ENTH

.0000E+00	.0000E+00	.0000E+00	.0000E+00	1.3739E+06
1.3929E+06	.0000E+00	.0000E+00	.0000E+00	.0000E+00
.0000E+00	.0000E+00	.0000E+00	1.4069E+06	1.4227E+06
1.4283E+06	1.4340E+06	1.4396E+06	1.4451E+06	1.4507E+06
1.4563E+06	1.4619E+06	1.4675E+06	1.4731E+06	1.4787E+06
1.4843E+06	1.4899E+06	1.4955E+06	1.5011E+06	1.5067E+06
1.5123E+06	1.5179E+06	1.5236E+06	1.5293E+06	1.5349E+06
1.5406E+06	1.5464E+06	1.5520E+06	1.5578E+06	1.5634E+06
1.5692E+06	1.5749E+06	1.5807E+06	1.5865E+06	1.5924E+06
1.5983E+06	1.6041E+06	1.6100E+06	1.6159E+06	1.6218E+06
1.6278E+06	1.6337E+06	1.6397E+06	1.6551E+06	1.6590E+06
1.6598E+06	1.6607E+06	1.6613E+06	1.6615E+06	.0000E+00
.0000E+00	.0000E+00	.0000E+00	.0000E+00	.0000E+00
.0000E+00	.0000E+00	.0000E+00	.0000E+00	.0000E+00
.0000E+00	.0000E+00	.0000E+00	.0000E+00	.0000E+00
.0000E+00	.0000E+00	.0000E+00	.0000E+00	.0000E+00
.0000E+00	.0000E+00	.0000E+00	.0000E+00	.0000E+00
.0000E+00	.0000E+00	.0000E+00	.0000E+00	.0000E+00
.0000E+00	.0000E+00	.0000E+00	.0000E+00	.0000E+00
.0000E+00	.0000E+00	.0000E+00	.0000E+00	.0000E+00
.0000E+00	.0000E+00	.0000E+00	.0000E+00	.0000E+00
.0000E+00	.0000E+00	.0000E+00	.0000E+00	.0000E+00
.0000E+00	.0000E+00	.0000E+00	.0000E+00	.0000E+00
.0000E+00	.0000E+00	.0000E+00	.0000E+00	.0000E+00
.0000E+00	.0000E+00	.0000E+00	.0000E+00	.0000E+00
.0000E+00	.0000E+00	.0000E+00	.0000E+00	.0000E+00
.0000E+00	.0000E+00	.0000E+00	.0000E+00	.0000E+00
.0000E+00	.0000E+00	.0000E+00	.0000E+00	.0000E+00
.0000E+00	.0000E+00	.0000E+00	.0000E+00	.0000E+00
.0000E+00	.0000E+00	.0000E+00	.0000E+00	.0000E+00
.0000E+00	.0000E+00	.0000E+00	.0000E+00	.0000E+00
.0000E+00	1.6617E+06	.0000E+00	.0000E+00	.0000E+00
.0000E+00	.0000E+00	.0000E+00	.0000E+00	.0000E+00
.0000E+00	.0000E+00	.0000E+00	.0000E+00	.0000E+00
.0000E+00	.0000E+00	.0000E+00	.0000E+00	.0000E+00
.0000E+00	.0000E+00	.0000E+00	.0000E+00	.0000E+00
.0000E+00	.0000E+00	.0000E+00	.0000E+00	.0000E+00
.0000E+00	.0000E+00	.0000E+00	.0000E+00	.0000E+00
.0000E+00	.0000E+00	.0000E+00	.0000E+00	.0000E+00
.0000E+00	.0000E+00	.0000E+00	.0000E+00	.0000E+00
.0000E+00	.0000E+00	.0000E+00	.0000E+00	.0000E+00

```
   .0000E+00    .0000E+00    .0000E+00    .0000E+00    .0000E+00
   .0000E+00    .0000E+00    .0000E+00    .0000E+00    .0000E+00
   .0000E+00    .0000E+00    .0000E+00    .0000E+00    .0000E+00
   .0000E+00    .0000E+00    .0000E+00    .0000E+00
EOI
H2OV       224   IFLAG = 2
  T
   .0000E+00  6.0000E-02  3.0060E+01  6.0060E+01  9.0060E+01
  1.2006E+02  1.5006E+02  1.8006E+02  2.1006E+02  6.9006E+02
  1.2001E+03  1.7101E+03  2.1901E+03  2.7001E+03  3.2101E+03
  3.2401E+03  3.2701E+03  3.3001E+03  3.3301E+03  3.3601E+03
  3.3901E+03  3.4201E+03  3.4501E+03  3.4801E+03  3.5101E+03
  3.5401E+03  3.5701E+03  3.6001E+03  3.6301E+03  3.6601E+03
  3.6901E+03  3.7201E+03  3.7501E+03  3.7801E+03  3.8101E+03
  3.8401E+03  3.8701E+03  3.9001E+03  3.9301E+03  3.9601E+03
  3.9901E+03  4.0201E+03  4.0501E+03  4.0801E+03  4.1101E+03
  4.1401E+03  4.1701E+03  4.2001E+03  4.2301E+03  4.2601E+03
  4.2901E+03  4.3201E+03  4.3501E+03  4.3801E+03  4.4701E+03
  4.5601E+03  4.6801E+03  4.7701E+03  4.8601E+03  4.9801E+03
  5.0701E+03  5.1601E+03  5.2801E+03  5.3701E+03  5.4601E+03
  5.5801E+03  5.6701E+03  5.7751E+03  5.8801E+03  5.9701E+03
  6.0751E+03  6.1801E+03  6.2701E+03  6.3751E+03  6.4801E+03
  6.5701E+03  6.6751E+03  6.7801E+03  6.8701E+03  6.9751E+03
  7.0801E+03  7.1701E+03  7.2751E+03  7.3801E+03  7.4701E+03
  7.5751E+03  7.6301E+03  7.7701E+03  7.8751E+03  7.9801E+03
  8.0701E+03  8.1751E+03  8.2801E+03  8.3701E+03  8.3851E+03
  8.4001E+03  8.4301E+03  8.4451E+03  8.4601E+03  8.4901E+03
  8.5051E+03  8.5201E+03  8.5501E+03  8.5651E+03  8.5801E+03
  8.6101E+03  8.6251E+03  8.6401E+03  8.6551E+03  8.6701E+03
  8.6851E+03  8.7001E+03  8.7151E+03  8.7301E+03  8.7451E+03
  8.7601E+03  8.7751E+03  8.7901E+03  8.8051E+03  8.8201E+03
  8.8351E+03  8.8501E+03  8.8651E+03  8.8801E+03  8.8951E+03
  8.9101E+03  8.9251E+03  8.9401E+03  8.9551E+03  8.9701E+03
  8.9851E+03  9.0001E+03  9.0151E+03  9.0301E+03  9.0451E+03
  9.0601E+03  9.0751E+03  9.0901E+03  9.1051E+03  9.1201E+03
  9.1351E+03  9.1501E+03  9.1651E+03  9.1801E+03  9.1951E+03
  9.2101E+03  9.2251E+03  9.2401E+03  9.2551E+03  9.2701E+03
  9.2851E+03  9.3001E+03  9.3151E+03  9.3301E+03  9.3451E+03
  9.3601E+03  9.3751E+03  9.3901E+03  9.4046E+03  9.4142E+03
  9.4252E+03  9.4472E+03  9.4581E+03  9.4784E+03  9.4877E+03
  9.5051E+03  9.5208E+03  9.5348E+03  9.5533E+03  9.5691E+03
  9.5825E+03  9.5974E+03  9.6147E+03  9.6273E+03  9.6383E+03
  9.6825E+03  9.7413E+03  9.7792E+03  9.8392E+03  9.9956E+03
  1.0029E+04  1.0089E+04  1.0209E+04  1.0296E+04  1.0356E+04
  1.0476E+04  1.0536E+04  1.0595E+04  1.0655E+04  1.0713E+04
  1.0768E+04  1.0803E+04  1.0863E+04  1.1017E+04  1.1048E+04
  1.1108E+04  1.1228E+04  1.1276E+04  1.1319E+04  1.1379E+04
  1.1499E+04  1.1619E+04  1.1899E+04  1.1970E+04  1.2018E+04
  1.2078E+04  1.2136E+04  1.2193E+04  1.2256E+04  1.2316E+04
  1.2378E+04  1.2436E+04  1.2501E+04  1.2561E+04  1.2623E+04
  1.2682E+04  1.2716E+04  1.2776E+04  1.2896E+04  2.3097E+04
  3.2963E+04  4.2985E+04  5.3008E+04  6.0024E+04
MASS
   .0000E+00    .0000E+00    .0000E+00    .0000E+00    .0000E+00
```

```
1.7841E+00  1.6632E-01   .0000E+00   .0000E+00   .0000E+00
 .0000E+00   .0000E+00   .0000E+00  7.5598E-02  4.0823E-01
3.9311E-01  3.7799E-01  3.7799E-01  3.6287E-01  3.4775E-01
3.4775E-01  3.3263E-01  3.3263E-01  3.1751E-01  3.1751E-01
3.0239E-01  3.0239E-01  2.8728E-01  2.8728E-01  2.7216E-01
2.7216E-01  2.5704E-01  2.4192E-01  2.4192E-01  2.2680E-01
2.1168E-01  2.1168E-01  1.9656E-01  1.8144E-01  1.8144E-01
1.2096E-01  1.2096E-01  1.2096E-01  1.0584E-01  1.0584E-01
9.0718E-02  7.5599E-02  7.5599E-02  6.0479E-02  4.5359E-02
3.0239E-02  1.5120E-02   .0000E+00   .0000E+00   .0000E+00
 .0000E+00   .0000E+00   .0000E+00   .0000E+00  2.6954E+01
3.6095E+01  2.6702E+01  2.7280E+01  2.6945E+01  3.4667E+01
2.5712E+01  3.0406E+01  2.4914E+01  1.9420E+01  1.4277E+01
1.0290E+01  7.8446E+00  6.1357E+00  4.8502E+00  3.9505E+00
3.3884E+00  2.8435E+00  2.7228E+00  2.6150E+00  3.0168E+00
3.4351E+00  3.0675E+00  2.6076E+00  2.1007E+00  1.6713E+00
1.4327E+00  1.4105E+00  1.3978E+00  1.4089E+00  1.4779E+00
1.6127E+00  1.5026E+00  1.3558E+00   .0000E+00   .0000E+00
2.0412E+00   .0000E+00   .0000E+00  1.7539E+00   .0000E+00
 .0000E+00  1.2398E+00   .0000E+00  2.5099E+00   .0000E+00
4.1730E+00  1.7585E+00  6.0348E+00  9.5951E+00  1.1023E+01
1.0237E+01  8.9723E+00  1.0655E+01  1.2256E+01  1.2876E+01
1.2014E+01  4.9849E+01  1.3575E+02  1.0348E+02  9.8958E+01
7.5179E+01  7.8795E+01  8.0344E+01  8.0427E+01  7.9656E+01
7.8564E+01  7.7130E+01  7.5514E+01  7.3794E+01  5.6531E+01
5.5598E+01  5.9014E+01  6.0287E+01  6.0709E+01  6.0396E+01
5.9561E+01  5.8557E+01  4.0870E+01  9.5430E+00  1.4881E+00
1.1939E+00  4.4942E-01  3.4634E-01  2.8486E-01  2.4363E-01
2.1570E-01  1.9484E-01  1.7692E-01  1.9274E-01  3.5289E-02
5.7534E-02  5.1639E-02  4.8202E-02   .0000E+00  4.6345E-02
4.3052E-02  8.3769E+02  6.9852E+02  1.6024E+02  1.6128E+02
1.6028E+02  1.5884E+02  1.5781E+02  1.5696E+02  1.5635E+02
1.5430E+02  1.5373E+02  1.5460E+02  1.5567E+02  1.5652E+02
1.5749E+02  1.5859E+02  1.5730E+02  9.2167E+00  1.1582E+01
3.4210E+00  1.9871E+01  1.3584E+01  6.5035E+00  3.1484E+01
1.1251E+01  4.0915E+00  1.9866E+01  1.0863E+01  6.3638E+00
1.5334E+01  1.4862E+01  8.4046E-01  2.0545E+01  2.4444E+00
1.9105E-01  1.2855E+01  5.1902E+00  3.5388E+01  1.0679E+01
4.1096E+00  1.7030E+01  2.0038E+01  1.0295E+01  9.0415E+00
1.1663E+01  3.6049E+00  3.2609E+01  1.4882E+01  7.4348E-01
1.9538E+01  1.6291E+00  1.7562E+01  1.1482E+00  1.8711E+01
1.7744E+00  1.7416E+01  1.2443E+00  1.8396E+01  1.6504E+00
1.4045E+01  5.8503E+00   .0000E+00   .0000E+00   .0000E+00
 .0000E+00   .0000E+00   .0000E+00   .0000E+00
ENTH
 .0000E+00   .0000E+00   .0000E+00   .0000E+00   .0000E+00
2.6601E+06  2.8143E+06   .0000E+00   .0000E+00   .0000E+00
 .0000E+00   .0000E+00   .0000E+00  2.7235E+06  2.7100E+06
2.7667E+06  2.7710E+06  2.6948E+06  2.7410E+06  2.7857E+06
2.7053E+06  2.7711E+06  2.7066E+06  2.7720E+06  2.7069E+06
2.7611E+06  2.6979E+06  2.7813E+06  2.7131E+06  2.7977E+06
2.7040E+06  2.7665E+06  2.8339E+06  2.7259E+06  2.7897E+06
2.8601E+06  2.7286E+06  2.7946E+06  2.8690E+06  2.7421E+06
2.8224E+06  2.9799E+06  2.7999E+06  3.0020E+06  2.7641E+06
```

```
 2.9243E+06  3.1256E+06  2.7242E+06  2.8853E+06  3.1330E+06
 3.6010E+06  4.9562E+06   .0000E+00   .0000E+00   .0000E+00
  .0000E+00   .0000E+00   .0000E+00   .0000E+00  2.5659E+06
 2.5621E+06  2.5684E+06  2.5678E+06  2.5687E+06  2.5653E+06
 2.5718E+06  2.5693E+06  2.5699E+06  2.5702E+06  2.5708E+06
 2.5732E+06  2.5766E+06  2.5804E+06  2.5845E+06  2.5880E+06
 2.5912E+06  2.5942E+06  2.5966E+06  2.5986E+06  2.6001E+06
 2.6013E+06  2.6025E+06  2.6034E+06  2.6040E+06  2.6043E+06
 2.6046E+06  2.6053E+06  2.6065E+06  2.6084E+06  2.6110E+06
 2.6146E+06  2.6313E+06  2.7037E+06   .0000E+00   .0000E+00
 2.7029E+06   .0000E+00   .0000E+00  2.7102E+06   .0000E+00
  .0000E+00  2.7452E+06   .0000E+00  2.7065E+06   .0000E+00
 2.6973E+06  2.6082E+06  2.6082E+06  2.6097E+06  2.6118E+06
 2.6138E+06  2.6155E+06  2.6176E+06  2.6197E+06  2.6223E+06
 2.6250E+06  2.6426E+06  2.7019E+06  2.7582E+06  2.8552E+06
 2.9120E+06  2.9798E+06  3.0554E+06  3.1366E+06  3.2229E+06
 3.3132E+06  3.4072E+06  3.5044E+06  3.6041E+06  3.6615E+06
 3.7219E+06  3.7905E+06  3.8635E+06  3.9408E+06  4.0203E+06
 4.1013E+06  4.1829E+06  4.2395E+06  4.2429E+06  4.2430E+06
 4.2422E+06  4.2428E+06  4.2427E+06  4.2428E+06  4.2429E+06
 4.2429E+06  4.2430E+06  4.2429E+06  4.2430E+06  4.2430E+06
 4.2431E+06  4.2431E+06  4.2430E+06   .0000E+00  4.2432E+06
 4.2430E+06  4.2431E+06  2.7790E+06  2.7414E+06  2.7411E+06
 2.7407E+06  2.7404E+06  2.7401E+06  2.7399E+06  2.7398E+06
 2.7399E+06  2.7405E+06  2.7411E+06  2.7418E+06  2.7424E+06
 2.7430E+06  2.7436E+06  2.7443E+06  2.7446E+06  2.7443E+06
 2.7440E+06  2.7435E+06  2.7433E+06  2.7425E+06  2.7422E+06
 2.7423E+06  2.7423E+06  2.7416E+06  2.7416E+06  2.7416E+06
 2.7412E+06  2.7412E+06  2.7412E+06  2.7410E+06  2.7411E+06
 2.7410E+06  2.7409E+06  2.7406E+06  2.7405E+06  2.7409E+06
 2.7407E+06  2.7404E+06  2.7404E+06  2.7407E+06  2.7406E+06
 2.7406E+06  2.7458E+06  2.7440E+06  2.7412E+06  2.7405E+06
 2.7417E+06  2.7405E+06  2.7415E+06  2.7406E+06  2.7416E+06
 2.7405E+06  2.7416E+06  2.7405E+06  2.7417E+06  2.7405E+06
 2.7420E+06  2.7419E+06   .0000E+00   .0000E+00   .0000E+00
  .0000E+00   .0000E+00   .0000E+00   .0000E+00
EOI
H2          224   IFLAG = 2
  T
  .0000E+00  6.0000E-02  3.0060E+01  6.0060E+01  9.0060E+01
 1.2006E+02  1.5006E+02  1.8006E+02  2.1006E+02  6.9006E+02
 1.2001E+03  1.7101E+03  2.1901E+03  2.7001E+03  3.2101E+03
 3.2401E+03  3.2701E+03  3.3001E+03  3.3301E+03  3.3601E+03
 3.3901E+03  3.4201E+03  3.4501E+03  3.4801E+03  3.5101E+03
 3.5401E+03  3.5701E+03  3.6001E+03  3.6301E+03  3.6601E+03
 3.6901E+03  3.7201E+03  3.7501E+03  3.7801E+03  3.8101E+03
 3.8401E+03  3.8701E+03  3.9001E+03  3.9301E+03  3.9601E+03
 3.9901E+03  4.0201E+03  4.0501E+03  4.0801E+03  4.1101E+03
 4.1401E+03  4.1701E+03  4.2001E+03  4.2301E+03  4.2601E+03
 4.2901E+03  4.3201E+03  4.3501E+03  4.3801E+03  4.4701E+03
 4.5601E+03  4.6801E+03  4.7701E+03  4.8601E+03  4.9801E+03
 5.0701E+03  5.1601E+03  5.2801E+03  5.3701E+03  5.4601E+03
 5.5801E+03  5.6701E+03  5.7751E+03  5.8801E+03  5.9701E+03
 6.0751E+03  6.1801E+03  6.2701E+03  6.3751E+03  6.4801E+03
```

6.5701E+03	6.6751E+03	6.7801E+03	6.8701E+03	6.9751E+03
7.0801E+03	7.1701E+03	7.2751E+03	7.3801E+03	7.4701E+03
7.5751E+03	7.6801E+03	7.7701E+03	7.8751E+03	7.9801E+03
8.0701E+03	8.1751E+03	8.2801E+03	8.3701E+03	8.3851E+03
8.4001E+03	8.4301E+03	8.4451E+03	8.4601E+03	8.4901E+03
8.5051E+03	8.5201E+03	8.5501E+03	8.5651E+03	8.5801E+03
8.6101E+03	8.6251E+03	8.6401E+03	8.6551E+03	8.6701E+03
8.6851E+03	8.7001E+03	8.7151E+03	8.7301E+03	8.7451E+03
8.7601E+03	8.7751E+03	8.7901E+03	8.8051E+03	8.8201E+03
8.8351E+03	8.8501E+03	8.8651E+03	8.8801E+03	8.8951E+03
8.9101E+03	8.9251E+03	8.9401E+03	8.9551E+03	8.9701E+03
8.9851E+03	9.0001E+03	9.0151E+03	9.0301E+03	9.0451E+03
9.0601E+03	9.0751E+03	9.0901E+03	9.1051E+03	9.1201E+03
9.1351E+03	9.1501E+03	9.1651E+03	9.1801E+03	9.1951E+03
9.2101E+03	9.2251E+03	9.2401E+03	9.2551E+03	9.2701E+03
9.2851E+03	9.3001E+03	9.3151E+03	9.3301E+03	9.3451E+03
9.3601E+03	9.3751E+03	9.3901E+03	9.4046E+03	9.4142E+03
9.4252E+03	9.4472E+03	9.4581E+03	9.4784E+03	9.4877E+03
9.5051E+03	9.5208E+03	9.5348E+03	9.5533E+03	9.5691E+03
9.5825E+03	9.5974E+03	9.6147E+03	9.6273E+03	9.6383E+03
9.6825E+03	9.7413E+03	9.7792E+03	9.8392E+03	9.9956E+03
1.0029E+04	1.0089E+04	1.0209E+04	1.0296E+04	1.0356E+04
1.0476E+04	1.0536E+04	1.0595E+04	1.0655E+04	1.0713E+04
1.0768E+04	1.0803E+04	1.0863E+04	1.1017E+04	1.1048E+04
1.1108E+04	1.1228E+04	1.1276E+04	1.1319E+04	1.1379E+04
1.1499E+04	1.1619E+04	1.1899E+04	1.1970E+04	1.2018E+04
1.2078E+04	1.2136E+04	1.2193E+04	1.2256E+04	1.2316E+04
1.2378E+04	1.2436E+04	1.2501E+04	1.2561E+04	1.2623E+04
1.2682E+04	1.2716E+04	1.2776E+04	1.2896E+04	2.3097E+04
3.2963E+04	4.2985E+04	5.3008E+04	6.0024E+04	
MASS				
.0000E+00	.0000E+00	.0000E+00	.0000E+00	.0000E+00
.0000E+00	.0000E+00	.0000E+00	.0000E+00	.0000E+00
.0000E+00	.0000E+00	.0000E+00	.0000E+00	.0000E+00
.0000E+00	.0000E+00	.0000E+00	.0000E+00	.0000E+00
.0000E+00	.0000E+00	.0000E+00	.0000E+00	.0000E+00
.0000E+00	.0000E+00	.0000E+00	.0000E+00	.0000E+00
.0000E+00	.0000E+00	.0000E+00	.0000E+00	.0000E+00
.0000E+00	.0000E+00	.0000E+00	.0000E+00	.0000E+00
.0000E+00	.0000E+00	.0000E+00	.0000E+00	.0000E+00
.0000E+00	.0000E+00	.0000E+00	.0000E+00	.0000E+00
.0000E+00	.0000E+00	.0000E+00	.0000E+00	.0000E+00
.0000E+00	.0000E+00	.0000E+00	.0000E+00	6.3680E-14
.0000E+00	.0000E+00	.0000E+00	.0000E+00	4.7558E-14
.0000E+00	3.0351E-10	1.1059E-08	4.1463E-08	1.2818E-07
5.1694E-07	2.1231E-06	9.1796E-06	3.6628E-05	9.7912E-05
2.1638E-04	4.2279E-04	7.9511E-04	1.4363E-03	3.3015E-03
6.1303E-03	7.6064E-03	8.2009E-03	7.7046E-03	6.8228E-03
6.3696E-03	6.6763E-03	6.9600E-03	7.3180E-03	7.9023E-03
8.7895E-03	7.0544E-03	.0000E+00	.0000E+00	.0000E+00
.0000E+00	.0000E+00	.0000E+00	.0000E+00	.0000E+00
.0000E+00	.0000E+00	.0000E+00	.0000E+00	.0000E+00
.0000E+00	1.1876E-02	4.2298E-02	7.0657E-02	8.5481E-02
8.3089E-02	7.5746E-02	9.4183E-02	1.1384E-01	1.2564E-01

1.2252E-01	6.0583E-01	2.0400E+00	1.7154E+00	1.6246E+00
1.1893E+00	1.1981E+00	1.1725E+00	1.1250E+00	1.0668E+00
1.0061E+00	9.4329E-01	8.8087E-01	8.2003E-01	5.9769E-01
5.6025E-01	5.6547E-01	5.4876E-01	5.2460E-01	4.9525E-01
4.6339E-01	4.3218E-01	2.9053E-01	6.7013E-02	1.0426E-02
8.3553E-03	3.1452E-03	2.4238E-03	1.9935E-03	1.7051E-03
1.5096E-03	1.3636E-03	1.2381E-03	1.3489E-03	2.4697E-04
4.0265E-04	3.6139E-04	3.3734E-04	.0000E+00	3.2434E-04
3.0130E-04	5.8625E+00	1.7604E+00	3.0766E-01	1.1984E-01
2.9531E-02	6.3832E-03	2.1080E-03	7.1409E-04	2.9346E-04
8.2034E-05	2.1721E-05	4.2447E-06	4.7053E-07	4.6559E-08
3.3728E-09	8.7951E-11	4.3270E-13	.0000E+00	.0000E+00
.0000E+00	4.7987E-14	3.0316E-14	5.8141E-14	1.1000E-13
.0000E+00	1.5158E-14	8.3568E-14	.0000E+00	1.5158E-14
6.0633E-14	3.0444E-14	.0000E+00	3.1635E-14	.0000E+00
5.1231E-14	.0000E+00	5.9276E-14	1.1761E-13	.0000E+00
1.5158E-14	7.5978E-14	4.2190E-14	.0000E+00	1.5158E-14
1.5158E-14	4.4189E-13	5.3303E-13	.0000E+00	.0000E+00
3.0955E-14	.0000E+00	2.8579E-14	.0000E+00	2.9697E-14
.0000E+00	2.7901E-14	.0000E+00	2.9267E-14	.0000E+00
5.3356E-14	3.0316E-14	.0000E+00	.0000E+00	.0000E+00
.0000E+00	.0000E+00	.0000E+00	.0000E+00	

ENTH

.0000E+00	.0000E+00	.0000E+00	.0000E+00	.0000E+00
.0000E+00	.0000E+00	.0000E+00	.0000E+00	.0000E+00
.0000E+00	.0000E+00	.0000E+00	.0000E+00	.0000E+00
.0000E+00	.0000E+00	.0000E+00	.0000E+00	.0000E+00
.0000E+00	.0000E+00	.0000E+00	.0000E+00	.0000E+00
.0000E+00	.0000E+00	.0000E+00	.0000E+00	.0000E+00
.0000E+00	.0000E+00	.0000E+00	.0000E+00	.0000E+00
.0000E+00	.0000E+00	.0000E+00	.0000E+00	.0000E+00
.0000E+00	.0000E+00	.0000E+00	.0000E+00	.0000E+00
.0000E+00	.0000E+00	.0000E+00	.0000E+00	.0000E+00
.0000E+00	.0000E+00	.0000E+00	.0000E+00	.0000E+00
.0000E+00	.0000E+00	.0000E+00	.0000E+00	4.9641E+06
.0000E+00	.0000E+00	.0000E+00	.0000E+00	4.9874E+06
.0000E+00	4.9962E+06	4.9989E+06	5.0009E+06	5.0069E+06
5.0257E+06	5.0497E+06	5.0773E+06	5.1050E+06	5.1281E+06
5.1503E+06	5.1702E+06	5.1864E+06	5.2001E+06	5.2100E+06
5.2178E+06	5.2253E+06	5.2313E+06	5.2348E+06	5.2364E+06
5.2372E+06	5.2376E+06	5.2379E+06	5.2381E+06	5.2380E+06
5.2379E+06	5.2379E+06	.0000E+00	.0000E+00	.0000E+00
.0000E+00	.0000E+00	.0000E+00	.0000E+00	.0000E+00
.0000E+00	.0000E+00	.0000E+00	.0000E+00	.0000E+00
.0000E+00	5.2556E+06	5.2629E+06	5.2744E+06	5.2878E+06
5.3001E+06	5.3109E+06	5.3256E+06	5.3434E+06	5.3624E+06
5.3803E+06	5.5050E+06	6.0167E+06	6.3944E+06	6.9568E+06
7.3838E+06	7.8646E+06	8.3869E+06	8.9440E+06	9.5285E+06
1.0139E+07	1.0771E+07	1.1419E+07	1.2080E+07	1.2460E+07
1.2858E+07	1.3306E+07	1.3785E+07	1.4286E+07	1.4801E+07
1.5323E+07	1.5846E+07	1.6208E+07	1.6222E+07	1.6216E+07
1.6212E+07	1.6213E+07	1.6213E+07	1.6213E+07	1.6212E+07
1.6212E+07	1.6212E+07	1.6213E+07	1.6212E+07	1.6212E+07
1.6212E+07	1.6213E+07	1.6212E+07	.0000E+00	1.6213E+07

```
  1.6212E+07  1.6213E+07  2.3611E+06  2.0734E+06  2.0692E+06
  2.0638E+06  2.0582E+06  2.0554E+06  2.0531E+06  2.0523E+06
  2.0536E+06  2.0607E+06  2.0680E+06  2.0768E+06  2.0845E+06
  2.0912E+06  2.0921E+06   .0000E+00   .0000E+00   .0000E+00
   .0000E+00   .0000E+00   .0000E+00  3.3554E+06   .0000E+00
   .0000E+00   .0000E+00   .0000E+00   .0000E+00   .0000E+00
   .0000E+00   .0000E+00   .0000E+00   .0000E+00   .0000E+00
   .0000E+00   .0000E+00  3.3554E+06   .0000E+00   .0000E+00
   .0000E+00   .0000E+00   .0000E+00   .0000E+00   .0000E+00
   .0000E+00  1.9738E+06  2.3967E+06   .0000E+00   .0000E+00
   .0000E+00   .0000E+00   .0000E+00   .0000E+00   .0000E+00
   .0000E+00   .0000E+00   .0000E+00   .0000E+00   .0000E+00
   .0000E+00   .0000E+00   .0000E+00   .0000E+00   .0000E+00
   .0000E+00   .0000E+00   .0000E+00   .0000E+00
EOI
&& ------------------CORE/CONCRETE INTERACTION GASES---
    CO      =33  IFLAG=2
 T
   9.438E+03  9.498E+03  1.064E+04  1.184E+04  1.304E+04
1.424E+04
  1.544E+04  1.664E+04  1.784E+04  1.904E+04  2.024E+04
2.144E+04
  2.264E+04  2.384E+04  2.504E+04  2.624E+04  2.744E+04
2.864E+04
  2.984E+04  3.104E+04  3.224E+04  3.344E+04  3.464E+04
3.584E+04
  3.704E+04  3.824E+04  3.944E+04  4.064E+04  4.184E+04
4.304E+04
  4.424E+04  5.024E+04  7.2E+04
 MASS
   1.008E-05  1.737E-05  2.197E-04  2.245E-03  3.565E-03
3.059E-03
  1.560E-03  6.050E-05  5.273E-05  5.074E-05  1.027E-01
1.530E-01
  5.522E-02  1.075E-02  1.249E-02  1.423E-02  1.721E-02
2.142E-02
  2.515E-02  2.776E-02  2.935E-02  2.953E-02  2.874E-02
2.765E-02
  2.661E-02  2.526E-02  2.461E-02  2.346E-02  2.059E-02
2.104E-02
  1.469E-02  8.333E-03  0.
 ENTH
   1.757E+06  1.881E+06  2.211E+06  2.253E+06  2.268E+06
2.042E+06
  1.799E+06  1.800E+06  1.803E+06  1.805E+06  2.177E+06
2.189E+06
  2.217E+06  2.277E+06  2.307E+06  2.329E+06  2.059E+06
1.839E+06
  2.083E+06  2.059E+06  1.837E+06  2.014E+06  2.184E+06
2.158E+06
  2.134E+06  2.116E+06  1.967E+06  1.940E+06  2.058E+06
1.924E+06
  1.924E+06  1.924E+06  0.
```

```
EOI
    CO2     =33  IFLAG=2
 T
   9.438E+03  9.498E+03  1.064E+04  1.184E+04  1.304E+04
1.424E+04
  1.544E+04  1.664E+04  1.784E+04  1.904E+04  2.024E+04
2.144E+04
  2.264E+04  2.384E+04  2.504E+04  2.624E+04  2.744E+04
2.864E+04
  2.984E+04  3.104E+04  3.224E+04  3.344E+04  3.464E+04
3.584E+04
  3.704E+04  3.824E+04  3.944E+04  4.064E+04  4.184E+04
4.304E+04
  4.424E+04  5.024E+04  7.2E+04
 MASS
   2.149E-03  4.391E-03  8.594E-03  1.770E-02  2.075E-02
1.700E-02
  1.221E-02  8.391E-03  7.530E-03  7.801E-03  7.848E-03
6.534E-03
  5.251E-03  5.388E-03  6.088E-03  6.795E-03  8.072E-03
1.103E-02
  1.434E-02  1.713E-02  1.945E-02  2.053E-02  2.083E-02
2.118E-02
  2.130E-02  2.107E-02  2.272E-02  2.545E-02  2.601E-02
2.890E-02
  2.779E-02  2.667E-02  0.
 ENTH
   1.788E+06  1.946E+06  2.226E+06  2.298E+06  2.325E+06
2.113E+06
  1.833E+06  1.834E+06  1.836E+06  1.839E+06  2.028E+06
2.245E+06
  2.289E+06  2.334E+06  2.366E+06  2.389E+06  2.107E+06
1.875E+06
  2.136E+06  2.093E+06  1.872E+06  2.064E+06  2.236E+06
2.208E+06
  2.187E+06  2.167E+06  2.000E+06  1.994E+06  2.104E+06
1.960E+06
  1.960E+06  1.96E+06  0.
EOI
    H2      =33  IFLAG=2
 T
   9.438E+03  9.498E+03  1.064E+04  1.184E+04  1.304E+04
1.424E+04
  1.544E+04  1.664E+04  1.784E+04  1.904E+04  2.024E+04
2.144E+04
  2.264E+04  2.384E+04  2.504E+04  2.624E+04  2.744E+04
2.864E+04
  2.984E+04  3.104E+04  3.224E+04  3.344E+04  3.464E+04
3.584E+04
  3.704E+04  3.824E+04  3.944E+04  4.064E+04  4.184E+04
4.304E+04
  4.424E+04  5.024E+04  7.2E+04
 MASS
   2.274E-03  3.807E-03  7.752E-03  1.631E-02  1.470E-02
```

```
3.001E-02
  4.061E-02  2.767E-02  2.482E-02  2.447E-02  1.993E-02
1.106E-02
  6.595E-03  7.356E-03  8.546E-03  9.736E-03  1.177E-02
1.465E-02
  1.720E-02  1.898E-02  2.008E-02  2.019E-02  1.965E-02
1.891E-02
  1.820E-02  1.728E-02  1.683E-02  1.495E-02  1.157E-02
1.129E-02
  8.562E-03  5.833E-03  0.
 ENTH
   2.299E+07  2.444E+07  2.823E+07  2.894E+07  2.922E+07
2.442E+07
  2.351E+07  2.352E+07  2.355E+07  2.358E+07  2.538E+07
2.827E+07
  2.886E+07  2.937E+07  2.974E+07  3.001E+07  2.670E+07
2.400E+07
  2.699E+07  2.670E+07  2.397E+07  2.615E+07  2.822E+07
2.791E+07
  2.763E+07  2.740E+07  2.556E+07  2.512E+07  2.669E+07
2.504E+07
  2.504E+07  2.504E+07  0.
EOI
    H2OV   =33  IFLAG=2
 T
   9.438E+03  9.498E+03  1.064E+04  1.184E+04  1.304E+04
1.424E+04
  1.544E+04  1.664E+04  1.784E+04  1.904E+04  2.024E+04
2.144E+04
  2.264E+04  2.384E+04  2.504E+04  2.624E+04  2.744E+04
2.864E+04
  2.984E+04  3.104E+04  3.224E+04  3.344E+04  3.464E+04
3.584E+04
  3.704E+04  3.824E+04  3.944E+04  4.064E+04  4.184E+04
4.304E+04
  4.424E+04  5.024E+04  7.2E+04
 MASS
   8.396E-03  1.715E-02  3.357E-02  6.913E-02  8.106E-02
6.643E-02
  4.768E-02  3.278E-02  2.942E-02  3.048E-02  3.060E-02
2.545E-02
  2.059E-02  2.128E-02  2.407E-02  2.688E-02  3.196E-02
4.365E-02
  5.668E-02  6.764E-02  7.676E-02  8.100E-02  8.213E-02
8.347E-02
  8.399E-02  8.306E-02  8.941E-02  1.099E-01  1.246E-01
1.412E-01
  1.24E-01  1.067E-01  0.
 ENTH
  3.453E+06  3.773E+06  4.341E+06  4.488E+06  4.544E+06
4.114E+06
  3.543E+06  3.545E+06  3.551E+06  3.556E+06  3.939E+06
4.380E+06
  4.471E+06  4.561E+06  4.626E+06  4.673E+06  4.100E+06
5.629E+06
```

```
  4.130E+06  4.072E+06  3.624E+06  4.012E+06  4.362E+06
4.306E+06
  4.259E+06  4.219E+06  3.882E+06  3.891E+06  4.094E+06
3.804E+06
  3.804E+06  3.804E+06  0.
EOI
&& ------------------------------------------------------------

&& ------------------END OF GAS
SOURCES----------------------------

H-BURN
STRUC
&& ---------------HEAT SINK STRUCTURES--

DOME ROOF  SLAB 11 5 310.9 10.0 0.0 0 2.323E3
0.0 5.563E-3 1.113E-2 1.676E-2 2.286E-2 3.2E-2 5.486E-2
1.036E-1
2.012E-1 3.962E-1 7.010E-1 1.159
FE FE CONC CONC CONC CONC CONC CONC CONC CONC CONC

WALL1 WALL SLAB 11 5 310.9 10.0 0.0 0 4.343E3
0.0 5.563E-3 1.113E-2 1.676E-2 2.286E-2 3.2E-2 5.486E-2 1.036E-1
2.012E-1 3.962E-1 7.01E-1 1.159
FE FE CONC CONC CONC CONC CONC CONC CONC CONC CONC

FLOOR FLOOR SLAB 11 5 310.9 10.0 0.0 0 1.045E3
0.0 5.563E-3 1.113E-2 1.676E-2 2.286E-2 3.2E-2 5.486E-2 1.036E-1
2.012E-1 3.962E-1 7.01E-1 1.159
FE FE CONC CONC CONC CONC CONC CONC CONC CONC CONC

WALL2 WALL SLAB 8 7 310.9 10.0 0. 0. 10.666E3
0.0 3.048E-3 9.144E-3 2.134E-2 4.572E-2 9.449E-2 1.92E-1
2.896E-1
3.993E-1
CONC CONC CONC CONC CONC CONC CONC CONC

WALL3 WALL SLAB 2 1 310.9 10.0 0. 2.747E3
0.0 1.250E-2 2.53E-2
FE FE

&& ------------------------------------------------------------

AEROSOL=8  UO2=0.  PU=0.  U=0. MNO=0. MGO=0. TIO2=0. CAO=0.
H2OV=0.1
SOURCE=12
&& ---------------AEROSOL SOURCES FROM RPV--------------

UO2=4  IFLAG=1
&& -------------CSI-------------------------------------
T=
0.0 9.438E3 9.498E3 1.0E10
MASS=
0.0 0.0633 0.0 0.0
```

```
EOI
&& ------------------------------------------------------------
PU=4  IFLAG=1
&& ------------CSOH-------------------------------------------
T=
0.0 9.438E3 9.498E3 1.0E10
MASS=
0.0 0.383 0.0 0.0
EOI
&& ------------------------------------------------------------
U=4  IFLAG=1
&& ------------------TE----------------------------------------
T=
0.0 9.438E3 9.498E3 1.0E10
MASS=
0.0 0.0217 0.0 0.0
EOI
&& ------------------------------------------------------------
MNO=4  IFLAG=1
&& ---------------REFRACTORY-----------------------------------
T=
0.0 9.438E3 9.498E3 1.E10
MASS=
0.0 .153 0.0 0.0
EOI
&& ------------------------------------------------------------
MGO=4  IFLAG=1
&& ------------------OTHER-------------------------------------
T=
0.0 9.438E3 9.498E3 1.0E10
MASS=
0.0 2.02 0.0 0.0
EOI
&& ------------------------------------------------------------------
&& ------------------------------------------------------------
TIO2=4  IFLAG=1
&& -----------HIGH PRESSURE EJECTION-MODE-1--------------------
T=
0.0 9.438E3 9.498E3 1.0E10
MASS=
0.0 0.833 0.0 0.0
EOI
&& ---------------HIGH PRESSURE EJECTION MODE 2---------------
CAO=4  IFLAG=1
T=
0.0 9.438E3 9.498E3 1.0E10
MASS=
0.0 0.833 0.0 0.0
EOI
&& ------------------------------------------------------------
&& ------------END RPV AEROSOL SOURCE--------------------------

&& ------------CORE/CONCRETE AEROSOL SOURCE--------------------
&& ---------------OTHER----------------------------------------
```

```
 MGO      =26  IFLAG=2
 T
  9.438E+03  1.064E+04  1.184E+04  1.304E+04  1.424E+04
1.544E+04
  1.664E+04  1.784E+04  1.904E+04  2.024E+04  2.144E+04
2.264E+04
  2.384E+04  2.504E+04  2.624E+04  2.744E+04  2.864E+04
2.984E+04
  3.104E+04  3.224E+04  3.344E+04  3.464E+04  3.584E+04
3.704E+04
  3.824E+04  7.2E+04
 MASS
  1.644E-03  2.119E-02  4.401E-02  6.080E-02  7.830E-02
6.881E-02
  5.079E-02  4.494E-02  4.140E-02  2.607E-02  9.981E-03
7.937E-03
  9.643E-03  1.267E-02  1.628E-02  2.057E-02  2.353E-02
2.351E-02
  2.165E-02  1.906E-02  1.609E-02  1.490E-02  1.276E-02
9.505E-03
  1.557E-02  0.
EOI
&& ------------------------------------------------------------
 MNO      =26  IFLAG=2
&& -------------------------REFRACTORY----------------------
 T
  9.438E+03  1.064E+04  1.184E+04  1.304E+04  1.424E+04
1.544E+04
  1.664E+04  1.784E+04  1.904E+04  2.024E+04  2.144E+04
2.264E+04
  2.384E+04  2.504E+04  2.624E+04  2.744E+04  2.864E+04
2.984E+04
  3.104E+04  3.224E+04  3.344E+04  3.464E+04  3.584E+04
3.704E+04
  3.824E+04  7.2E+04
 MASS
  9.357E-05  1.295E-03  2.242E-03  2.641E-03  2.829E-03
1.801E-03
  1.023E-03  7.716E-04  5.766E-04  4.186E-04  3.036E-04
2.550E-04
  3.186E-04  4.252E-04  5.517E-04  7.031E-04  8.097E-04
8.110E-04
  7.466E-04  6.538E-04  5.454E-04  5.004E-04  4.275E-04
3.187E-04
  5.262E-04  0.
EOI
&& ------------------------------------------------------------
 U        =26  IFLAG=2
&& -------------------------TE-------------------------------
 T
  9.438E+03  1.064E+04  1.184E+04  1.304E+04  1.424E+04
1.544E+04
  1.664E+04  1.784E+04  1.904E+04  2.024E+04  2.144E+04
2.264E+04
```

```
  2.384E+04  2.504E+04  2.624E+04  2.744E+04  2.864E+04
2.984E+04
  3.104E+04  3.224E+04  3.344E+04  3.464E+04  3.584E+04
3.704E+04
  3.824E+04  7.2E+04
 MASS
  8.420E-06  1.135E-04  2.152E-04  3.035E-04  3.837E-04
3.079E-04
  2.251E-04  2.098E-04  2.135E-04  1.958E-04  1.367E-04
9.765E-05
  1.072E-04  1.301E-04  1.582E-04  1.951E-04  2.272E-04
2.389E-04
  2.333E-04  2.189E-04  1.972E-04  1.935E-04  1.718E-04
1.321E-04
  1.741E-04  0.
EOI
&& ------------------------------------------------------------------
 PU       =25  IFLAG=2
&& -------------------------CSOH
(CS2O)-----------------------------
 T
  9.438E+03  1.064E+04  1.184E+04  1.304E+04  1.424E+04
1.544E+04
  1.664E+04  1.784E+04  1.904E+04  2.024E+04  2.144E+04
2.264E+04
  2.384E+04  2.504E+04  2.624E+04  2.744E+04  2.864E+04
2.984E+04
  3.104E+04  3.224E+04  3.344E+04  3.464E+04  3.584E+04
3.704E+04
  3.824E+04
 MASS
  3.925E-06  2.155E-05  4.037E-05  2.037E-05  0.          0.
  0.         0.         0.         0.         0.          0.
  0.         0.         0.         0.         0.          0.
  0.         0.         0.         0.         0.          0.
  0.
EOI
&&
------------------------------------------------------------------
 UO2        =25  IFLAG=2
&&
-----------------------------CSI--------------------------------

 T
  9.438E+03  1.064E+04  1.184E+04  1.304E+04  1.424E+04
1.544E+04
  1.664E+04  1.784E+04  1.904E+04  2.024E+04  2.144E+04
2.264E+04
  2.384E+04  2.504E+04  2.624E+04  2.744E+04  2.864E+04
2.984E+04
  3.104E+04  3.224E+04  3.344E+04  3.464E+04  3.584E+04
3.704E+04
  3.824E+04
```

```
 MASS
   7.720E-06  6.620E-05  1.415E-04  8.532E-05  4.267E-06
4.828E-07
   7.253E-08  2.545E-08  1.275E-08  5.920E-09  2.680E-09
1.630E-09
   1.980E-09  1.870E-09  1.670E-09  9.400E-10  0.          0.
   0.         0.         0.         0.         0.          0.
   0.
EOI
&&
-------------------------------------------------------------------


&& ---------------------END OF AEROSOL
SOURCES-------------------------
&& --------------------------------
FISSION SOURCE=16
&& -------------------FISSION SOURCE FOR RPV AEROSOLS-------------
&& ------------------CSI-----------------------------------------
CS=4  IFLAG=1
T=
0.0 9.438E3 9.498E3 1.0E10
MASS=
0.0 0.0323 0.0 0.0
EOI
&&
-------------------------------------------------------------------
I=4  IFLAG=1
T=
0.0 9.438E3 9.498E3 1.0E10
MASS=
0.0 0.031 0.0 0.0
EOI
&&
-------------------------------------------------------------------
&&
---------------------------------CSOH----------------------------
CS2=4  IFLAG=1
T=
0.0 9.438E3 9.498E3 1.0E10
MASS=
0.0 0.34 0.0 0.0
EOI
&&
-------------------------------------------------------------------

&&
-------------------------------TE--------------------------------
TE=4  IFLAG=1
T=
0.0 9.438E3 9.498E3 1.0E10
MASS=
0.0 0.0217 0.0 0.0
EOI
```

```
&&
-------------------------------------------------------------------------

&&
-------------------------REFRACTORY-------------------------------

RF=4  IFLAG=1
T=
0.0 9.438E3 9.498E3 1.0E10
MASS=
0.0 0.153 0.0 0.0
EOI
&&
-------------------------------------------------------------------------

&&
-------------------------OTHER-------------------------------------

OTH=4  IFLAG=1
T=
0.0 9.438E3 9.498E3 1.0E10
MASS=
0.0 2.02 0.0 0.0
EOI

&& -------------------------XENON-------------------------------
XE=4  IFLAG=1
T=
0.0 9.438E3 9.498E3 1.0E10
MASS=
0.0 4.308 0.0 0.0
EOI
&&
-------------------------------------------------------------------------
&&
-------------------------KR-------------------------------------
KR=4  IFLAG=1
T=
0.0 9.438E3 9.498E3 1.0E10
MASS=
0.0 0.2217 0.0 0.0
EOI
&&
-------------------------------------------------------------------------

&& ----------FISSION SOURCES FOR CORE/CONCRETE
AEROSOLS----------

 OTH        =26  IFLAG=2
 T
  9.438E+03  1.064E+04  1.184E+04  1.304E+04  1.424E+04
1.544E+04
  1.664E+04  1.784E+04  1.904E+04  2.024E+04  2.144E+04
```

```
 2.264E+04
   2.384E+04  2.504E+04  2.624E+04  2.744E+04  2.864E+04
 2.984E+04
   3.104E+04  3.224E+04  3.344E+04  3.464E+04  3.584E+04
 3.704E+04
   3.824E+04  7.2E+04
  MASS
   1.644E-03  2.119E-02  4.401E-02  6.080E-02  7.830E-02
 6.881E-02
   5.079E-02  4.494E-02  4.140E-02  2.607E-02  9.981E-03
 7.937E-03
   9.643E-03  1.267E-02  1.628E-02  2.057E-02  2.353E-02
 2.351E-02
   2.165E-02  1.906E-02  1.609E-02  1.490E-02  1.276E-02
 9.505E-03
   1.557E-02  0.
 EOI
 &&
 ---------------------------------------------------------------
  RF         =26  IFLAG=2
  T
   9.438E+03  1.064E+04  1.184E+04  1.304E+04  1.424E+04
 1.544E+04
   1.664E+04  1.784E+04  1.904E+04  2.024E+04  2.144E+04
 2.264E+04
   2.384E+04  2.504E+04  2.624E+04  2.744E+04  2.864E+04
 2.984E+04
   3.104E+04  3.224E+04  3.344E+04  3.464E+04  3.584E+04
 3.704E+04
   3.824E+04  7.2E+04
  MASS
   9.357E-05  1.295E-03  2.242E-03  2.641E-03  2.829E-03
 1.801E-03
   1.023E-03  7.716E-04  5.766E-04  4.186E-04  3.036E-04
 2.550E-04
   3.186E-04  4.252E-04  5.517E-04  7.031E-04  8.097E-04
 8.110E-04
   7.466E-04  6.538E-04  5.454E-04  5.004E-04  4.275E-04
 3.187E-04
   5.262E-04  0.
 EOI
 &&
 ---------------------------------------------------------------
  TE         =26  IFLAG=2
  T
   9.438E+03  1.064E+04  1.184E+04  1.304E+04  1.424E+04
 1.544E+04
   1.664E+04  1.784E+04  1.904E+04  2.024E+04  2.144E+04
 2.264E+04
   2.384E+04  2.504E+04  2.624E+04  2.744E+04  2.864E+04
 2.984E+04
   3.104E+04  3.224E+04  3.344E+04  3.464E+04  3.584E+04
 3.704E+04
   3.824E+04  7.2E+04
```

```
 MASS
  8.420E-06  1.135E-04  2.152E-04  3.035E-04  3.837E-04
3.079E-04
  2.251E-04  2.098E-04  2.135E-04  1.958E-04  1.367E-04
9.765E-05
  1.072E-04  1.301E-04  1.582E-04  1.951E-04  2.272E-04
2.389E-04
  2.333E-04  2.189E-04  1.972E-04  1.935E-04  1.718E-04
1.321E-04
  1.741E-04  0.
EOI
&&
-------------------------------------------------------------------
 CS2        =25  IFLAG=2
 T
  9.438E+03  1.064E+04  1.184E+04  1.304E+04  1.424E+04
1.544E+04
  1.664E+04  1.784E+04  1.904E+04  2.024E+04  2.144E+04
2.264E+04
  2.384E+04  2.504E+04  2.624E+04  2.744E+04  2.864E+04
2.984E+04
  3.104E+04  3.224E+04  3.344E+04  3.464E+04  3.584E+04
3.704E+04
  3.824E+04
 MASS
  3.702E-06  2.033E-05  3.808E-05  1.921E-05  0.          0.
  0.         0.         0.         0.         0.          0.
  0.         0.         0.         0.         0.          0.
  0.         0.         0.         0.         0.          0.
  0.
EOI
&&
-------------------------------------------------------------------
 CS         =25  IFLAG=2
 T
  9.438E+03  1.064E+04  1.184E+04  1.304E+04  1.424E+04
1.544E+04
  1.664E+04  1.784E+04  1.904E+04  2.024E+04  2.144E+04
2.264E+04
  2.384E+04  2.504E+04  2.624E+04  2.744E+04  2.864E+04
2.984E+04
  3.104E+04  3.224E+04  3.344E+04  3.464E+04  3.584E+04
3.704E+04
  3.824E+04
 MASS
  3.949E-06  3.386E-05  7.237E-05  4.364E-05  2.183E-06
2.470E-07
  3.710E-08  1.302E-08  6.522E-09  3.028E-09  1.371E-09
8.337E-10
  1.013E-09  9.565E-10  8.542E-10  4.808E-10  0.          0.
  0.         0.         0.         0.         0.          0.
  0.
EOI
```

```
&&
-------------------------------------------------------------------
 I          =25  IFLAG=2
 T
  9.438E+03  1.064E+04  1.184E+04  1.304E+04  1.424E+04
1.544E+04
  1.664E+04  1.784E+04  1.904E+04  2.024E+04  2.144E+04
2.264E+04
  2.384E+04  2.504E+04  2.624E+04  2.744E+04  2.864E+04
2.984E+04
  3.104E+04  3.224E+04  3.344E+04  3.464E+04  3.584E+04
3.704E+04
  3.824E+04
 MASS
  3.771E-06  3.234E-05  6.911E-05  4.168E-05  2.084E-06
2.358E-07
  3.543E-08  1.243E-08  6.228E-09  2.892E-09  1.309E-09
7.963E-10
  9.672E-10  9.135E-10  8.158E-10  4.592E-10  0.          0.
  0.         0.         0.         0.         0.          0.
  0.
EOI
&&
-------------------------------------------------------------------

TE132 = 4  IFLAG=1  HOST=13
T
0.0 9438.0 9498.0 1.0E10
MASS
0.0 3.186E-03 0.0 0.0
EOI
&& ---------------------------------------------------------------
TE131M = 4  IFLAG=1  HOST=13
T
0.0 9438.0 9498.0 1.0E10
MASS
0.0 1.196E-04 0.0 0.0
EOI
&& ----------END OF FISSION SOURCE ON CORE/CONCRETE AEROSOL
&& ---------------------------------------------------------------
&& -------------- CONTAINMENT SPRAY INPUT --------------------
ENGINEER SPRAYS 2 1 1 0.
SOURCE=1
H2OL=5
IFLAG=1
T=    0.   12000.  12090. 16200. 60000.
MASS= 0.   252.52   599.  346.67 346.67
TEMP= 315. 315.    324.22 330.97 330.97
EOI
SPRAY SPHITE=18.25 EOI
EOI

CELL=2
```

```
CONTROL=20
  0 0 0 0
  0 0 0 0
  0 0 0 0
  0 0 0 0
  0 0 0 0
GEOMETRY 1.E8 1.E30
ATMOS=3  1.E5 300.
  H2OV=0.050
  O2=0.2
  N2=0.75
EOF
```

DISTRIBUTION:
U. S. Government Printing Office
Receiving Branch (Attn: NRC Stock)
8610 Cherry Lane
Laurel, MD 20707
300 copies for R4

U.S. Department of Energy (2)
Albuquerque Operations Office
P.O. Box 5400
Albuquerque, NM 87185
Attn: J. R. Roeder, Dir.
Transportation Safeguards
D. L. Krenz, Dir.
Energy Research Technology
For: C. B. Quinn
R. N. Holton

Argonne National Laboratory (2)
9700 Cass Avenue
Argonne, IL 60439
Attn: L. Baker
B. C-J. Chen

Brookhaven National Laboratory (4)
Upton, NY 11973
Attn: G. A. Greene
M. Kahtib-Rahbar
H. Ludewig
T. Pratt

Los Alamos National Laboratory (3)
Los Alamos, NM 87545
Attn: R. J. Henninger
P. Y. Pan
L. L. Smith

Oak Ridge National Laboratories (4)
P.O. Box Y
Oak Ridge, TN 37830
Attn: S. A. Hodge
T. S. Kress
M. L. Tobias
S. Greene

Sandia National Laboratories
Organization 6400 (20)
Albuquerque, NM 87185
Attn: R. Cochrell

Battelle's Columbus Laboratories (3)
505 King Avenue
Columbus, OH 43201
Attn: R. S. Denning
A. Fentiman
P. Cybulskis

General Electric Company
175 Curtner Avenue, MC 766
San Jose, CA 95125
Attn: Jyh-Tong Teng

General Electric Company
P.O. Box 3508
Sunnyvale, CA 94088
Attn: E. L. Gluekler

Jack Tills & Associates, Inc.
209 Eubank, NE
Albuquerque, NM 87123
Attn: J. Tills

Power Authority State of New York
10 Columbus Circle
New York, NY 10019

Risk Management Asociates
2309 Dietz Farm Road
Albuquerque, NM 87107
Attn: P. Bieniaritz

Stone & Webster (2)
P.O. Box 2325
Boston, MA 02107
Attn: J. Metcalf
E. Warman

Technology for Energy
Corporation (2)
One Energy Center
Pellissippi Parkway
Knoxville, TN 37922
Attn: J. Carter
H. A. Mitchell

Westinghouse Electric Corporation
P.O. Box 355
Pittsburgh, PA 15230
Attn: N. Lipasulo

OEC
200 Rue de la Loi
1049 Brussels
BELGIUM
Attn: E. Della-Loggia
SdM2/77

AEE Winfrith (2)
Dorchester
Dorset
UNITED KINGDOM
Attn: A. T. D. Butland
P. N. Smith

AERE Harwell
Didcot
Oxfordshire OX11 ORA
UNITED KINGDOM
Attn: J. Gittus, AETB

Culham Laboratory
Culham
Abingdon
Oxfordshire OX14 3DB
UNITED KINGDOM
Attn: F. Briscoe

UKAEA Safety and Reliability
Directorate (6)
Culcheth
Wigshaw Lane
Warrington WA3 4NE
Cheshise
UNITED KINGDOM
Attn: F. Abbey
P. N. Clough
J. F. Collier
I. H. Dunbar
S. Ramsdale
R. L. D. Young

ENEA-DISP
DISP/ALCO/PROCS
Via Vitaliano Brancati, 48
00144 Roma, Italy
Attn: Dr. Maurizio Colagrossi

Joint Research Center (JRC)
21020 ISPRA (Varese), Italy
Attn: Dr. Antonio Markovina

JAYCOR
11011 Torreyana Road
P.O. Box 85154
San Diego, CA 92138
Attn: Dr. Paul Nakayama

U.S. Nuclear Regulatory Commission (18)
Division of Accident Evaluation
Office of Nuclear Regulatory Research
Washington, DC 20555
Attn: G. Arlotto
O. Bassett
S. B. Burson (5)
L. Chan
M. Cunningham
R. T. Curtis
J. Han
T. M. Lee
C. N. Kelber
G. Marino
R. Meyer
R. Minogue
M. Silberberg
R. W. Wright

U.S. Nuclear Regulatory Commission (12)
Office of Nuclear Reactor Regulation
Washington, DC 20555
Attn: V. Benaroya
R. Bernero
W. R. Butler
J. K. Long
J. F. Meyer
J. Mitchell
R. L. Palla
J. Rosenthal
Z. Rosztoczy
T. Speis
C. G. Tinkler
D. D. Yue

U.S. Department of Energy
RRT/DOE
NE 530
Washington, DC 20545
Attn: H. Alter

U.S. Department of Energy
Office of Nuclear Safety Coordination
Washington, DC 20545
Attn: R. W. Barber

Hanford Engineering Development Laboratory
Richland, WA 99352
Attn: G. R. Armstrong

Pacific Northwest Laboratory (3)
Battelle Blvd.
Richland, WA 99352
Attn: E. Coombes
P. C. Owczarski
C. Wheeler

Massachusetts Institute of Technology (2)
Cambridge, MA 02139
Attn: M. Golay
M. S. Kazimi

University of California at Los Angeles
Nuclear Energy Laboratory
405 Hilgard Avenue
Los Angeles, CA 90024
Attn: I. Catton

University of Missouri
Nuclear Engineering Department
Columbia, MO 65211
Attn: S. Loyalka

University of Wisconsin
Nuclear Engineering Department
Madison, WI 53706
Attn: M. Corradini

EG&G Idaho (4)
P.O. Box 1625
Idaho Falls, ID 83415
Attn: P. D. Bayless
R. Gottula
C. Allison
K. C. Wagner

Electric Power Research Institute
3412 Hillview Avenue
Palo Alto, CA 94303
Attn: R. Sehgal

Fauske & Associates, Inc.
16W070 83rd Street
Burr Ridge, IL 60521
Attn: M. G. Plys

Battelle Institute e.V. (3)
Am Romerhof 35
D-6000 Frankfurt am Main 90
FEDERAL REPUBLIC OF GERMANY
Attn: K. Fischer
L. Wolf
T. Kanzleiter

Gesellschaft fur Reaktorsicherheit mbH
Postfach 101650
Glockengasse 2
D-5000 Koln 1
FEDERAL REPUBLIC OF GERMANY
Attn: J. Langhans

Kerntorschungszentrum Karlsruhe (3)
Postfach 3640
D-7500 Karlsruhe 1
FEDERAL REPUBLIC OF GERMANY
Attn: Dr. Heusener
J. P. Hosemann
W. Schoeck

Division of Nuclear Safety Research
Nuclear Safety Research Center
Tokai Research Establishment
Japan Atomic Energy Research Institute
Tokai, Ibaraki-ken, 319-11
JAPAN
Attn: K. Soda

Power Reactor and Nuclear Fuel Development Corporation
Oarai Engineering Center
4002 Narita, Oarai-machi,
Ibaraki-ken, 311-13
JAPAN
Attn: H. Hiroi

Power Reactor and Nuclear Fuel Development Corporation
Fast Breeder Reactor Development Project
9-13, 1-Chome, Akasaka
Minato-ku, Tokyo
JAPAN
Attn: A. Watanabe

Rensselaer Polytechnic Institute
Department of Nuclear Engineering
Troy, NY 12180-3590
Attn: Prof. Richard Lahey

Technische Universitat Munchen
Forschungsgelande
8046 Garching
Republic of Germany
Attn: Prof. Dr. Ing. Helmut Karwat

Burns & Roe, Inc.
800 Kinderkamack Road
Oradell, NJ 07649
Attn: F. J. Patti

Sandia Distribution:
1271 M. J. Clauser
3141 S. A. Landenberger (5)
3151 W. L. Garner
6400 A. W. Snyder
6410 J. W. Hickman
6411 A. S. Benjamin
6411 A. C. Peterson
6412 A. L. Camp
6415 F. E. Haskin
6422 D. A. Powers
6422 J. E. Brockman
6423 P. A. Pickard
6423 A. Furutani
6423 K. Muramatsu
6423 G. Schumacher
6425 W. J. Camp
6425 J. Berthier
6425 I. Cook
6425 W. Frid
6425 S. Unwin
6427 M. Berman
6427 J. T. Hitchcock
6430 N. R. Ortiz
6440 D. A. Dahlgren
6442 W. A. von Riesemann
6442 L. D. Buxton
6444 J. M. McGlaun
6446 L. L. Bonzon
6447 D. L. Berry
6449 K. D. Bergeron (10)
6449 K. K. Murata
6449 P. E. Rexroth
6449 F. J. Schelling
6449 P. R. Shire
6449 G. Valdez
6449 D. C. Williams
6450 J. A. Reuscher
8024 P. W. Dean

NRC FORM 335 (2-84) NRCM 1102, 3201, 3202

U.S. NUCLEAR REGULATORY COMMISSION

BIBLIOGRAPHIC DATA SHEET

SEE INSTRUCTIONS ON THE REVERSE

1 REPORT NUMBER (Assigned by TIDC add Vol. No., if any)

NUREG/CR-4343
SAND85-1639

2 TITLE AND SUBTITLE

INTEGRATED SEVERE ACCIDENT CONTAINMENT ANALYSIS WITH THE CONTAIN COMPUTER CODE

3 LEAVE BLANK

4 DATE REPORT COMPLETED

MONTH	YEAR
August	1985

5 AUTHOR(S)

K. D. Bergeron J. L. Tills
D. C. Williams
P. E. Rexroth

6 DATE REPORT ISSUED

MONTH	YEAR
December	1985

7 PERFORMING ORGANIZATION NAME AND MAILING ADDRESS (Include Zip Code)

Containment Modeling Division
Sandia National Laboratories
Albuquerque, NM 87185

8 PROJECT/TASK/WORK UNIT NUMBER

Task 7

9 FIN OR GRANT NUMBER

A-1198

10 SPONSORING ORGANIZATION NAME AND MAILING ADDRESS (Include Zip Code)

Division of Accident Evaluation
Office of Nuclear Regulatory Research
U.S. Nuclear Regulatory Commission
Washington, DC 20555

11a TYPE OF REPORT

Technical

b PERIOD COVERED (Inclusive dates)

12 SUPPLEMENTARY NOTES

13 ABSTRACT (200 words or less)

Analysis of physical and radiological conditions inside the containment building during a severe (core-melt) nuclear reactor accident requires quantitative evaluation of numerous highly disparate yet coupled phenomenologies. These include two-phase thermodynamics and thermal-hydraulics, aerosol physics, fission product phenomena, core-concrete interactions, the formation and combustion of flammable gases, and performance of engineered safety features. In the past, this complexity has meant that a complete containment analysis would require application of suites of separate computer codes each of which would treat only a narrower subset of these phenomena, e.g., a thermal-hydraulics code, an aerosol code, a core-concrete interaction code, etc. In this paper, we describe the development and some recent applications of the CONTAIN code, which offers an integrated treatment of the dominant containment phenomena and the interactions among them. We describe the results of a series of containment phenomenology studies, based upon realistic accident sequence analyses in actual plants, which highlight various phenomenological effects that have potentially important implications for source term and/or containment loading issues, and which are difficult or impossible to treat using a less integrated code suite. The results described show that analyses with non-integrated, separate-effects codes can neglect interactions that are important to the source term and, furthermore, it is impossible to generalize whether the errors in such treatments would be "conservative" or "non-conservative". It is concluded that integrated phenomenological analysis will play an increasingly important role as the technology for severe accident analysis matures.

14 DOCUMENT ANALYSIS - a KEYWORDS/DESCRIPTORS

Reactor containment; computer code; severe accidents; aerosol behavior; thermal-hydraulic behavior; fission products; sensitivity studies.

b IDENTIFIERS/OPEN-ENDED TERMS

Studies of severe accident containment phenomenology.

15 AVAILABILITY STATEMENT

NTIS
GPO Sales

16 SECURITY CLASSIFICATION

(This page) Unclassified
(This report) Unclassified

17 NUMBER OF PAGES

18 PRICE

☆ U.S. Government Printing Office 1985-676-049/21022